ASD-TDR-7-943a(1)

EXPANDABLE SPACE STRUCTURE

INTERIM TECHNICAL DOCUMENTARY REPORT Nr. ASD-TDR-7-943a(1)

1 November 1962 - 31 January 1963

Materials and Processes Branch
Manufacturing Technology Laboratory
Aeromechanics Branch
Flight Dynamics Laboratory
Aeronautical Systems Division
Air Force Systems Command
United States Air Force
Wright-Patterson Air Force Base, Ohio

ASD Project Nr. 7-943a and Nr 1368

Task Nr. 136808

The needs and requirements for expandable semirigid space structures are discussed and problem areas are described. A representative space mission profile is defined at an altitude of 257 mi and 33.3 deg inclination. Preliminary design criteria, including structural loads and space environmental conditions, are established. Effects of thermal radiation, meteoroids, and space radiation are discussed. Results of thermal heat balance analyses programed on the IBM 7090 are presented. Structural factors of safety are defined. A structural configuration is chosen from the standpoint of strength, operational reliability, manufacturing feasibility, and minimum weight and cost. Preliminary tooling and fabrication studies are described.

(Prepared under Contract No. AF33(657)-9733
by Martin Company, Denver, Colorado
Aerospace Division of Martin-Marietta Corporation
Authors: P. M. Knox, Jr., A. Corell, E. Lane)

NOTICES

When US Government drawings, specifications, or other data are used for any purpose other than a definitely related Government procurement operation, the Government thereby incurs no responsibility nor any obligation whatsoever; and the fact that the Government may have formulated, furnished, or in any way supplied the said drawings, specifications or otherwise, as in any manner licsensing the holder or any other person or corporation, or conveying any rights or permission to manufacture, use, or sell any patented inventions that may in any way be related thereto.

Copies should not be returned to the Aeronautical Systems Division unless return is required by security considerations, contractual obligations, or notice on a specific document.

FOREWORD

This Interim Technical Documentary Report covers the work performed under Contract AF33(657)-9733 from 1 November 1962 through 31 January 1963. It is published for technical information only and does not necessarily represent the recommendations, conclusions or approval of the Air Force.

This contract with Martin Company, Denver, Colorado, was initiated under Project Nr. 7-943a and 1368, Task Nr. 136808, "Semirigid or Nonrigid Structures for Space Applications." The telescoping concept investigated in the study is identified as "Expandable Space Structure." The work effort under this contract is under the joint management of the Manufacturing Technology Laboratory, Directorate of Materials and Processes (ASRCTF) and the Flight Dynamics Laboratory, Directorate of Aeromechanics (ASRMDS-21). It is being accomplished under the technical direction of Mr. Thomas Campbell, Manufacturing Technology Laboratory.

Closely related efforts are covered under ASD Contracts AF33(616)-6641, "Multiwall Space Structures" and AF33(616)-7775 "Nonrigid and Semirigid Space Structures."

Paul M. Knox, Jr is the Project Manager in charge. Others who cooperated in this phase of the study and in the preparation of the report were: A. Corell, Project Engineer; A. E. Rhoads, Advanced Manufacturing; E. Lane, Structural Design; W. S. Paulson, Structural Analysis; and L. C. Gregory, Materials Engineering.

The Martin Company report number assigned to this report is ASD-CR-63-4.

Abstract - Summary

The needs and requirements for expandable semirigid space structures are discussed and problem areas are described. A representative space mission profile is defined at an altitude of 257 n mi and 33.3 deg inclination. Preliminary design criteria, including structural loads and space environmental conditions, are established. Effects of thermal radiation, meteoroids, and space radiation are discussed. Results of thermal heat balance analyses programed on the IBM 7090 are presented. Structural factors of safety are defined. A structural configuration is chosen from the standpoint of strength, operational reliability, manufacturing feasibility, and minimum weight and cost. Preliminary tooling and fabrication studies are discussed.

Tests completed to determine feasibility of deployment and stowage are discussed. These include the following operational mockups:

1) Full-scale structure with single ply bladder;

2) ¼-scale structure with double-ply bladder to simulate self-sealing.

Results of eight meteoroid puncture tests in representative panels are presented and data are analyzed.

The materials test program is defined. Results of thermal properties tests on fibrous insulations are described.

Manufacturing tests, tooling studies, value engineering activities and weight studies are discussed.

The plans for the remainder of Phase I, which include release of engineering drawings, operable mockup tests, environmental analyses and tests, manufacturing tests, tooling studies, and materials tests are presented.

TABLE OF CONTENTS

LIST OF ILLUSTRATIONS

LIST OF TABLES

I. INTRODUCTION

This research and development program was initiated by the Materials Laboratory of the Aeronautical Systems Division, Wright-Patterson Air Force Base, to determine and develop the manufacturing methods, processes, and related design data required for the efficient and practical use of available materials for expandable space structures.

Future operational mission requirements for space vehicles or stations will necessitate a substantial increase in payload size and weight, and therefore increased booster requirements. Alleviation of these booster requirements can be aided by the design of efficient space structures. One such structural concept is the expandable semirigid or telescoping structure. The effort covered by this contract is to develop the manufacturing knowhow for a telescoping space structure and establish its feasibility by evaluation and test for use as a manned space station.

The predominating considerations for the conventional space structure are:

1) Sealing and control of air leakage due to meteoroid penetration;

2) Environmental control;

3) Systems integration;

4) Compatibility of materials with natural and induced environments;

5) Structural and mechanical considerations;

The concept of Expandable Space Structures (ESS) introduces several new problems:

1) Structural integrity of telescoping structures;

2) Mechanical feasibility of stowage and deployment in a space environment;

3) Tooling and manufacturing problems associated with stowage and deployment requirements.

To systematically evaluate the feasibility of the telescoping concept through design, fabrication, and environmental testing, a three-phase program was initiated:

Phase I - Material selection, design, and preliminary fabrication studies;

Phase II - Fabrication of the ESS and test panels;

Phase III - Test evaluation.

This quarterly progress report summarizes the results of the first half of Phase I.

SUMMARY

In the first half of Phase I, covered by this quarterly progress report, structural design criteria and space environmental criteria were defined for the space mission under consideration. The effects of nuclear radiation, meteoroids, and solar heating were analyzed and internal temperature control by active systems was studied. Thermal balance studies were programed on the IBM 7090. Structural configurations were optimized from the standpoint of strength, operational reliability, manufacturing feasibility, minimum weight and minimum cost, and the design concept was established. Preliminary tooling design studies were completed and a value analysis was started.

Two operational mockups were built and tested to determine the feasibility of deployment and stowage. These included one full-scale structure with single ply bladder, and a one-quarter-scale structure with a double-ply bladder to simulate self-sealing. Bladder folding characteristics will be determined and folding methods developed on these mockups.

Eight meteoroid penetration test panels were built and tested in the Hypervelocity Particle test facility at the Denver Research Institute. Hypervelocity puncture diameter data are presented (see Fig. III-5).

In the materials area, thermal properties tests were run on fibrous insulations, and sealant tests were started.

Several manufacturing tests, including machining of representative welded rings, were completed. Ring forging drawings of the main frames were released for procurement of test articles for machining tests.

Results of other Martin studies such as Manual Orbital Development System (MODS), Military Test Space Station (MTSS), and other Air Force studies have been incorporated in this program where applicable. A literature search is being continued, particularly in the area of materials for space environment.

Plans for completion of Phase I are shown in Section VIII. The critical problem areas remaining in Phase I are:

1) Structural sealing;

2) Bladder folding;

3) Warpage of frames during machining operation;

4) Design and fabrication tolerance control;

5) Cleanliness requirements.

II. VEHICLE DESIGN

Aspects of vehicle design described in this section include design criteria, vehicle description, configuration design studies, and structural and weight analysis.

A. PRELIMINARY DESIGN CRITERIA

During this reporting period an attempt has been made to identify the criteria that should be considered in the design of the vehicle. The criteria discussed here represent items that have been developed to date and are considered to be of primary interest to the program. Continuing effort on this program will further evaluate the design criteria to determine any necessary additions or changes.

The basic philosophy governing design of the vehicle is to develop an expanding structure that will prove feasibility of the concept. The expandable sections will be designed considering requirements of a manned space station. Portions of the vehicle not pertinent to proving feasibility of the concept, such as the end closures, will be designed to permit the telescoping structure to function properly, but need not be of the configuration that would be proposed for space flight.

1. Contractual Design Considerations

The contract statement of work contains the following design considerations, listed here for reference:

1) Performance in low-earth orbits (maximum 500 mi);

2) Maintain internal pressurization of 7 to 15 psi and loads resulting from same;

3) Radiation shielding of occupants and equipment (5 to 30 days);

4) Structural life expectancy of 1 yr;

5) Material shielding and self-sealing characteristics;

6) Minimum weight construction;

7) Thermal control - External surface temperature of -150 to 400°F;

8) Methods and reliability of deployment;

9) Vibration and dynamic loading during launch and boost trajectory;

10) Loads imposed on structure during deployment;

11) Ratio of deployed volume to packaged volume should be 5 to 1 or more;

12) Packagability and ease of ground handling;

13) Interaction of above stresses;

14) Ease of fabrication;

15) Modular concept so two similar modules, if made to rendezvous in space, would have easy and quick connection capability to each other.

Additional design constraints are:

1) The structural component shall be of a size equivalent to a cylinder 8 ft in diameter and 15 ft long;

2) The semirigid structural concept considered shall be the telescoping rigid section configuration;

3) The expanded structure shall provide a volume of at least five times the packaged volume.

2. Design Criteria

In compliance with the preceding considerations, the following preliminary design criteria have been established.

Mission Profile - The expandable space structure will be boosted into a 100 n mi elliptical orbit from which it will coast to a 257 n mi altitude for circular orbit injection.

Configuration Constraints - The 8-ft diameter 15-ft long module will telescope to form a compact boost package. The expansion ratio will be at least 5 to 1, based on the volume of the telescoping sections only, and assuming both ends are flat. Capability of incorporating radiator panels for an environmental control system will be demonstrated by analysis and layout.

Factors of Safety - The following safety factors will apply:

	Limit and Proof	Ult
Nonpressurized Structure		
Manned Operation	1.1	1.4
Unmanned Operation	1.0	1.25
Pressurized Structure	1.1	1.5
Skin Structure Subject to Tearing after Puncture*		1.5
Deployment and Pressure Cycles	4	

*Stresses to be compared to the tear limit of the skin.

Minimum regulated pressure will be used in conjunction with limit and ultimate loads when the pressure constitutes a relieving load. Maximum regulated pressure will be used for computing pressure loads. Limit temperatures will be used to determine the material properties.

Strength, Temperatures, and Deformation Requirements - The structure will be capable of sustaining all concurrent combinations of limit load and temperatures without loss of utility or integrity. The effects of structural deformations due to limit loads and temperatures will not be detrimental to vehicle functioning or integrity of the structure. The structure will be capable of sustaining all concurrent combinations of ultimate loads and limit temperatures without failure.

3. Design Conditions

Ground Handling and Transportation - Transportation and handling will be accomplished in the collapsed position. A limit load factor of $\pm 2g$ in the longitudinal direction and $\pm 1g$ in any side direction will be used to establish limit handling loads for all assembling, moving, and hoisting operations. A limit load factor of $\pm 2g$ in any side direction and $\pm 3g$ in the longitudinal direction will be used to establish limit loads for transportation.

Prelaunch and Boost - The station structure will be capable of withstanding static and dynamic loads imposed during prelaunch. The station structure will be capable of withstanding the static and dynamic loads and temperatures associated with maximum aerodynamic loads, maximum dynamic pressure, maximum acceleration, and the maximum temperature conditions during boost phase. The maximum acceleration imposed by the booster will be assumed to be 8.0g and 0.6g in the longitudinal and lateral directions, respectively.

Acoustics and Vibration - Experience with the Titan I and Titan II vehicles has shown that the acoustic level at the payload elevation produces no particular structural problem during the vehicle prelaunch and launch phases, and, therefore, shall not be considered in the vehicle design. Vibration will be considered in the overall vehicle design. The structurally-significant frequencies lie within the 0- to 50-cps band. Design criteria will be taken from Titan II accelerometer data. Panel flutter phenomenon will be considered in the design of the external skin panels of the outer telescoping section.

Maneuvering and Deployment in Orbit - Deployment will be accomplished after orbital injection. Consideration will be given to loads, pressures, and temperatures incurred during this period. The internal atmosphere of the station will be completely evacuated, and all expansion sections will be unlocked from the boost position before deployment commences. Deployment will be accomplished by controlled-pressure injection to the cabin interior. A positive alignment feature to prevent relative rotation of the sections during expansion will be included in the design. Kick-stage thrust loads and docking loads may be imposed on the station in either the collapsed or expanded position. The structural frequency design goal will be above 10 cps in the expanded and pressurized position. A maximum closing rate of 0.5 fps will be used to determine docking loads. Docking may be accomplished on the forward end of the vehicle only. The mass of the vehicle being rendezvoused with will be assumed to be 10,000 lb for purposes of computing rendezvous loads. Maximum weight of the ESS is assumed to be 8,000 lb.

Operation - The maximum internal working pressure will be 11 psig. The pressure structure will incorporate seals for maintenance of internal pressure for as long as practical (2 hr with less than 30% pressure loss is desired). Consideration will be given to self-sealing capability. The pressure sealing bladder will be repairable in orbit if punctured. No provisions will be made for collapse or re-entry of the station after deployment or orbital use.

Space Environment - The vehicle will be designed to withstand the anticipated space environment of a low-altitude orbit, and to protect the crew against such environment. The environment considered consists of:

1) Thermal radiation;

2) Space nuclear radiation;

3) Meteoroid field;

4) Ultraviolet radiation.

The thermal radiation for a low-orbit mission for a vehicle that maintains one face constantly toward the earth is shown in Fig. II-1. This data will be the basis for heat balance computations. The meteoroid environment, for design purposes, will be as shown in Fig. II-2.

Space radiation evaluations will be based on the data of Fig. II-3, II-4, II-5, and II-6, and Table II-1. Figures II-3, II-4, and II-5 are definitions of the Van Allen Belt. Limits on absorbed radiation by the crew are shown in Fig. II-6, and radiation levels are shown in Table II-1. Ultraviolet radiation will be as defined in Fig. II-7.

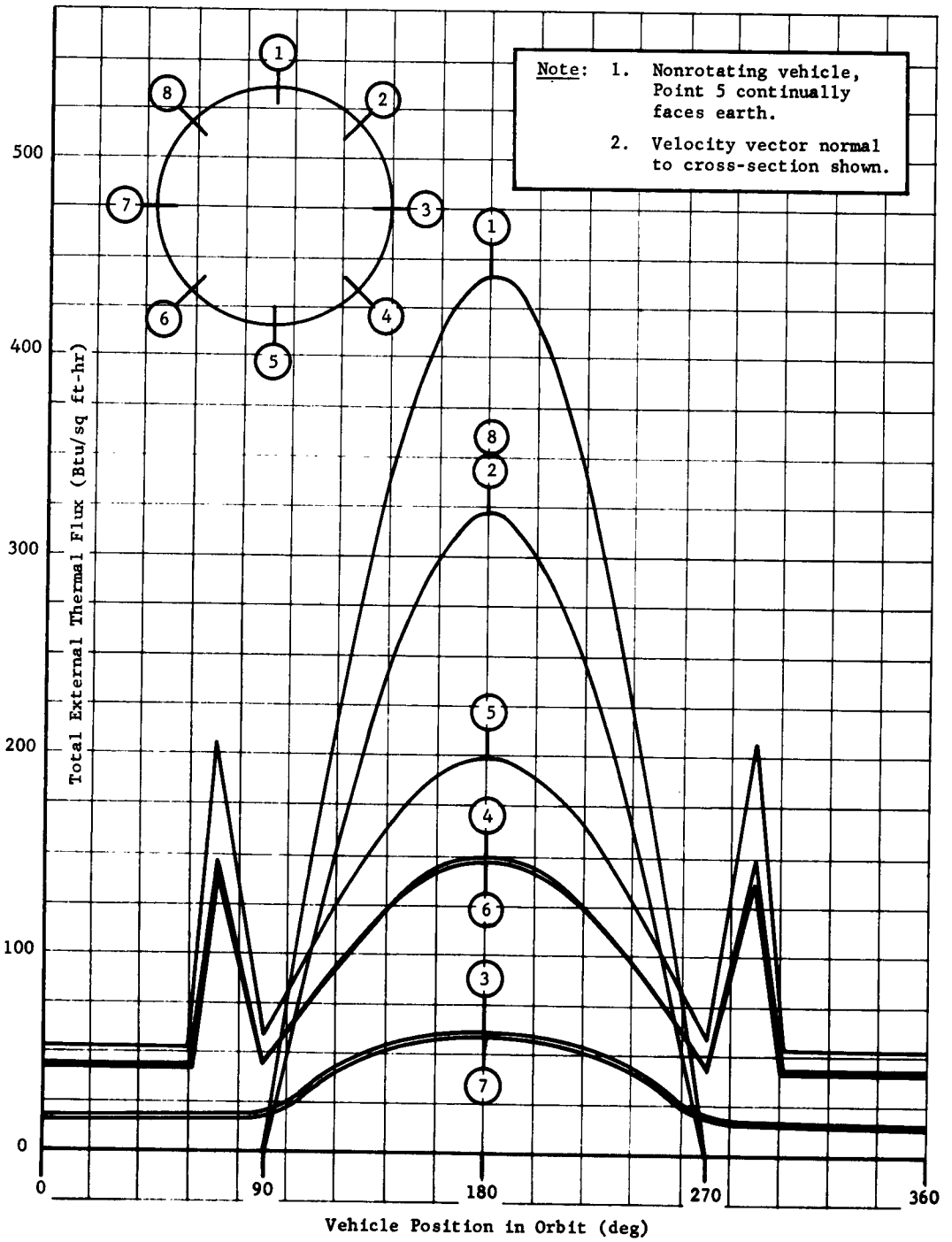

Fig. II-1 Total Incident Thermal Flux on External Cylindrical Surfaces of Vehicle in Orbit

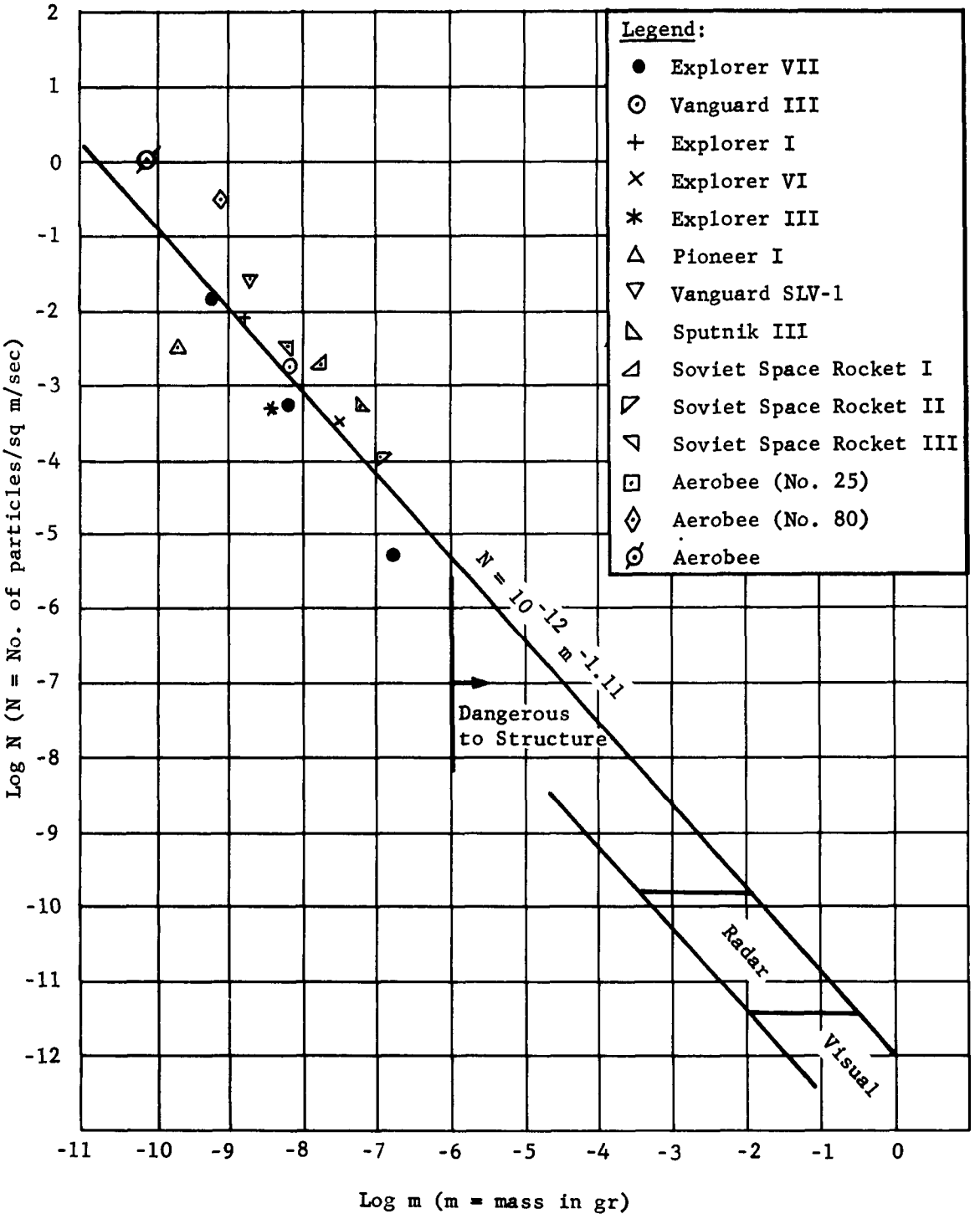

Fig. II-2 Meteoroids - Flux Density Versus Particle Mass

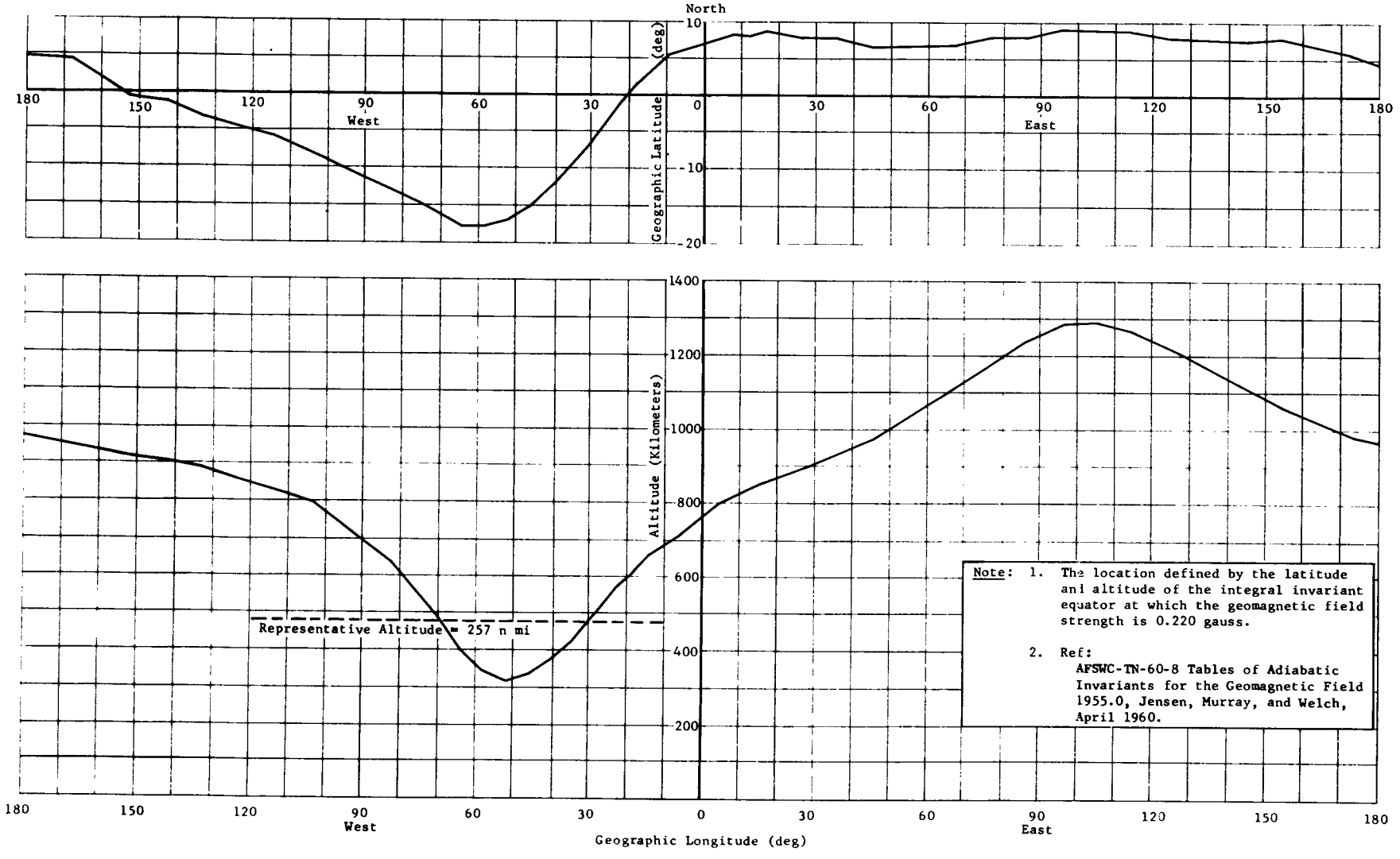

Fig. II-3 Location of the Minimum Altitude of the Van Allen Belt

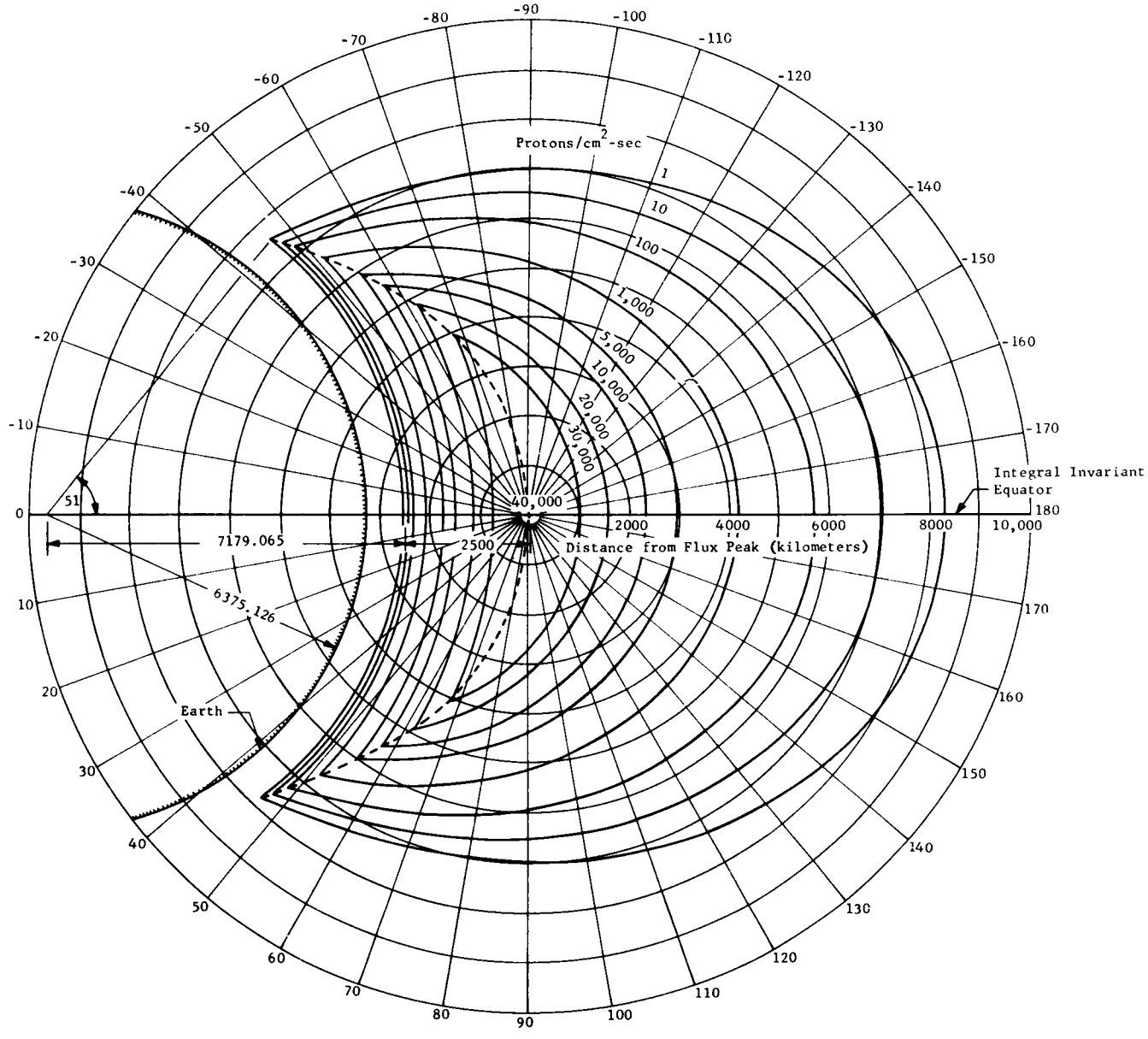

Fig. II-4 Proton Flux Contours Normal to the Plane of the Integral Invariant Equator

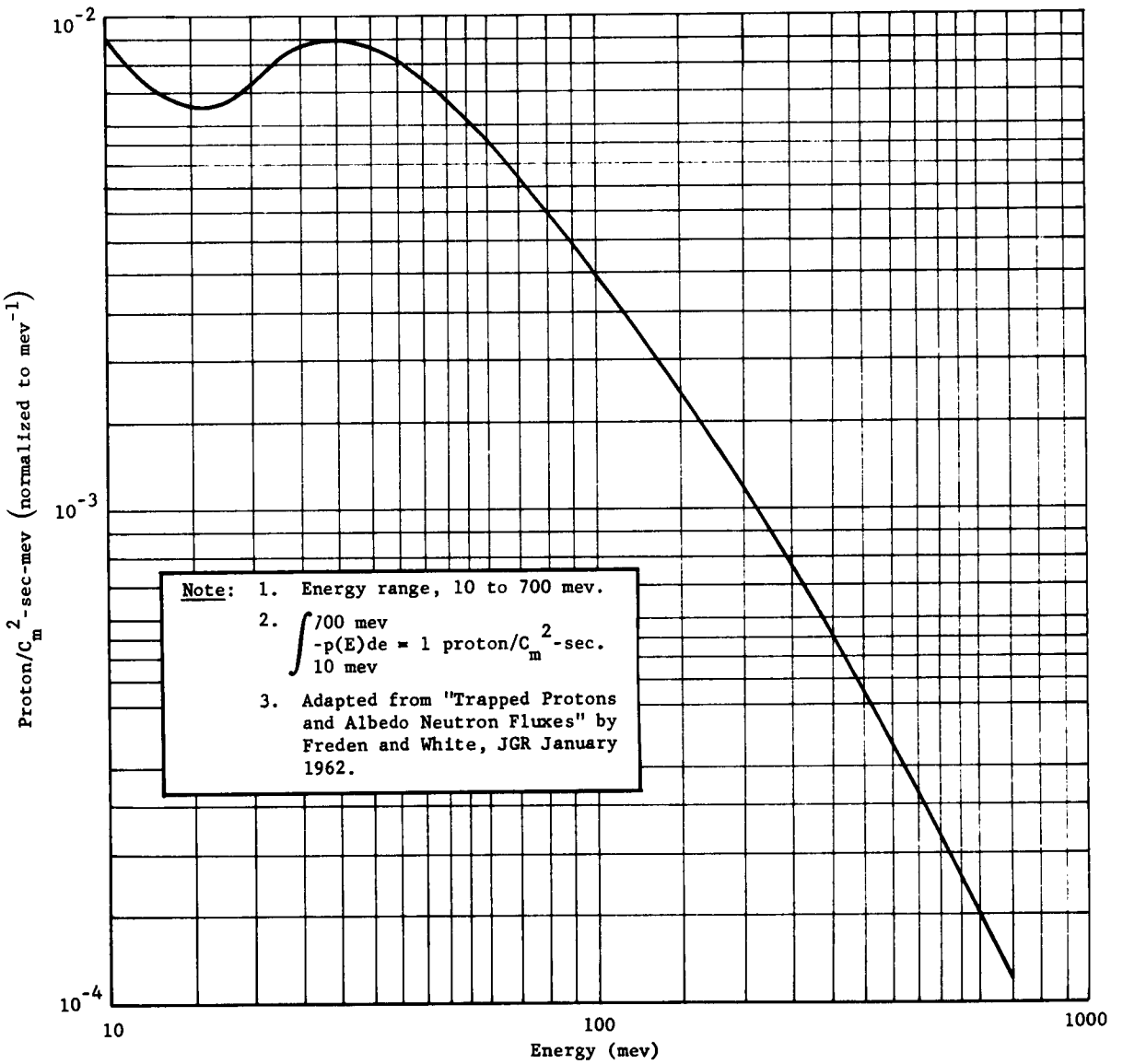

Fig. II-5 Incident Differential Kinetic Energy Spectrum for Unit Proton Flux in the Van Allen Belt

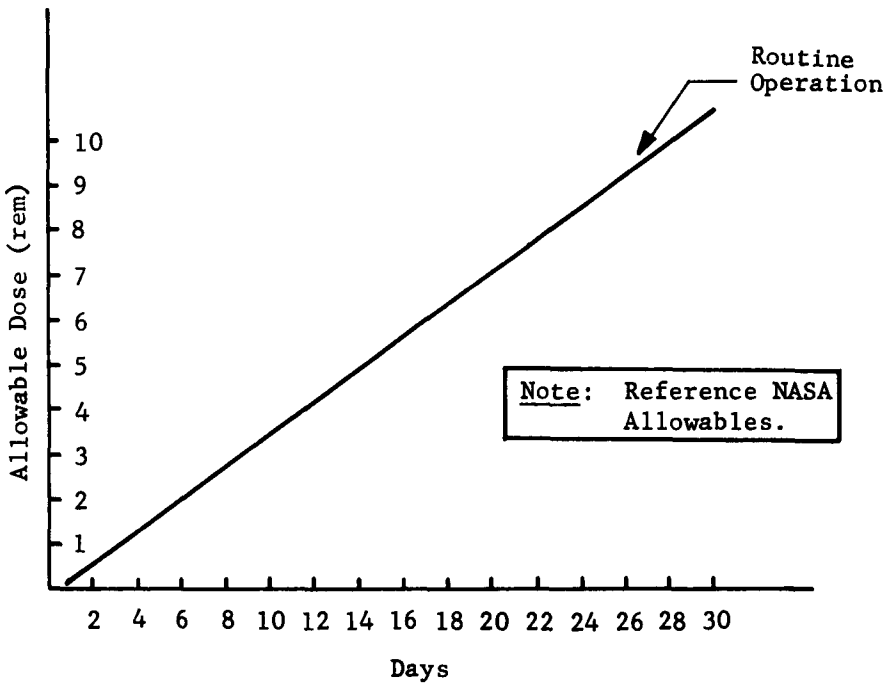

Fig. II-6 Limits of Absorbed Radiation - Crew Members

Table II-1 Space Radiation Design Criteria - Environment

Item	Criteria
Van Allen Protons Primary Secondary	Per Fig. II-5
Van Allen Electronics Primary Bremsstrahlung	Negligible (Relative to Van Allen Protons)
Cosmic Ray Protons	Negligible (Relative to Van Allen Protons)
Solar Flare Protons	0.00 (Orbit Is of Such Low Latitude and Altitude that Solar Flare Radiation Does Not Reach Vehicle)

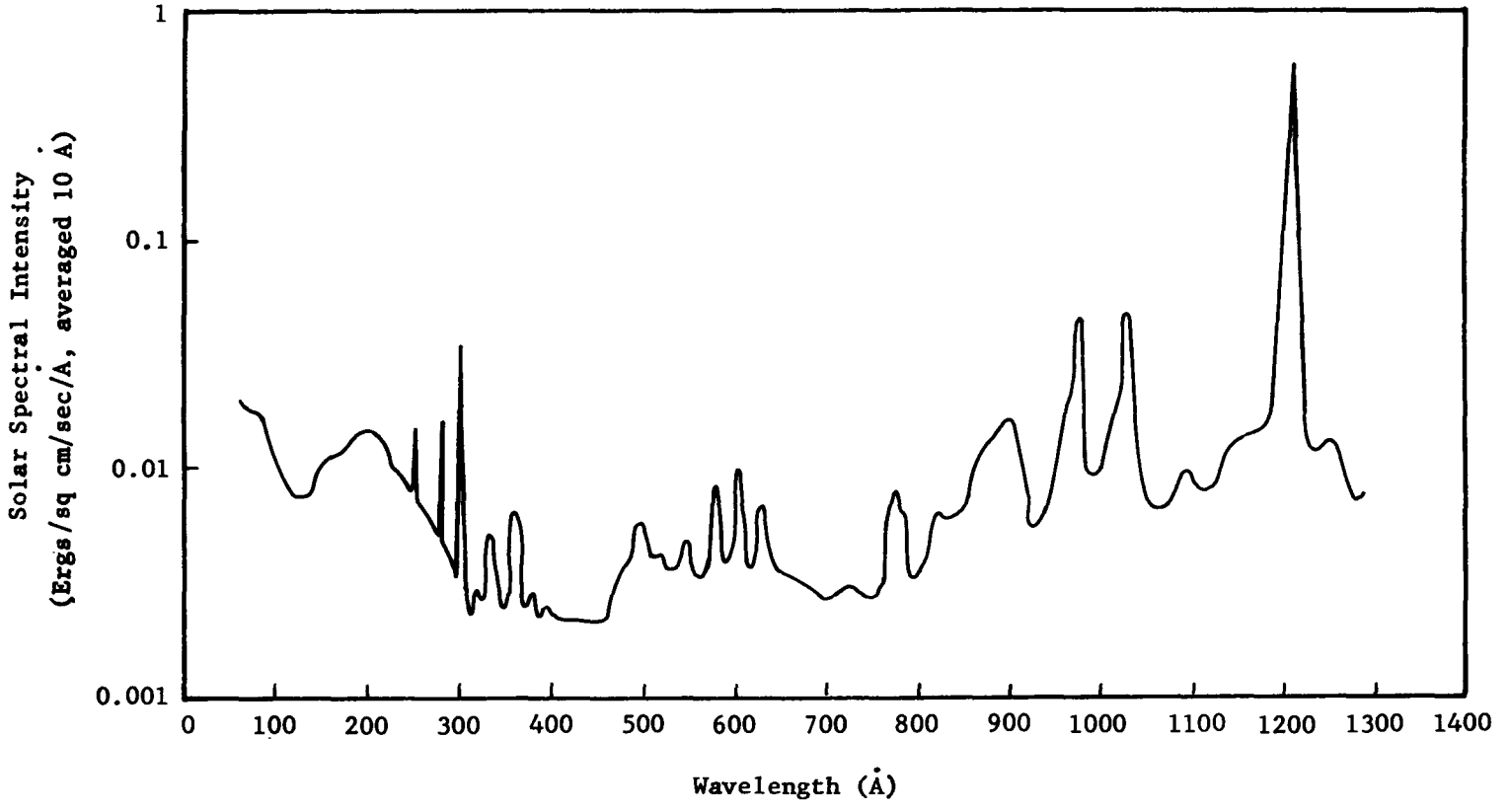

Fig. II-7 Electromagnetic Spectrum for Solar Radiation

B. VEHICLE DESCRIPTION

The Expandable Space Structure is a telescoping, semirigid vehicle (Fig. II-8 and II-9). It has a diameter of 8 ft and is 15 ft long when fully expanded. It has five telescoping interlocking sections, each approximately 30 in. long. The end closures are a flat bulkhead at the aft end and an elliptically-shaped dome at the forward end. A liner covers the interior wall of the cylindrical portion of the vehicle, and serves as a primary pressure seal after deployment.

Aluminum alloys are used throughout as construction material for the primary structure. Natural and synthetic rubbers are used for gaskets and pressure liners.

1. Interlocking Section Configuration

Each telescoping section (Fig. II-10) has double-wall construction with a total wall thickness of 0.75 in. The external skin on the aft telescoping section is 0.020 in. thick. It serves primarily as a thermal shield and meteoroid bumper. The panels are floating with respect to the primary structure. The batt-type insulation in the wall cavity is attached to the external skin panels. These panels are removable to allow access to primary structure.

The 0.020 thickness of the shield is typical for all sections, except for the outer telescoping section. There the external skin panels are exposed to aerodynamic environment, and, therefore, must be considerably thicker to withstand aerodynamic heating and pressures.

The inner skin of the vehicle wall is 0.040 in. thick. It is the primary structure for inertial loads, and, with the interlocking frames, reacts internal pressure loads. All joints and splices of the primary structure are pressure sealed.

At the forward and aft extremities of each telescoping section, machined frames interlock with the mating frames of the adjacent sections.

To prevent rotation of one section with respect to an adjacent section, torsional restraints have been incorporated in the form of a track and shoe arrangement along the longitudinal axis.

Structure Expanded

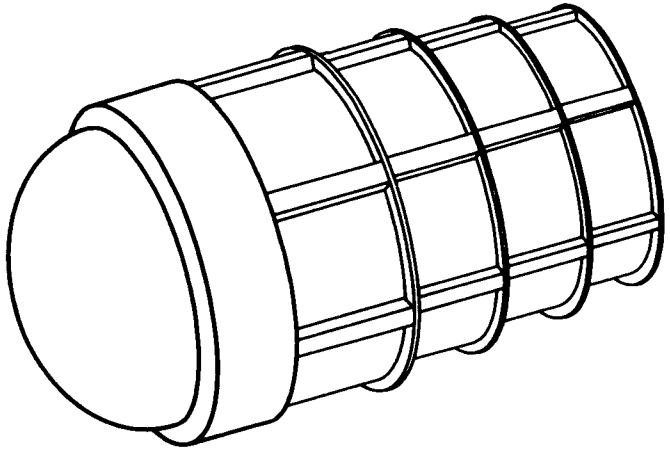

Structure Contracted

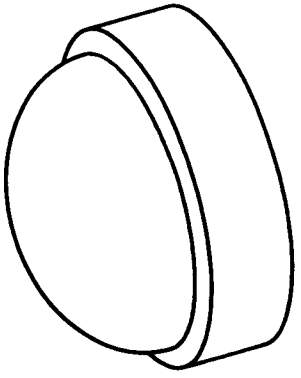

Fig. II-8 ESS External View

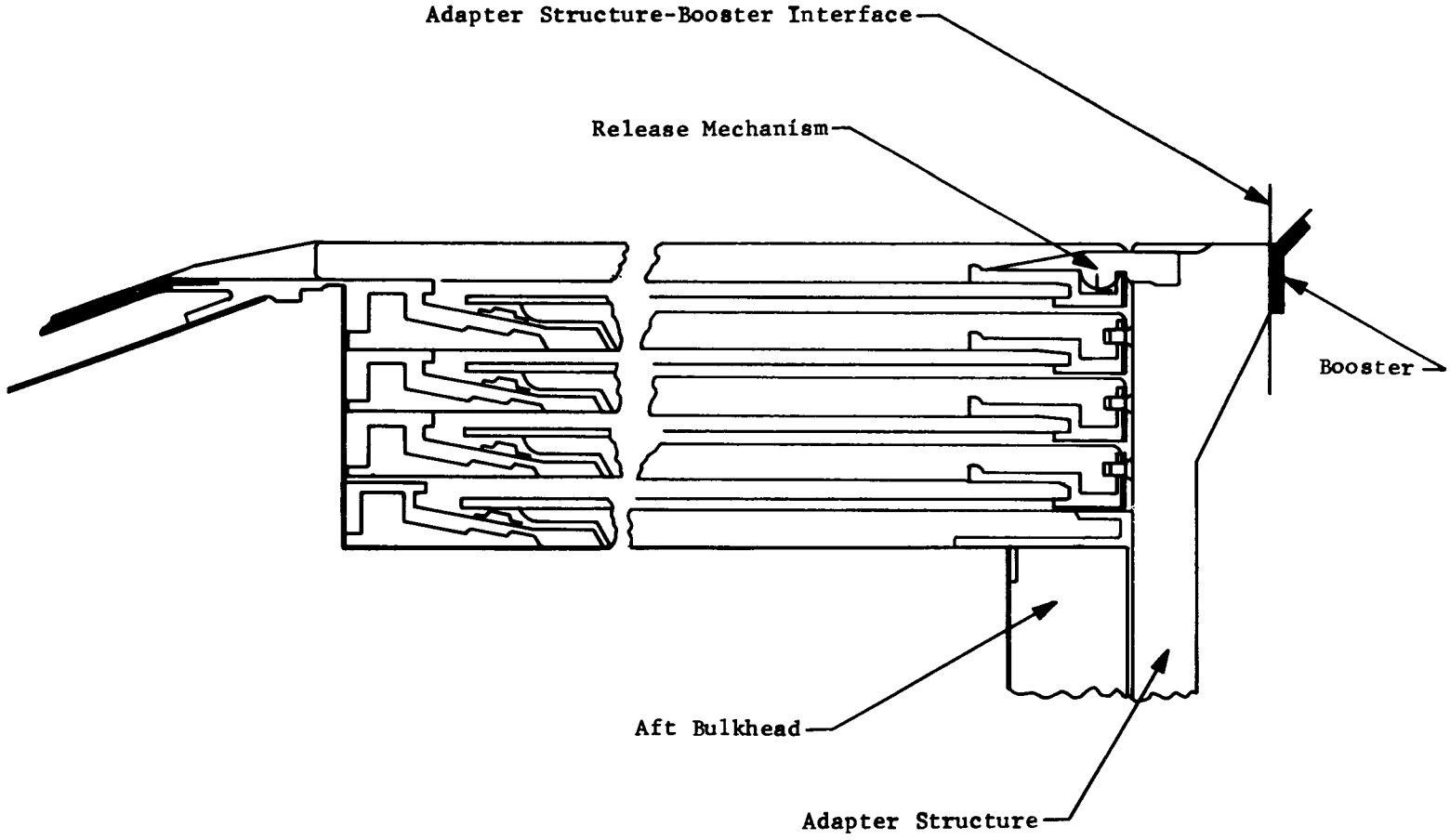

Fig. II-9 Longitudinal Section (Structure Contracted)

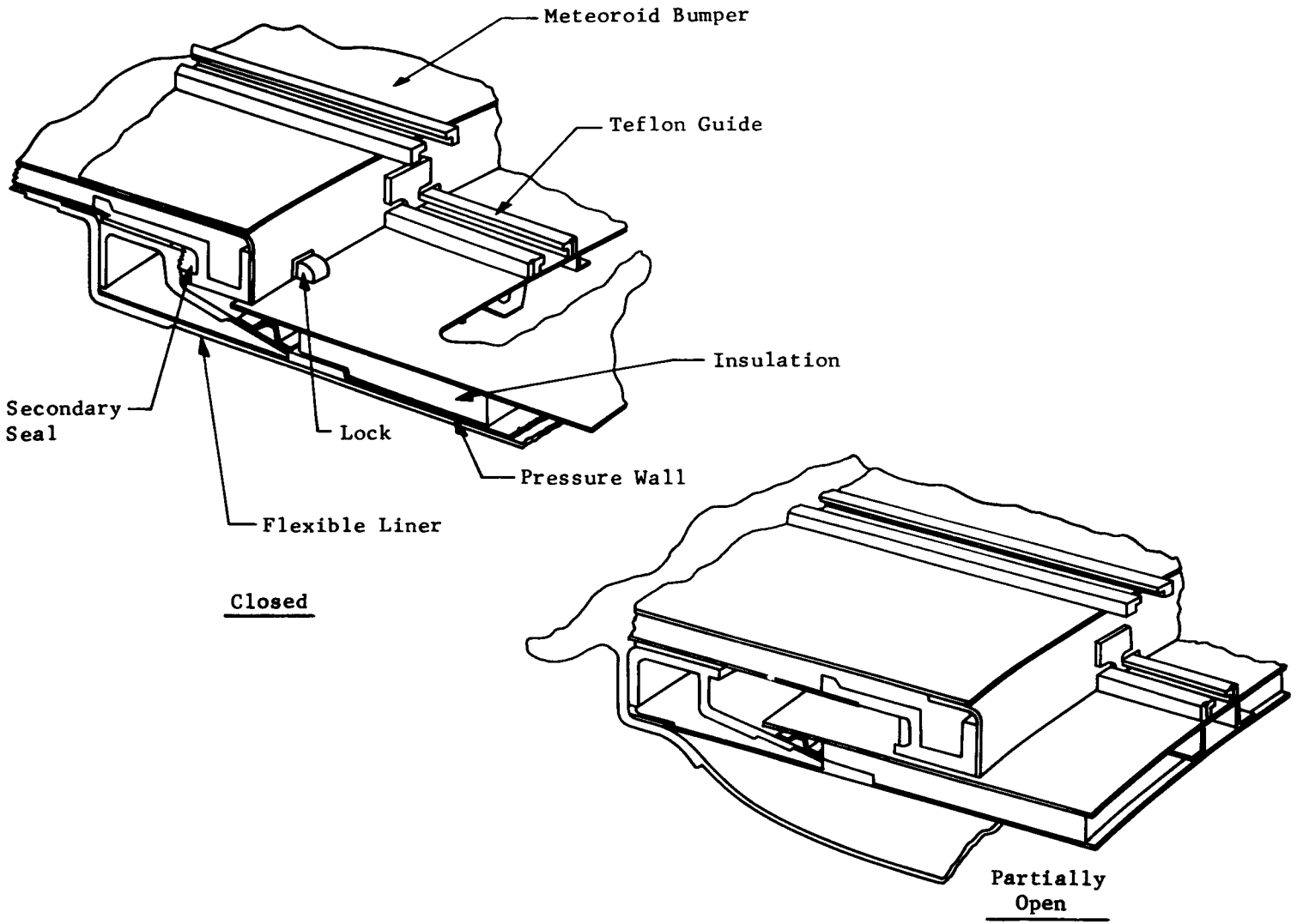

Fig. II-10 Typical Joint

2. End Closure Configuration

The end closures of the vehicle consist of an elliptical dome at the forward end and a flat bulkhead at the aft end.

The aft bulkhead is a honeycomb panel with aluminum skins and core. The total thickness of this panel is approximately 3 in. with 0.040-in. faces. This panel can be used as a closure of an operational vehicle with minor modifications.

The dome at the forward end is single-wall construction, and does not represent the type of construction that will be used in a space environment. Since the aft bulkhead design represents a typical closure for this environment, a salvaged tank dome from a Titan vehicle has been proposed as a cost saving measure. If a future operational vehicle will require a closure that is shaped similar to the dome used, the double-wall construction can easily be adapted.

3. Vehicle Sealing

The vehicle design includes primary and secondary sealing systems to provide compartment sealing after deployment of the structure.

The primary sealing is obtained from a reinforced rubber bladder that covers the entire cylindrical portion of the vehicle.

The secondary compartment sealing is provided by the sealed structure. All joints and splices of the inboard skin panels are sealed, and gaskets are used at the interlocking joints.

4. Operation

When the expandable structure is attached to the launch vehicle, the telescoping sections are locked in a retracted position by an interlock arrangement.

Positive venting is provided for areas of the vehicle that require venting during the boost phase.

The deployment of the structure is accomplished by internal pressurization. Tests performed on an operable mockup have indicated that a very small pressure differential will be required to deploy the vehicle. Once the structure is fully deployed, the internal pressure is increased to operating pressure (11 psi), providing high loads between the interlocking frames. The design incorporates a device that automatically locks the vehicle in the deployed configuration.

C. CONFIGURATION DESIGN STUDIES

Configuration design studies described here include expansion ratio, walls of telescoping sections, end closures, interlocking frames, bladder installation, packaging and ease of ground handling, extension and contraction locks, and internal thermal control.

1. Expansion Ratio

Study results of the effects of various factors on the expansion ratio of the expandable vehicle are presented here. The expansion ratio of an expandable structure is the ratio of the total internal volume of the expanded configuration to the total internal volume of the contracted configuration. In telescoping-type expandable structures, parameters affecting expansion ratio, as defined, are as follows (Fig. II-11):

1) Number of telescoping sections, N;

2) Volumes enclosed by end structure (domes), V_D;

3) Overlap of sections at joints in the extended position, j;

4) Differences in radii of telescoping sections, Δr;

5) Differences in lengths of telescoping sections, $\Delta \ell$.

Figure II-11 reveals that a fixed volume enclosed by a dome significantly affects expansion ratio. This effect is illustrated in Fig. II-12, where values of Δr, $\Delta \ell$, and j are held constant, and expansion ratios are plotted for various values of V_D and N. Data points are given for spherical and ellipsoidal domes to illustrate that as dome volume enclosure efficiency increases, expansion ratio decreases.

Figure II-12 shows that the effect of fixed-end dome volume on expansion ratio becomes less severe as the ratio of the expanded length to the contracted length increases. It also illustrates that maximum expansion ratios can be obtained when end closures are flat bulkheads with zero volumes, since they minimize internal volumes of contracted configurations. Further, the achievement of certain expansion ratios is impossible when fixed-dome volumes are large relative to total internal volume.

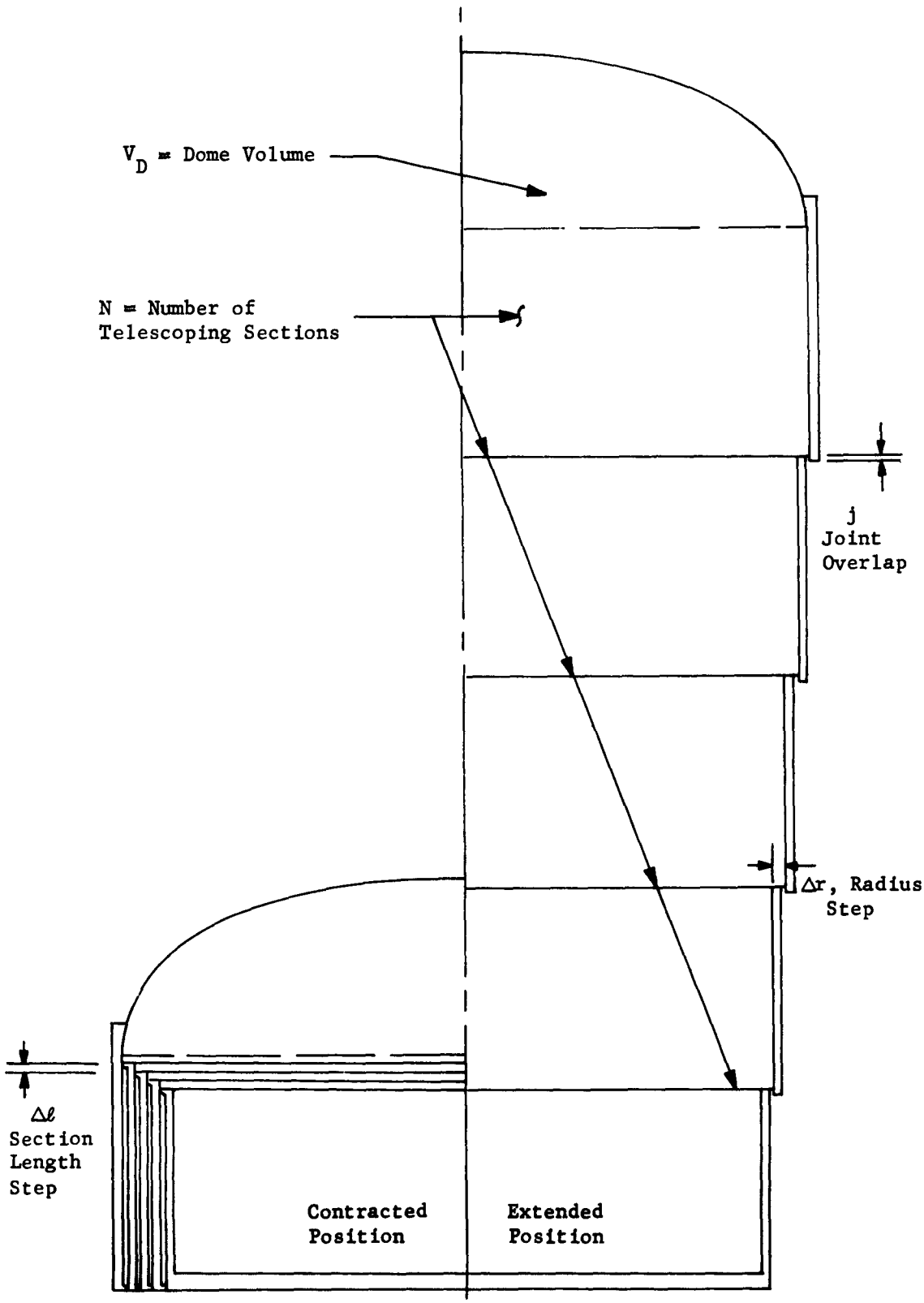

Fig. II-11 Expansion Ratio Variables

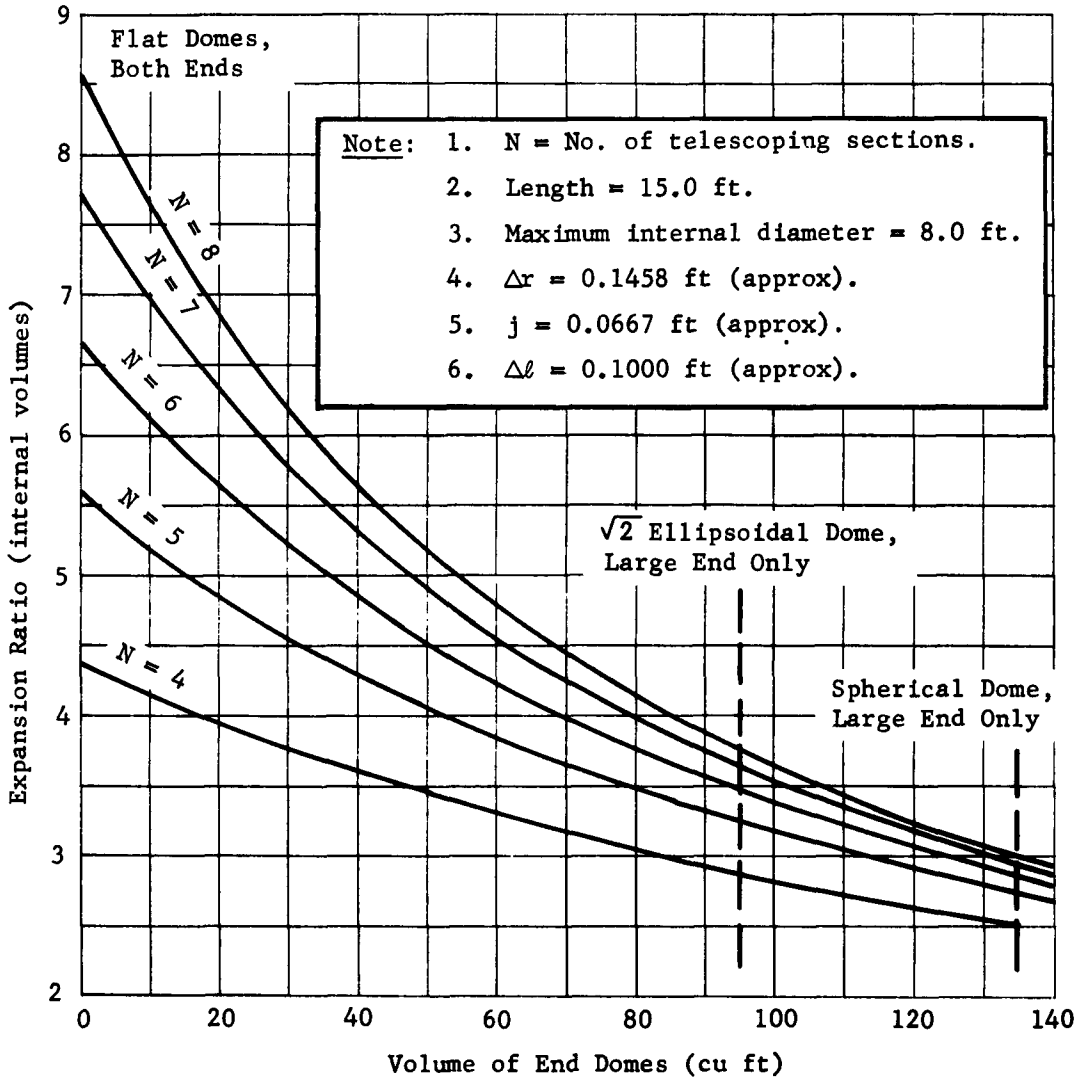

Fig. II-12 Expansion Ratio Versus Dome Volume

Figure II-13 illustrates the relative effects on expansion ratio of the parameters Δr, $\Delta \ell$, and j when end closures are flat bulkheads.

The validity of considering fixed-end volumes as a variable factor in determining expansion ratio depends on mission requirements. For example, an expandable structure placed atop a booster as the total payload must be equipped with a nose fairing. This fairing, enclosing a fixed volume, constitutes a large part of the total contracted volume of the boost phase configuration. In this case, the nose fairing volume could be filled or replaced with a fixed-end closure on the forward end of the expandable structure. Maximum use could be made of payload volume, enhancing the value of the expandable structure vehicle by increasing available volume for storing supplies and equipment. In this case, the forward-end closure volume should not be considered in computing expansion ratio of the structure.

The vehicle to be designed and built under this contract is one requiring a capability of manned occupancy for 5 to 30 days. This would require packaging of substantial amounts of supplies and equipment inside the vehicle. The entire fixed volume of the forward-end closure is considered logical space for packaging a portion of supplies and equipment, and should not be considered in expansion ratio determination. On this basis, the expansion ratio of the Expandable Space Structure is 5.88:1. If the volume of the fixed-end closure were included in expansion ratio determination, the value would be 3.34:1. Volumes used for these determinations are those shown in Fig. II-14.

2. Walls of Telescoping Sections

The double-wall construction chosen for the cylindrical telescoping sections evolved from studies conducted under this contract, and from past space cabin design studies by Martin-Denver.

The design studies were aimed at providing a wall design of minimum weight with good thermal qualities that would also provide maximum protection from meteoroid penetration.

Thermal Considerations - A wall construction of high thermal efficiency has been achieved through careful detail design of the wall. Special care has been taken to eliminate thermal leaks between the outside floating panels and the inner load-carrying skin. The members connecting the panels are of fiberglas construction where needed to reduce thermal conduction. The batt-type insulation, which partially fills the cavity between the wall panels, also aids in maintaining an acceptable thermal environment of the cabin.

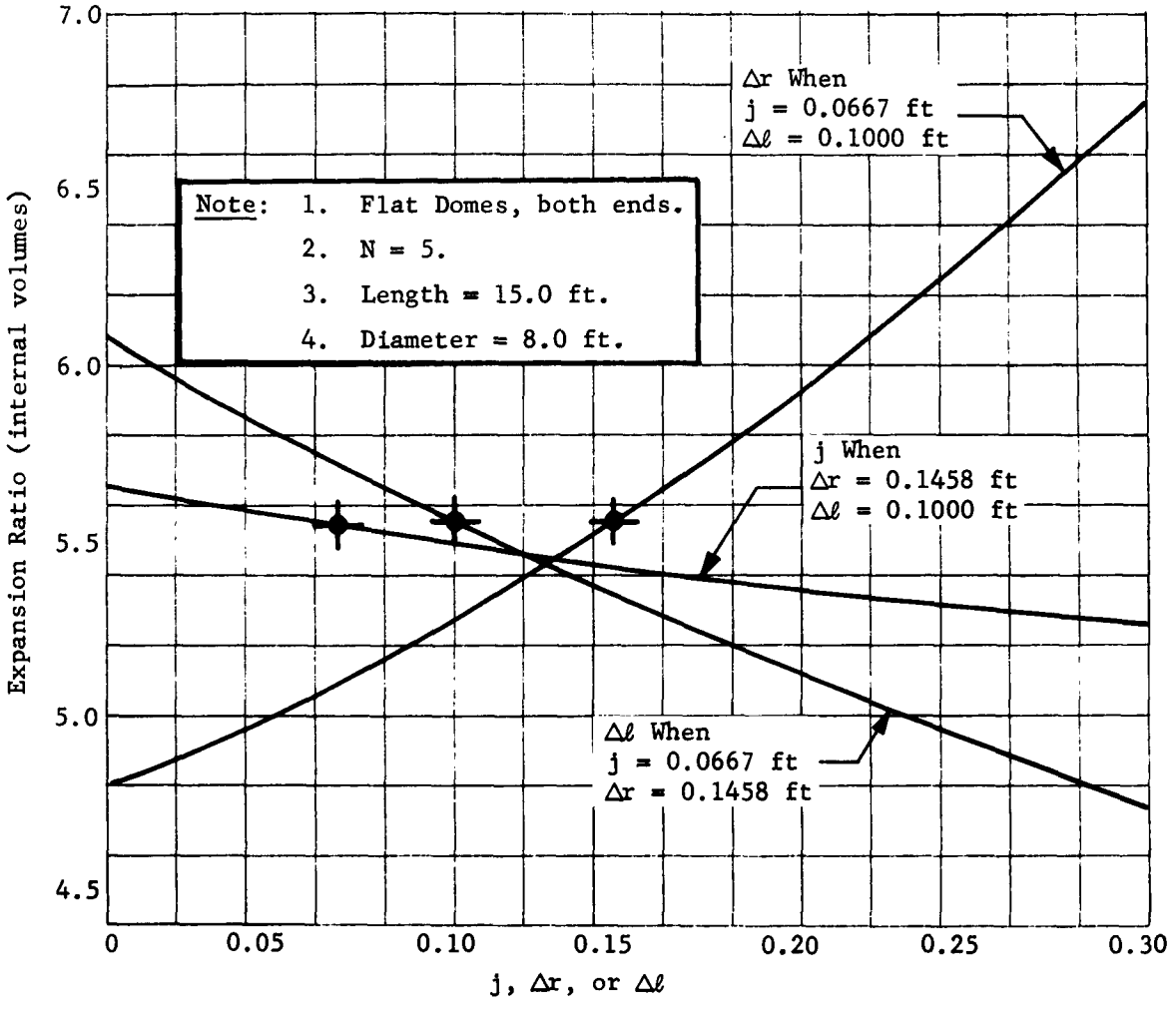

Fig. II-13 Expansion Ratio Versus Joint Overlap, Radius Step, and Section Length Step

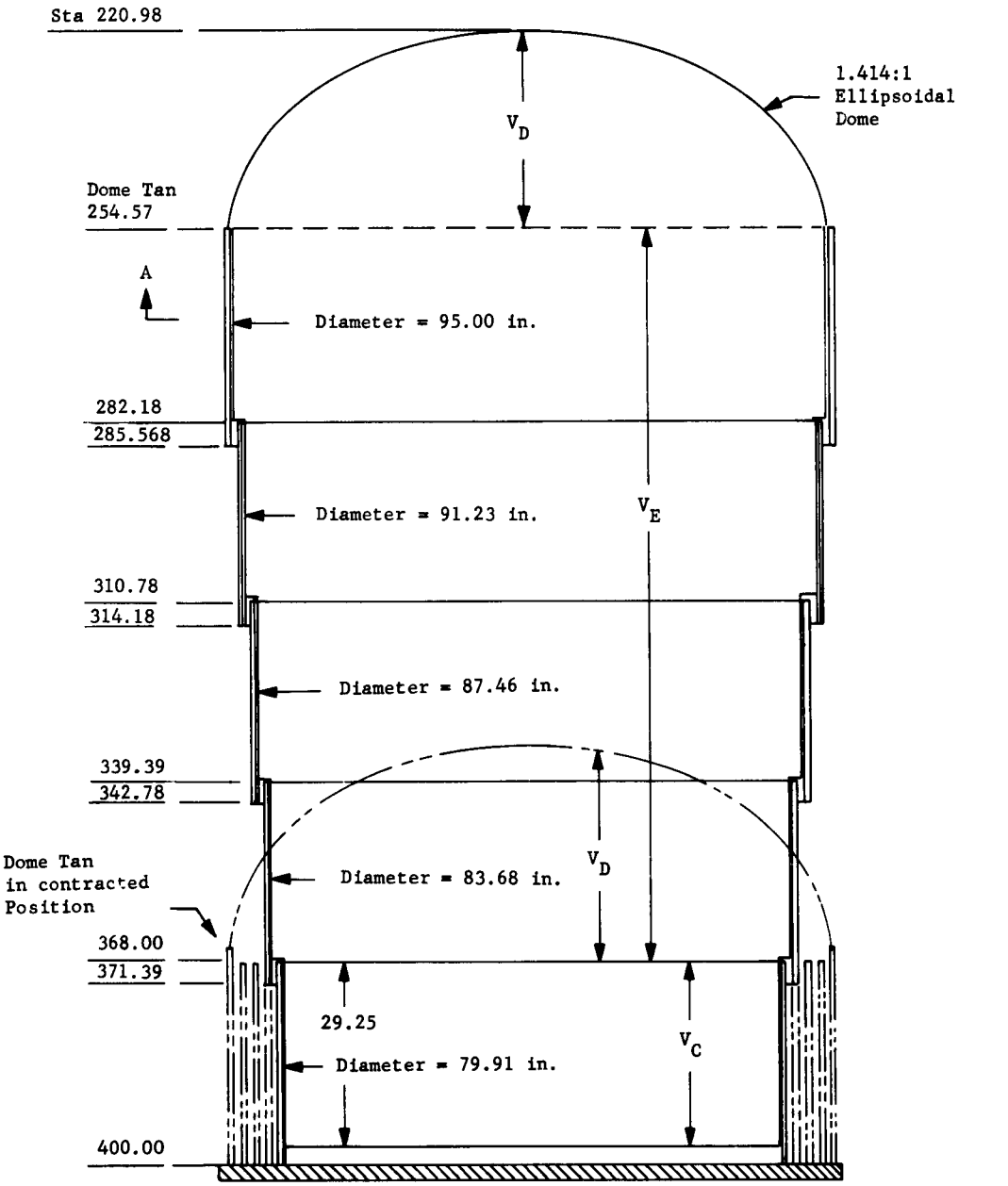

Legend:

V_E, Volume in Expanded Position

V_C, Volume in Contracted Position

V_D, Fixed Volume End Closure

Note:

1. V_E = 853,300 cu in.
2. V_C = 145,500 cu in.
3. V_D = 158,000 cu in.
4. V_E V_C = 5.88.
5. $V_E + V_D/V_C + V_D$ = 3.34.

Fig. II-14 Longitudinal Section of Vehicle

Meteoroid Considerations - The double-wall construction is highly efficient from a weight standpoint to provide adequate meteoroid penetration protection. The double wall weighs one-third as much as a single wall for the same level of meteoroid protection.

Figure II-15 presents probability curves on which the total skin thickness of 0.060 in. of the double wall is based. The figure shows that for the most severe case, the 30-day mission, a probability of 0.772 exists that no puncture of the wall will occur, and a probability of 0.971 that not more than one will occur.

The zero puncture curves indicate the cost in weight of obtaining high probabilities of no punctures. The 30-day mission curve, showing probabilities of one puncture, exhibits a distinct knee in the vicinity of t = 0.06 in., indicating that selection of thicker walls would increase meteoroid protection only slightly.

If the crew can survive a meteoroid puncture without serious hardship, as seems reasonable in a vehicle with near-normal earth surface atmosphere, the puncture could be sealed by the crew. On this basis, the 0.06-in. wall thickness is a reasonable compromise between safety and weight.

The type of double-wall construction chosen for the vehicle, compared with sandwich-type construction, is considered to be superior because of its inherent structural design simplicity, improved thermal control through minimizing conduction load paths, fabrication simplicity, handling simplicity, lower cost, structural reliability through visual access to all surfaces of primary structure, superior environmental control design flexibility relating to radiator panels, and maintainability.

3. End Closures

Forward Dome - The major consideration in selecting an ellipsoidal dome for the forward end closure is cost reduction. A substantial cost saving to the program was possible because of the availability in scrap inventory of an existing dome that would provide pressure continuity. The type of end-closure design does not affect the telescoping action of the sliding sections, and does not affect the deployment in a thermal environment during functional testing. Since it is desirable to evaluate heat balance characteristics of the telescoping sections in the absence of heat inputs to end closures, the forward dome will be isolated from the thermal flux by test facility shielding.

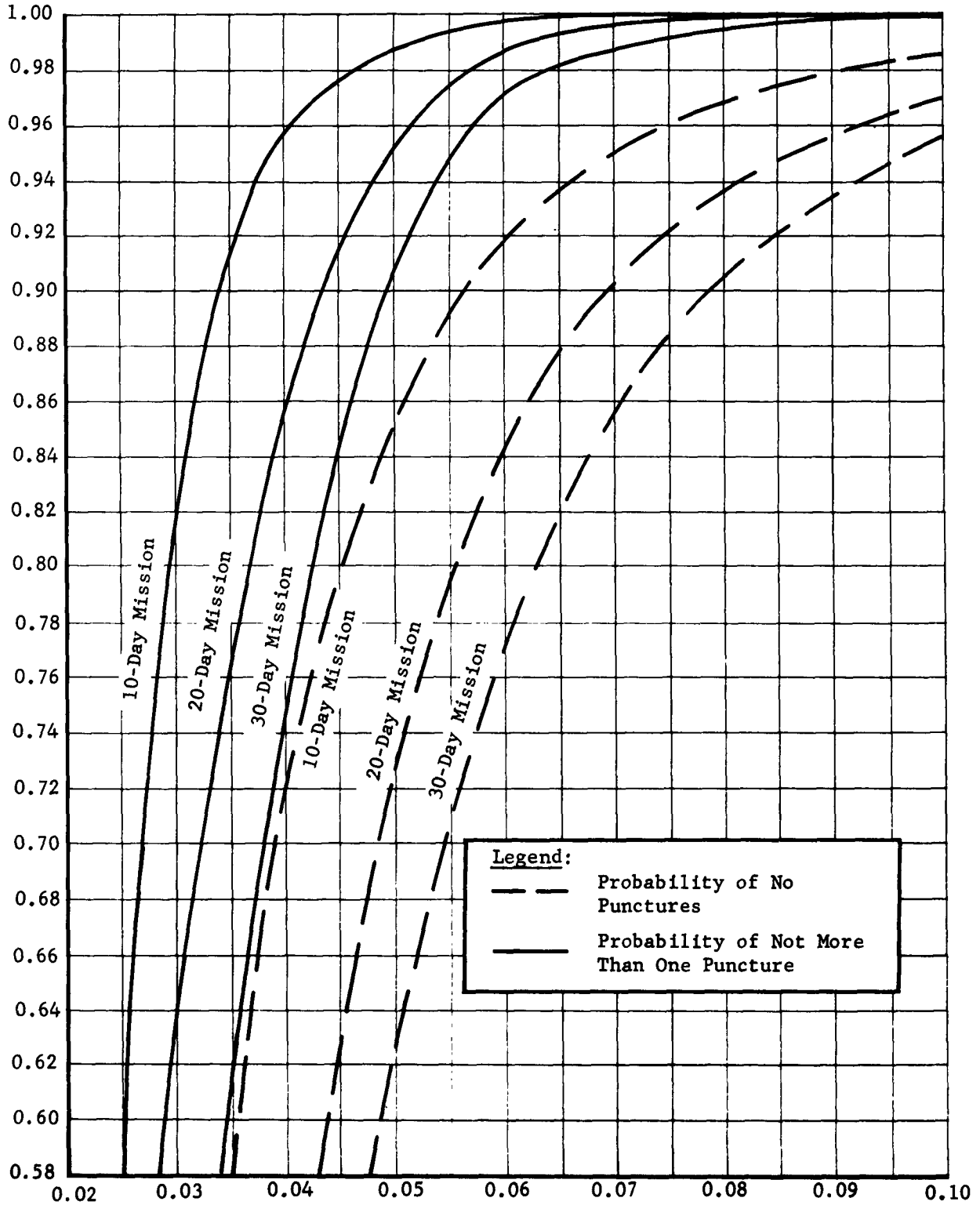

Fig. II-15 Meteoroid Puncture Risk Versus Double-Wall Thickness of Aluminum

Aft Closure - A flat bulkhead representative of a flight vehicle has been selected for the aft closure. Three primary considerations influenced this choice. First, a flat closure is considered to be fundamental shape for certain mission applications of a telescoping expandable vehicle. Second, a flat closure minimizes the overall length of the booster-payload vehicles. Third, the aft bulkhead has a greater influence on sliding clearances than the forward bulkhead.

Subjecting the bulkhead directly to thermal flux during Phase III testing would not further the objectives of this program. On this basis, room temperature curing, adhesive-bonded sandwich construction with aluminum honeycomb core and aluminum face sheets was chosen for the bulkhead. The core and face sheets will permit venting of the bulkhead structure to ambient. The chosen design was evaluated on the basis of weight and cost against the following configurations:

1) Flat membrane with peripheral frame;

2) Flat membrane skin with beam-type backup structure (wagon wheel);

3) Adhesive bonded sandwich with balsa wood core and aluminum face sheets;

4) Adhesive bonded sandwich of fiberglas honeycomb core and aluminum face sheets;

5) Adhesive bonded sandwich of paper honeycomb core and aluminum face sheets.

4. Interlocking Frames - Telescoping Section

An overlapping or interlocking frame configuration at section joints for structural continuity in the expanded position is dictated by the nature of the telescoping action. On this premise, candidate frame configurations were conceived and evaluated to obtain an optimum configuration.

The following factors were considered when the various frame configurations were evaluated:

1) Weight;

2) Deployment performance reliability;

3) Adaptability to promising gasket seal configurations;

4) Adaptability to conventional structural sealing methods;

5) Ease of fabrication;

6) Susceptibility to heat transfer by conduction;

7) Suitability for installation of thermal control radiator and bladder systems;

8) Tolerance control during deployment;

9) Simplicity of design;

10) Strength considerations, strength analysis;

11) Cost.

Study configurations that were eventually discarded in favor of more promising ones are shown in Fig. II-16 thru II-21. Figure II-21 shows the interlocking frame configurations that are considered to be optimum, and are the configurations that have been chosen.

Based on unfavorable results from tolerance control tests of rolled and welded segmented rings subsequently machined (Sec VI), and on the basis of results of cost studies, the frames will be machined from roll-forged one-piece rings.

The ring rolled forgings will be stress-relieved before machining to minimize distortions in the finished frames.

To control the alignment of one frame inside the other, and thereby achieve control of frame action during deployment, a circumferential teflon positioning strip is installed on the inner frame, and guide shoes spaced at intervals around the circumference are attached to the base of the outer frame. These components will position one frame with respect to the other as the frames approach the interlocking position. The guide shoes will exert forces to position the outer frame inboard, and thereby control alignment by controlling relative sag of the inboard frame relative to the outboard frame. The circumferential teflon strip on the inboard frame and the ramp on the outboard frame leg will force the frames into assuming similar conditions of roundness before gasket surface contact.

Tolerance control of plus or minus 0.005 in. will be maintained on the metal-to-metal station plane contact surfaces so uniform monocoque load paths for longitudinal loads will exist. Eccentric loads at the joints will be transferred between the pressure skins by a diagonal leg integrally machined in the inboard frame.

Tolerance studies indicate that maintaining adequate gasket depression will be no problem. Complete sealing can be achieved with gasket depression of 0.02 in.

5. Bladder Installation

Bladder installation design studies were based on the following requirements:

1) Vehicle bladder shall provide complete sealing of the telescoping portion of the structure under limit and ultimate pressures;

2) Bladder shall be attached to the structure at each interlocking frame joint so it will fold and unfold as individual panels;

3) The creation of potential leak points in installing the bladder shall be minimized;

4) The restriction of natural folding tendencies shall be minimized;

5) Edges and corners of structure that would tend to chafe or tear the bladder material shall be eliminated by the addition of anti-chafe devices;

6) Use of sealants that would tend to bond the bladder to the structure shall be minimized.

Using these requirements as criteria, the bladder installation design will provide for the bladder to attach to the inboard frame of each interlocking joint with devices that do not penetrate the bladder wall. Radiator panel bulkhead fittings that must penetrate the bladder will be installed as shown in Fig. II-22. The bladder makes use of the bladder material itself, eliminating need for additional gaskets.

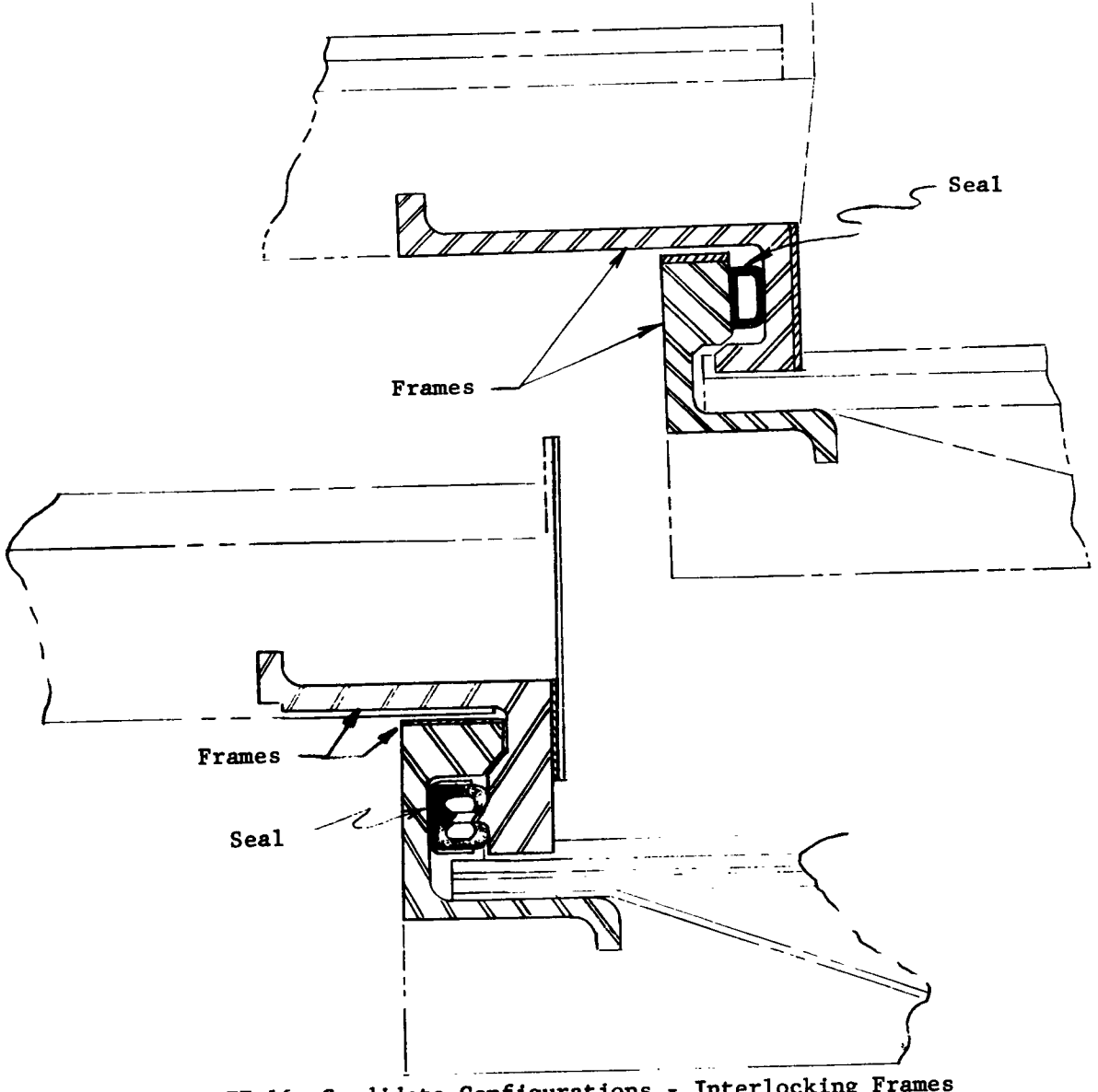

Fig. II-16 Candidate Configurations - Interlocking Frames

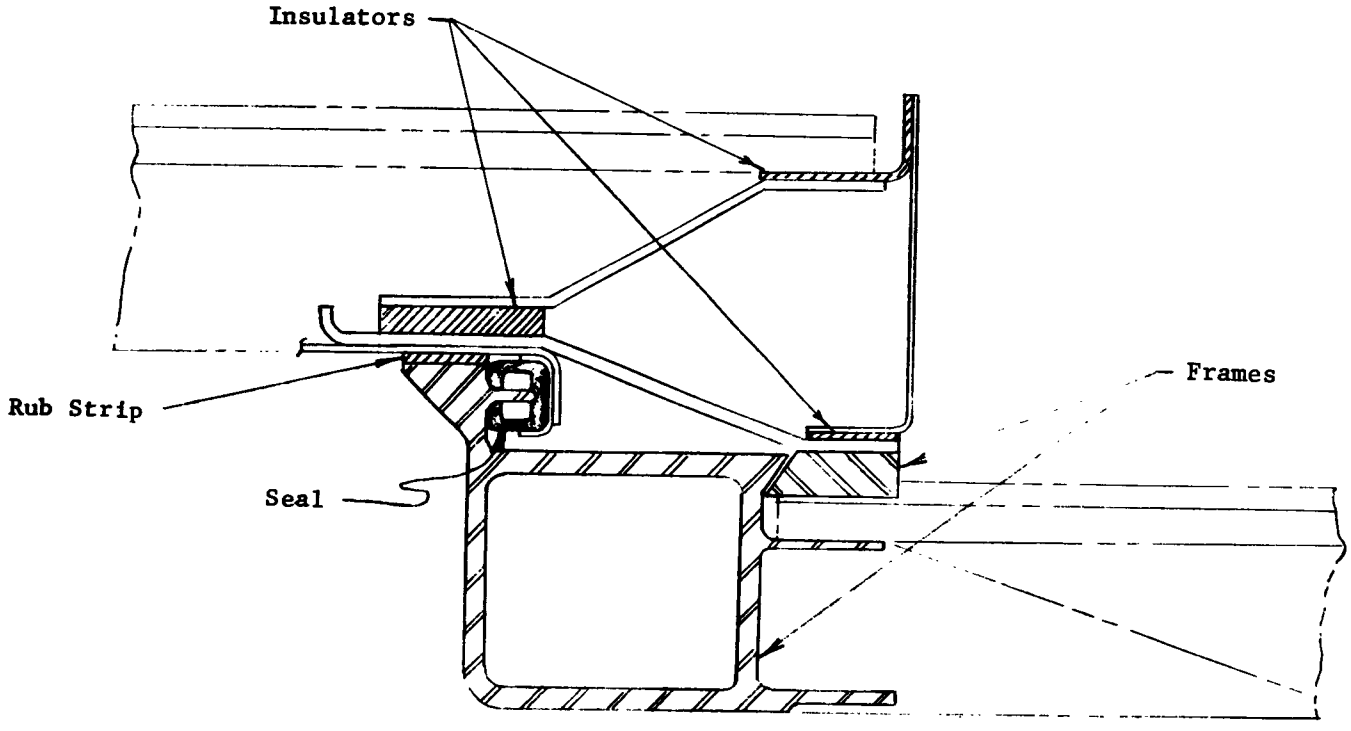

Fig. II-17 Candidate Configuration - Interlocking Frames

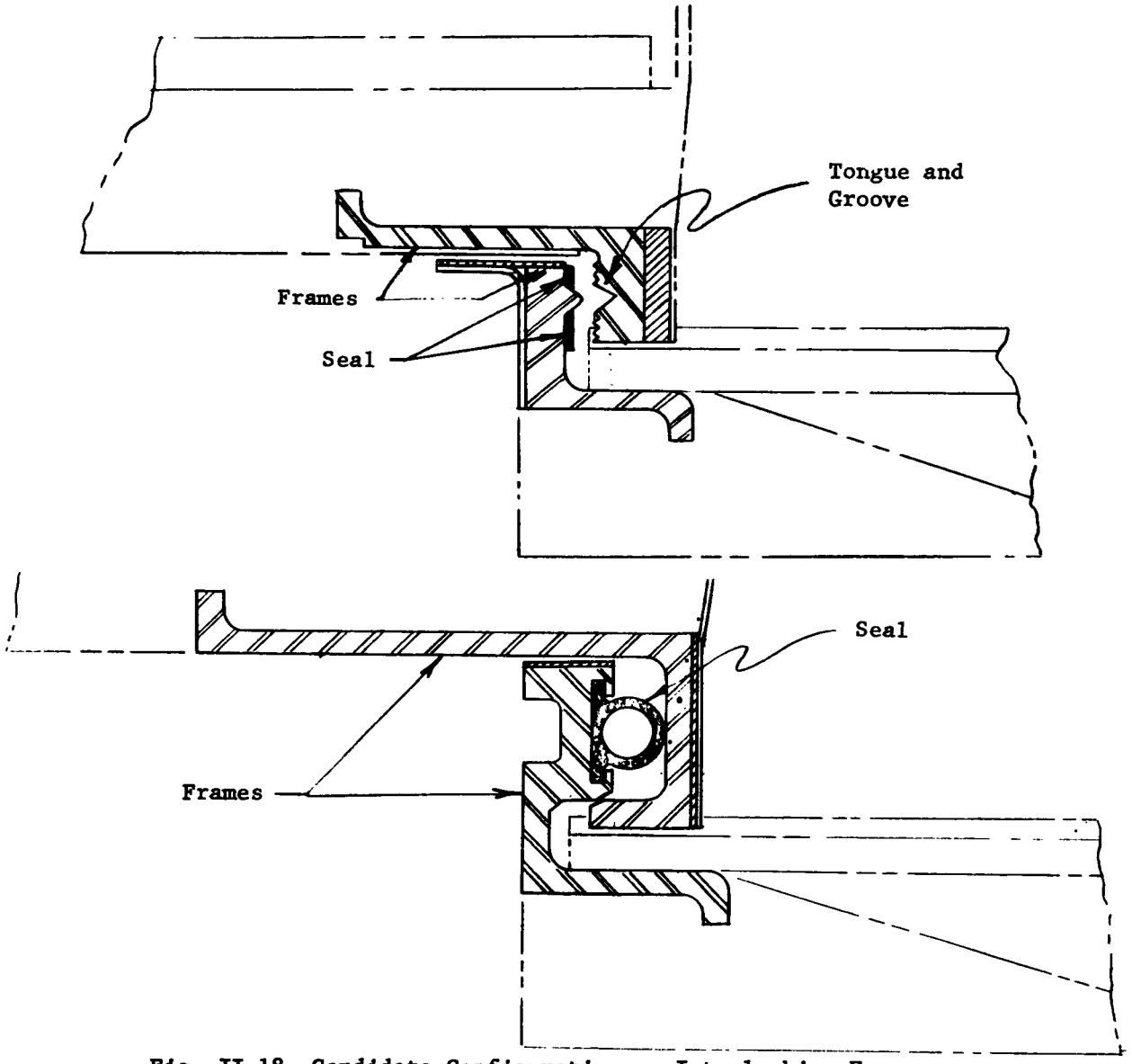

Fig. II-18 Candidate Configurations - Interlocking Frames

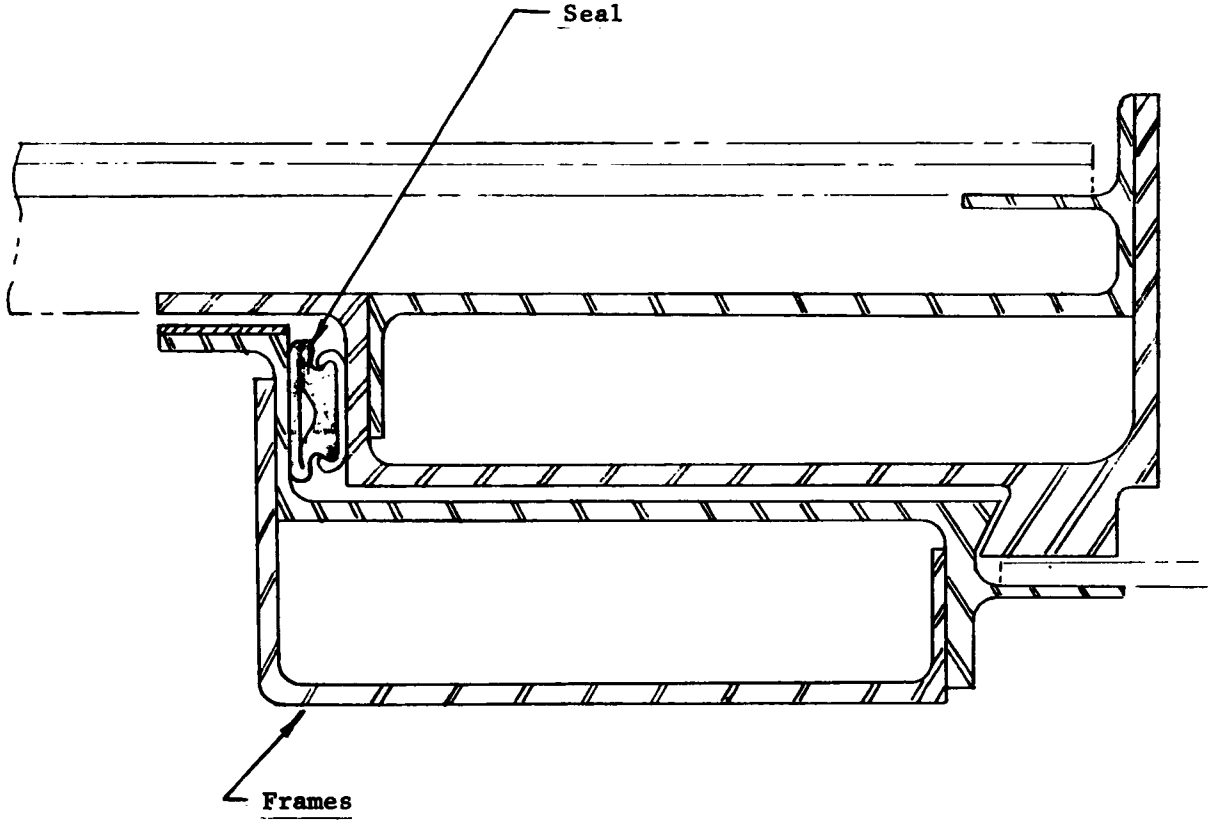

Fig. II-19 Candidate Configuration - Interlocking Frames

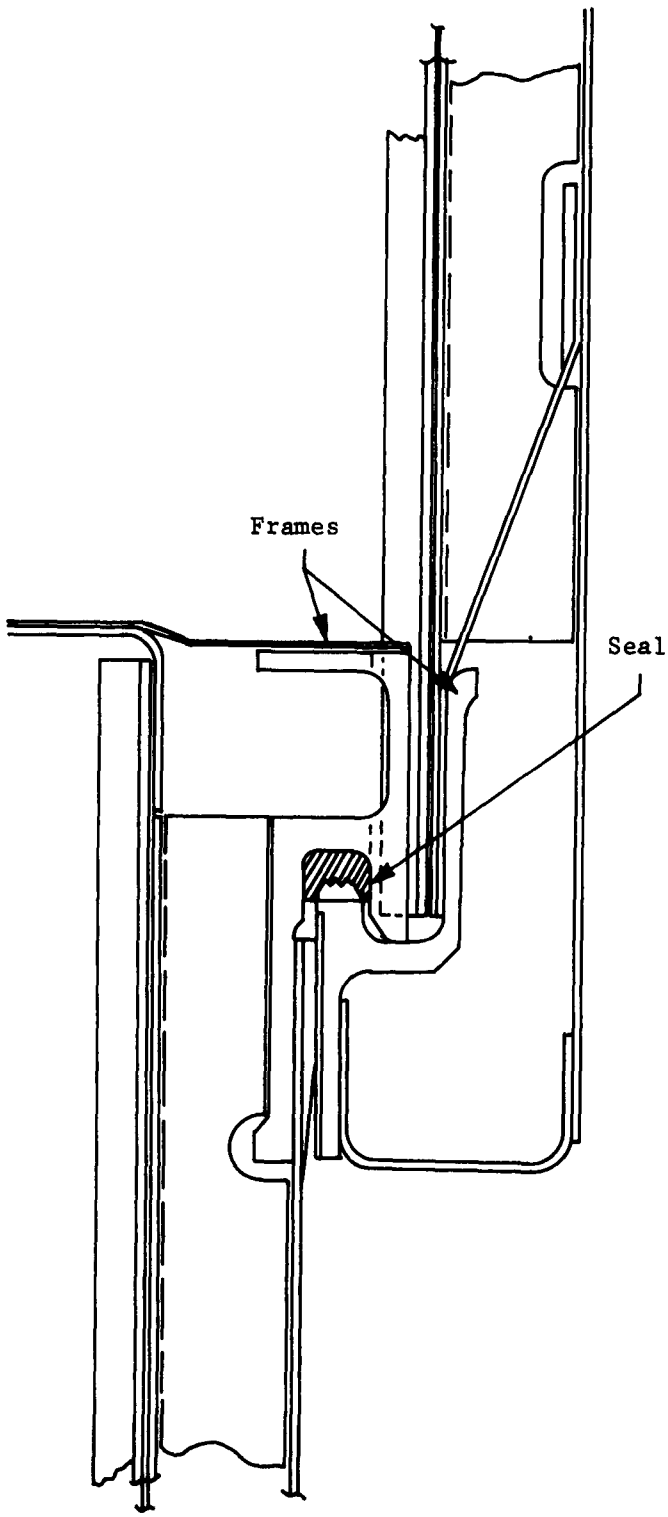

Fig. II-20 Candidate Configuration - Interlocking Frames

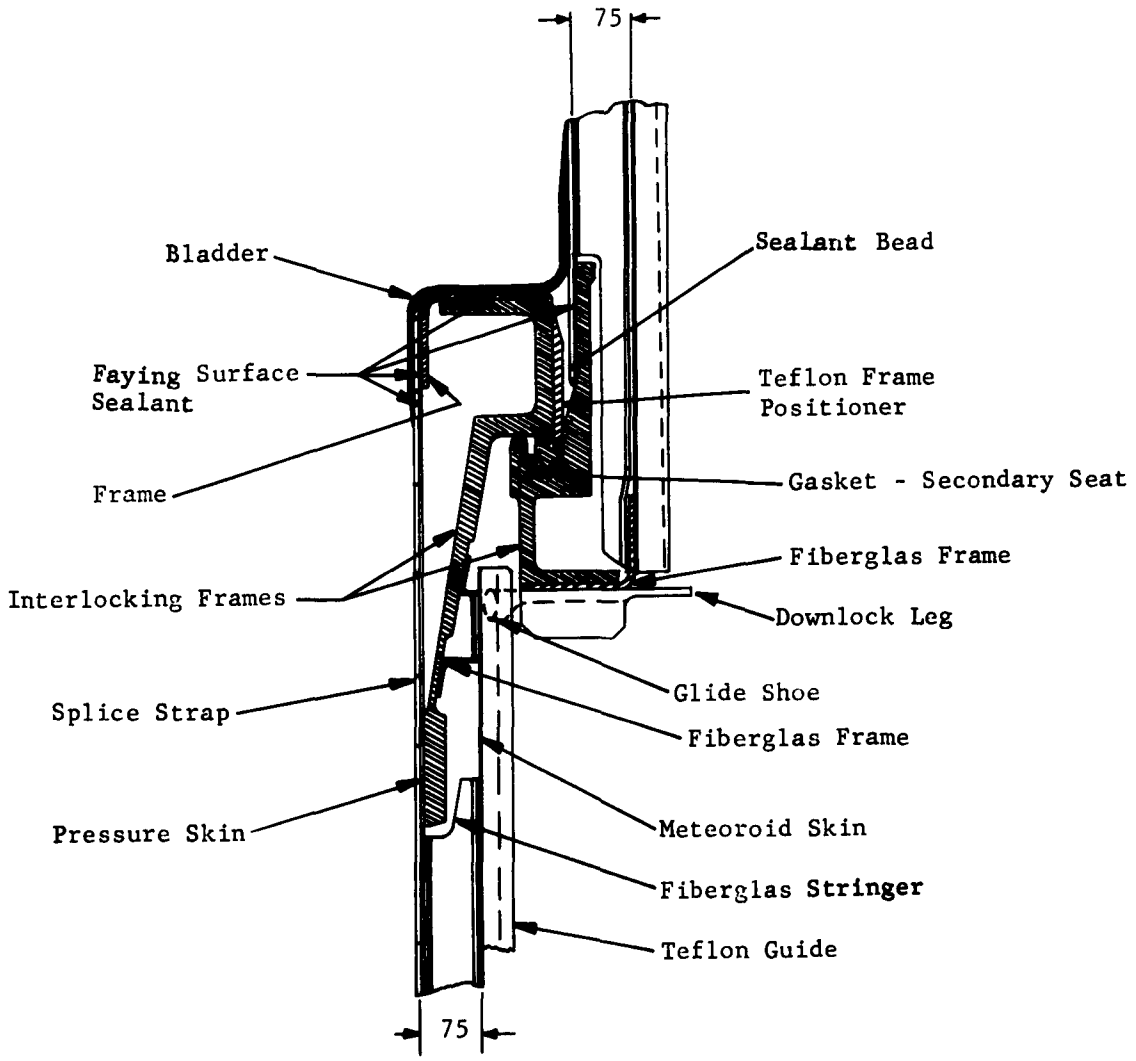

Fig. II-21 Interlocking Frames Configuration - Expandable Space Structure Vehicle

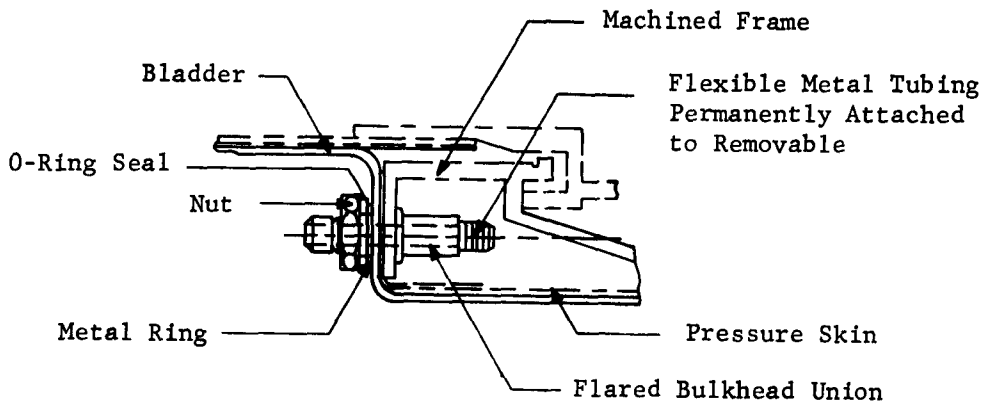

Fig. II-22 Radiator Bulkhead Fitting Installation

6. Insulation Installation

Various methods of installing insulation in the cavity walls of the telescoping sections were considered. Each allowed a gap to exist in the cavity between the insulation and one adjacent wall. These were:

1) Batts retained by straps on the outboard surface of the inner pressure wall;

2) Batts retained by stud pins and clips attached to the outboard surface of the inner pressure wall;

3) Batts retained by mechanical devices on the inboard surface of the external skins;

4) Batts retained by adhesive bonding to the inboard surface of the external skins.

The chosen design is the adhesive bonding of batts to the inboard surfaces of the external skins. Adhesives used are being tested to verify performance in the orbital environment. Relative thermal growth between the external skin and the insulation will be allowed by strip bonding.

Since the insulation system efficiency is affected insignificantly by whether the gap exists on the outboard or inboard side of the insulation, the insulation is installed on the outer skin, leaving the gap between insulation and the inner skin. The chief advantage of this is to permit access to the inner skin and other primary structure by the concurrent removal of the external skin panel-insulation assemblies.

7. Packaging and Ease of Ground Handling

To facilitate handling and testing of the vehicle, an adapter ring structure attached to the base of the vehicle has been studied and has been tentatively adopted. In addition, a skirt extending forward from the forward frame of the outer telescoping section has been tentatively adopted. Handling loads will be applied at the adapter ring and/or forward skirt, isolating these loads in the outer telescoping section.

During handling operations, resistance to aft movement of the inner telescoping sections will be provided by the adapter ring, while resistance to forward movement will be provided by interlocking lug-type components attached to the aft frames of these sections. By attaching the outer telescoping section to the adapter ring, control of the inner sections will be achieved.

For a flight vehicle, the adapter ring structure concept could be used. All segments of the expandable structure would be held in position by attaching the outer telescoping cylinder to the adapter structure, and the adapter structure to the booster, both joints using quick-release structural disconnects. When deployment of the vehicle is desired, the quick-release structural disconnects would be actuated, releasing the expandable vehicle from the adapter structure.

8. Extension and Contraction Locks

Extension Locks - A design study was conducted to determine a reliable, lightweight method of retaining the telescoping sections in a deployed position without internal pressure. Emphasis was placed on ease of operation and on the requirement that during testing one person could operate all extension lock devices. A relatively simple device was designed to meet the requirement that the locks be released in the deployed position, remain so during contraction, yet be actuated in the contracted position for relocking on return to the deployed position. This device will be installed intermittently around the bases of the telescoping sections.

Contraction Locks - A design study was conducted to determine a simple, lightweight method of securing the inner telescoping sections in a down position during ground handling and flight before deployment, yet is reliable for release when deployment action is initiated. The product of the study was a series of lug-like structural members, positioned intermittently around the aft frames of the inner telescoping sections and extending outboard to overlap the bases of adjacent telescoping sections. Attaching the outer telescoping section to the external structure also secures the inner sections by successive retention of one adjacent section to the other.

9. Internal Thermal Control

The ultimate rejection of internally-generated heat from an earth-orbiting space station can be accomplished by a radiator. If the vehicle is manned, the average allowable radiator temperature should be somewhat less than 70°F, since the internal atmosphere in which heat is being generated would be controlled at approximately 70°F. Heat is primarily transferred from its source to the circulating environmental gases by forced convection. It is then transported to a heat exchanger that transfers it to a coolant that circulates through radiator panels mounted on the external surface of the vehicle. The heat is then transferred from the coolant to the radiator and radiated to space.

A portion of the heat flux from the sun and the earth, which is incident on the radiator surface, is absorbed by the radiators and must be re-radiated to space with the internally-generated heat being rejected from the space station. The magnitude of the heat flux from the sun and the earth that is absorbed by the radiator is a function of the space station shape, its orientation in orbit, orbit altitude and inclination, and the absorptivity characteristics of the radiator for solar direct, earth-reflected solar, and earth-emitted thermal radiation.

Total absorbed heat flux (sum of direct solar, earth-reflected solar, and earth-emitted) was calculated with the IBM 7090 Digital Computer, and the results are shown on Fig. II-23. For these calculations, the vehicle configuration was assumed to be approximated by five right-circular cylindrical sections connected in series, with their common longitudinal axis parallel to the velocity vector. Each cylindrical section was divided into eight segments as shown in Fig. II-24, and the vehicle was oriented so Segment 5 continuously faces the earth.

The internal heat removal rate is determined from the instantaneous steady-state heat balance on the radiator:

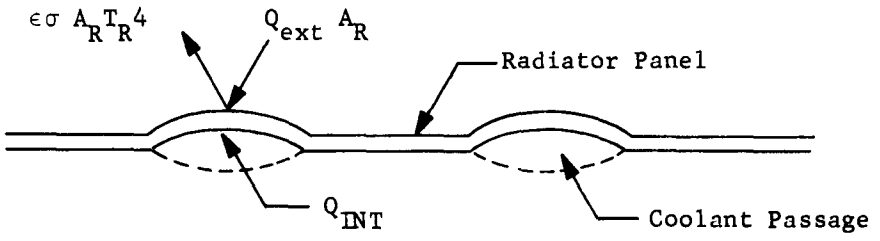

$$Q_{INT} + Q_{ext} A_R = \epsilon\sigma A_R T_R^4,$$

or,

$$Q_{INT} = \left(\epsilon\sigma T_R^4 - Q_{ext}\right) A_R,$$

where:

Q_{INT} = internal heat removal rate (Btu/hr),

Q_{ext} = total absorbed external heat flux (Btu/hr-sq ft),

A_R = radiator area (sq ft),

ϵ = infrared emissivity (dimensionless),

σ = Stefan-Boltzmann constant $\left(0.1714 \times 10^{-8}\right.$ Btu/hr-sq ft-$\left.°R^4\right)$,

T_R = radiator temperature (°R).

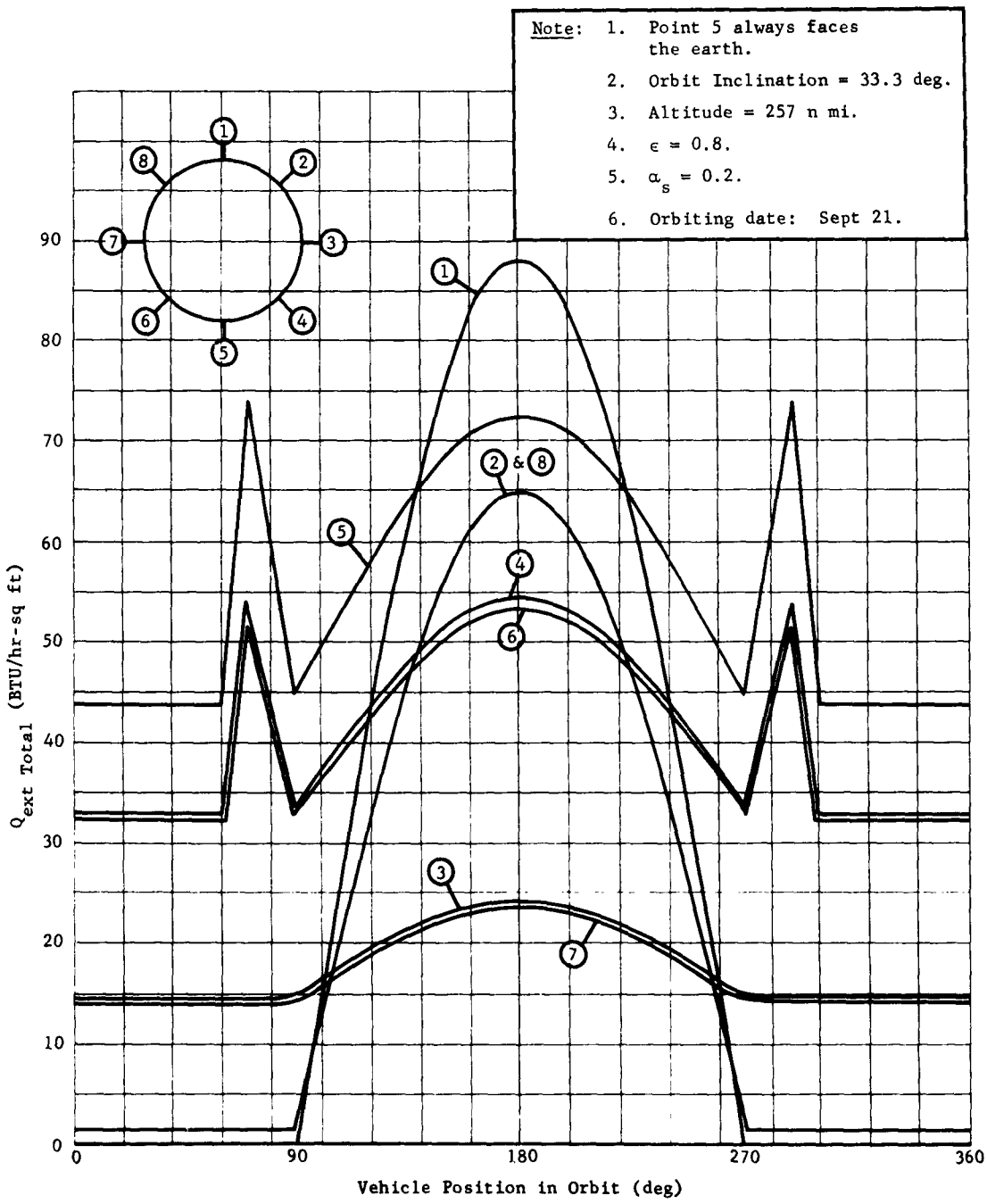

Fig. II-23 Total External Heat Flux Absorbed by Radiator Panels in Orbit

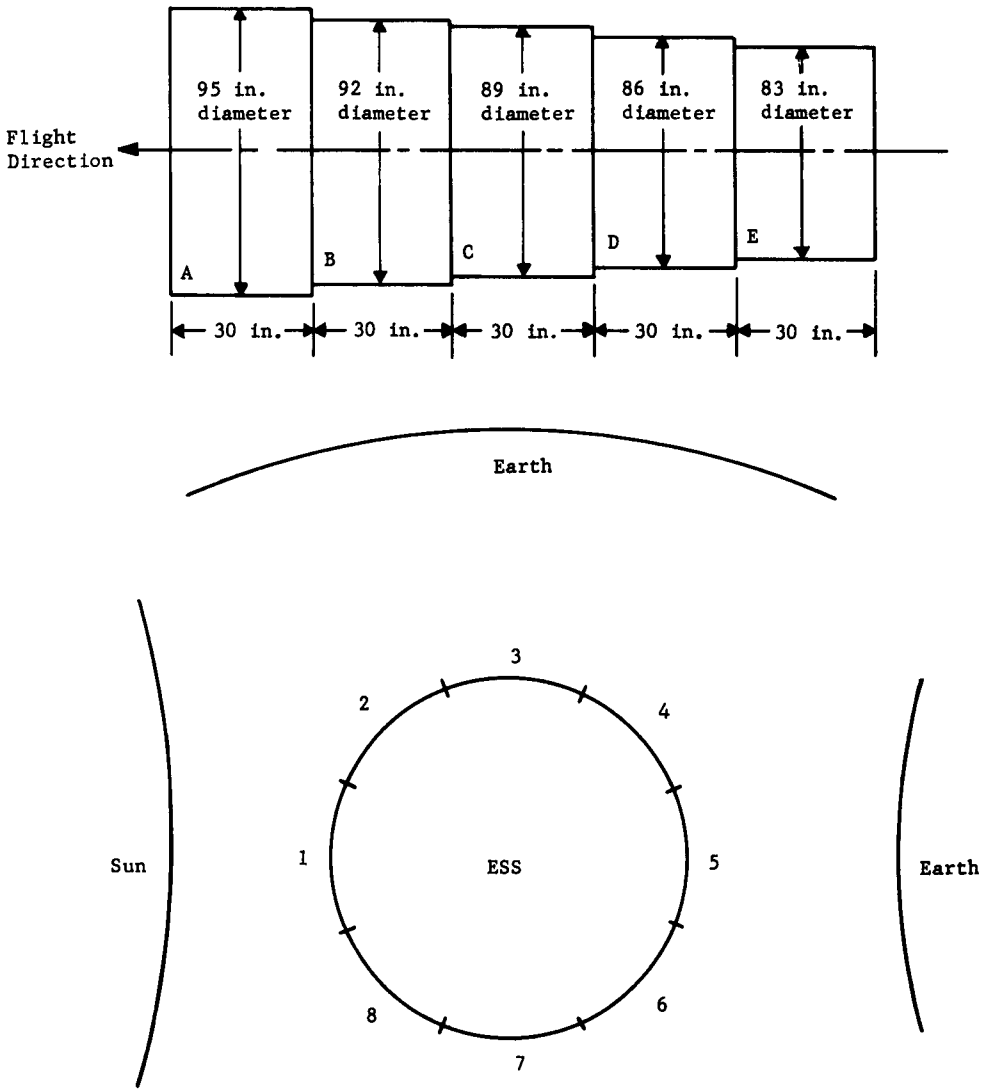

Fig. II-24 Vehicle Configuration and Orientation (180-deg Position)

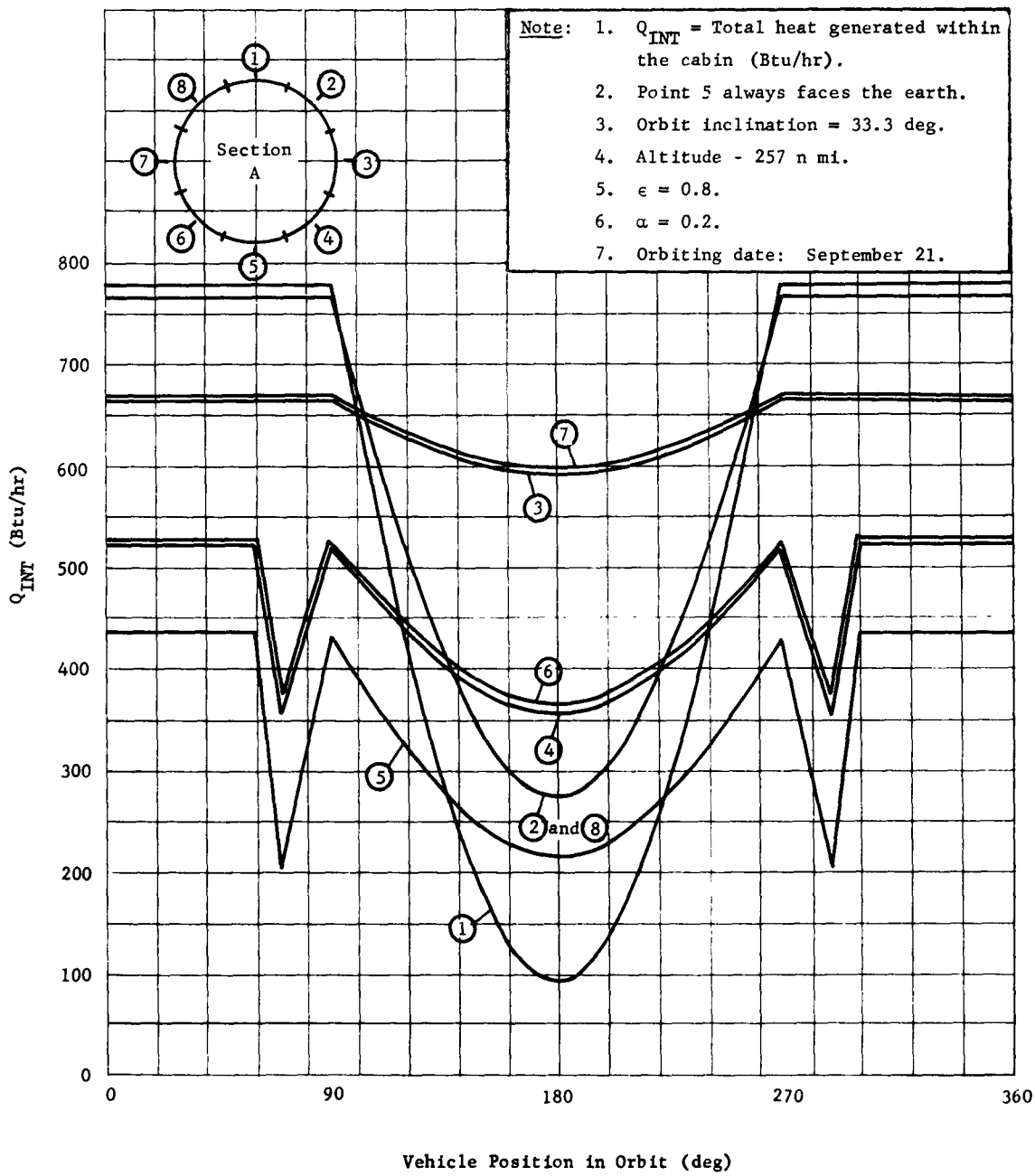

Fig. II-25 Total Internally-Generated Heat Versus Vehicle Position in Orbit

The internal heat removal rate, Q_{INT}, for all eight segments of each section was calculated as a function of the space station's position in orbit, assuming $\epsilon = 0.8$ and $T_R = 60°F$. The results of these calculations for Section A are shown in Fig. II-25. The maximum continuous internal heat removal rate per segment corresponds to the Q_{INT} value when the space station is at the 180-deg position in orbit (maximum Q_{ext} when the vehicle is directly between sun and earth). The Q_{INT} values for all segments (when the space station at the 180-deg position in orbit) are shown on Table II-2.

The total value for Q_{INT} of 12,489 Btu/hr indicates that approximately 3.5 kw of heat generated internally by equipment could be dissipated by the radiator panels after making allowances of 1000 Btu/hr of heat generation for a two-man crew.

The preceding study is preliminary in nature. In the study, the radiator panels are assumed to make up the entire outer skin surface, and are considered 100% efficient relative to surface area. A compensating factor is that the value taken for Q_{INT} of each radiator section is that value for maximum continual capability of the radiator section. This means that the radiator, in reality, could dissipate considerably more heat when on the side not exposed to the heat flux.

Table II-2 Internally-Generated Heat for Vehicle Position in Orbit

Section A		Section B		Section C	
Segment	Q_{INT}(Btu/hr)	Segment	Q_{INT}(Btu/hr)	Segment	Q_{INT}(Btu/hr)
1	92	1	79	1	85
2	274	2	254	2	256
3	591	3	562	3	546
4	356	4	334	4	333
5	215	5	198	5	201
6	365	6	343	6	342
7	597	7	568	7	559
8	274	8	254	8	256
Total	2,764	Total	2,592	Total	2,578

Section D		Section E	
Segment	Q_{INT}(Btu/hr)	Segment	Q_{INT}(Btu/hr)
1	83	1	81
2	247	2	239
3	534	3	517
4	322	4	312
5	194	5	188
6	330	6	319
7	540	7	523
8	247	8	239
Total	2,497	Total	2,418

Section	Q_{INT}(Btu/hr)
A	2,764
B	2,592
C	2,578
D	2,497
E	2,418
Grand Total	12,849

D. STRUCTURAL ANALYSIS

Structural analyses described here includes interlocking frames analysis, pressure skins and riveted joints, skin panels of outer telescoping section, and temperature effects on the primary structure.

1. Frame Analysis - Interlocking Frames

When internal cabin pressure is applied, the frames will be subjected to a complex loading system, including pressure load and uniform shear, moment, and longitudinal load from the barrel skin. These loads are reacted by the joining frame and the hoop continuity and roll resistance of the frame itself. The frames are shown in their loaded and deflected positions in Fig. II-26.

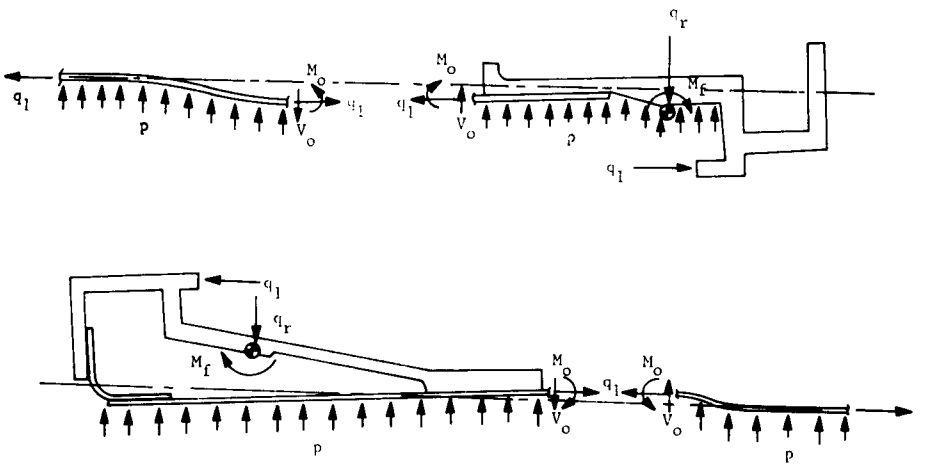

Fig. II-26 Interlocking Frames - Free Bodies

The critical areas are:

1) Skin adjacent to the frames, where high combined longitudinal and bending stresses occur due to skin-frame discontinuity;

2) Throat (or hook) of the frame, where high bending stresses occur because of the eccentrically-applied longitudinal loads;

3) Fasteners joining the skin to the frames, where the discontinuity at the joint may cause high combined shear and tension in the fasteners.

The critical areas of 1) and 3) were evaluated in the following manner. General equations were derived that yielded the indeterminate moment and shear, total stress in the skin, and the deflection and rotation at the point where the skin joins the frames. The equations were derived by balancing forces on the skin and frames, and equating rotation and deflection at the skin-frame junction.

The ring is assumed to be rigid with respect to secondary bending, i.e., the cross-sectional shape will not distort due to secondary bending. This assumption is valid if secondary bending is kept small. Another method of analysis that accounts for the bending may be used in future frame analysis.

The equations derived are:

$$M_o = (p)\frac{\left[\frac{R_e}{2} - \ell a\right] - \frac{\left[\frac{A}{t}\left(1 - \frac{\mu}{2}\right) - \ell\right]\left[b - \left(\frac{1}{2D\lambda^2}\right)\beta\right]}{\left[1 + \left(\frac{1}{2D\lambda^2}\right)\left(\frac{1}{\lambda} + b\right)\alpha\right]}}{\left[1 + \left(\frac{1}{D\lambda}\right)\beta\right] + \frac{\left[\alpha\left(\frac{1}{D\lambda}\right)\left(\frac{1}{2\lambda} + b\right)\right]\left[b - \left(\frac{1}{2D\lambda^2}\right)\beta\right]}{\left[1 + \left(\frac{1}{2D\lambda^2}\right)\left(\frac{1}{\lambda} + b\right)\alpha\right]}},$$

$$V_o = (p)\frac{\dfrac{\left[\dfrac{R_e}{2} - \ell a\right]\left[\alpha\left(\dfrac{1}{D\lambda}\right)\left(\dfrac{1}{2\lambda} + b\right)\right]}{\left[1 + \left(\dfrac{1}{D\lambda}\right)\beta\right]} + \left[\dfrac{A}{t}\left(1 - \dfrac{\mu}{2}\right) - \ell\right]}{\left[1 + \left(\dfrac{1}{2D\lambda^2}\right)\left(\dfrac{1}{\lambda} + b\right)\alpha\right] + \dfrac{\left[b - \left(\dfrac{1}{2D\lambda^2}\right)\beta\right]\left[\alpha\left(\dfrac{1}{D\lambda}\right)\left(\dfrac{1}{2\lambda} + b\right)\right]}{\left[1 + \left(\dfrac{1}{D\lambda}\right)\beta\right]}},$$

$$\sigma_{1o} = \frac{6M_o}{t^2} + \frac{pR}{2t},$$

$$\delta_o = \frac{M_o}{2D\lambda^2} - \frac{V_o}{2D\lambda^3} + \frac{pR^2}{tE}\left(1 - \frac{\mu}{2}\right),$$

$$\theta_o = \frac{M_o}{\lambda D} - \frac{V_o}{2D\lambda^2},$$

where:

$$\beta = \frac{EI}{R^2},$$

$$\alpha = \frac{AE}{R^2},$$

$$D = \frac{Et^3}{12\left(1-\mu^2\right)},$$

$$\lambda = \sqrt[4]{\frac{3\left(1-\mu^2\right)}{R^2 t^2}},$$

M_o = Indeterminate uniform moment (in.-lb/in.) at the skin-frame junction,

V_o = Indeterminate uniform shear (lb/in.) at the skin-frame junction,

σ_{1o} = Combined longitudinal and bending stress in skin at skin-frame junction $\left(lb/in.^2\right)$,

δ_o = Radial deflection at skin-frame junction (in.),

θ_o = Rotation of frame and skin at skin-frame junction (rad),

p = Internal cabin pressure (psig),

R = Radius of the frame (in.),

t = Thickness of the skin (in.),

I = Moment of inertia of the frame (in.^4) taken about a neutral axis in the plane of the ring frame,

A = Cross-sectional area of the frame (in.) on which internal cabin pressure acts,

ℓ = Longitudinal lengths of frame (in.) on which internal cabin pressure acts,

e = Eccentricity of longitudinal applied loads on the frame (in.),

a = Distance from the centroid of the frame cross section to the resultant load of the internal pressure acting on the frame (in.),

b = The distance from the centroid of the frame cross section to the skin-frame junction (in.),

E = Modulus of elasticity of the frame and skin material (lb/in.^2),

μ = Poissons ratio of the frame and skin material (in./in.).

The preceding equations were programed on the IBM 1620 computer with equations to compute all of the section properties in the previous list. This provided the capability of evaluating several frame shapes. It was found that in most areas manufacturing requirements controlled gages. The analysis of these frames gave the following results:

Outside frame: $M_o = 7.6$ in.-lb/in., $V_o = 13.3$ lb/in.

$\sigma_{lo} = 35{,}017$ lb/in.^{2}, $\delta_o = 0.012$ in., $\theta_o = 0.0074$ rad.

Inside frame: $M_o = 2.7$ in.-lb/in., $V_o = 3.3$ lb/in.,

$\sigma_{lo} = 16{,}400$ lb/in.^{2}, $\delta_o = 0.057$ in., $\theta_o = 0.015$ rad.

The critical area described in 2), the throat of the frame, is sized by computing a simple bending stress caused by eccentrically-applied loads.

2. Pressure Skins and Riveted Joints

The pressure skins of the cylindrical segments are critical for pressure loads, the largest radius segment being the most critical. The strength requirement for the skin is the allowable strength to preclude propagation of tearing in case of meteoroid puncture, rather than the tensile strength of the material. A tear strength of 30,000 psi was chosen arbitrarily for 2000-series aluminum alloy sheet, because adequate data are not available at this time. However, this value is somewhat substantiated by fracture resistance test data produced by Frankford Arsenal on 2000-series forgings and 7000-series sheet. Tests, consisting of notched specimen tests and possibly actual meteoroid impact tests on stressed skins, will be performed to obtain better fracture resistance data for sheet material. By using the 30,000-psi tear strength value, a considerable margin is shown for the 0.040 minimum gage skins.

The skin material in the riveted joints is critical for tensile and bearing strength around the rivets. In case of meteoroid damage in this area, tear propagation will be stopped by a rivet hole.

3. Skin Panels of Outer Telescoping Section

Parametric design curves are being generated for use in designing the outer meteoroid shield and pressure skin for boost loads. The meteoroid shield must resist dynamic pressures during boost. The pressure skin must resist combined axial loads, moment loads, and shear loads.

The varying parameters for the meteoroid skin curves are panel length, panel width, skin thickness, and critical pressure. The varying parameters for the pressure skin are panel length, panel width, and critical compressive and shear stress. Interaction of shear and compression stress is being accounted for in determining the most critical condition. These curves will provide the capability of selecting the optimum skin and stiffener combinations.

4. Temperature Effects on Primary Structure

The effects of temperature on primary structure can assume two forms of significance relative to the structure itself. They are thermal stresses arising from differential temperatures, and reduced strength allowables due to temperatures higher than room temperature.

The significance of the latter is considered negligible, because final temperatures are expected to be between 0 and 100°F. The former may have a relative minor influence on the design of the frames and skin joints. The thermal stresses resulting from temperature differentials will be superimposed on the stresses resulting from pressure loads. The magnitude of thermal stresses will be determined after final temperature analysis is complete.

E. WEIGHT ANALYSIS

Structural weight and mass and inertia distributions are described here.

1. Structural Weight Statement

Table II-3 presents the preliminary weight breakdown of the ESS structure that will be built during this program.

Table II-3 ESS Structure Weights (Estimated)

Item	Weight (lb)
Forward Dome (Weight for Air Lock and Hatch Are Estimated)	215
Frames, Forward	165
Frames, Rear	167
Aft Bulkhead	120
Meteoroid Shield (And Associated Hardware)	142
Pressure Skin (And Associated Hardware)	225
Guides and Rails	58
Bladder (And Associated Hardware)	62
Insulation	109
Total	**1263**

2. Mass and Inertia Distributions

Mass and inertia assumptions were made to arrive at logical loading conditions for the structure:

1) The vehicle is a manned space station, and is equipped to perform certain test functions in orbit;

2) It will be boosted into orbit by a standard Titan II booster;

3) The total boost weight, including a propulsion module, is 8000 lb.

Existing data, where available, were used in determining equipment, propulsion, and structure requirements for a nominal boost and orbital configuration. These data were taken from current programs at the Martin Company. The assumed weight breakdown is presented in Table II-4.

Table II-4 Weight Breakdown

Item	Weight (lb)
BASIC VEHICLE	(4813)
ESS Structure	1263
Nose Fairing	250
Adapter	100
Kick Stage (Propulsion and Guidance)	3200
EQUIPMENT	(3187)
Controls	102
Navigation	102
Communication	127
Instrumentation	325
Power System	810
Furnishings	551
Accommodations	171
Environmental Controls	773
Food (60 Man-Days)	134
Water	38
Rendezvous and Docking	54
TOTAL	8000

Mass distributions and inertia are shown in Fig. II-27, II-28, II-29, and II-30 for the boost and orbital configurations. Three phases of orbital operation are included: unexpanded, expanded, and ready for occupancy.

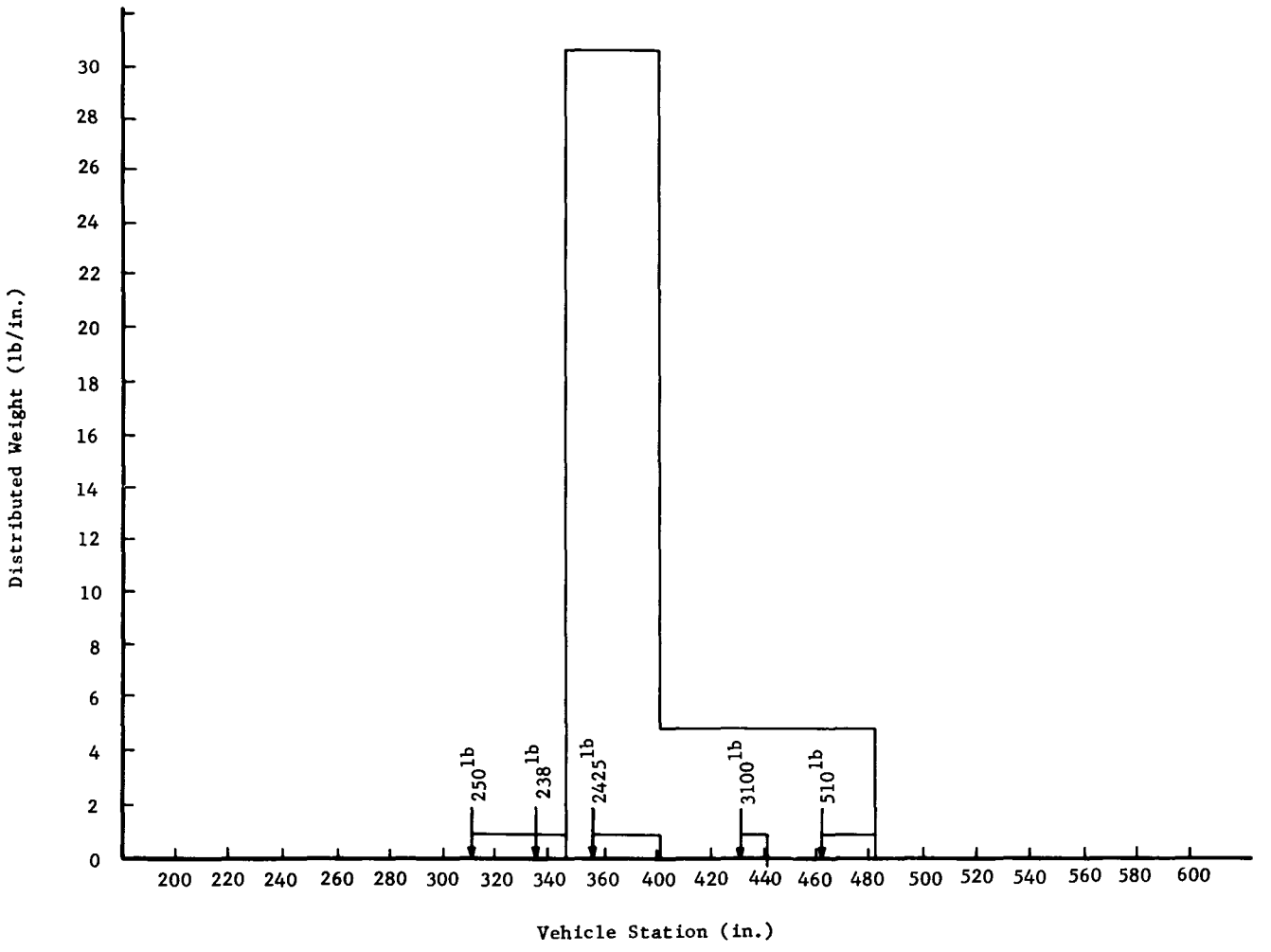

Fig. II-27 Distributed and Concentrated Weight Versus Vehicle Station

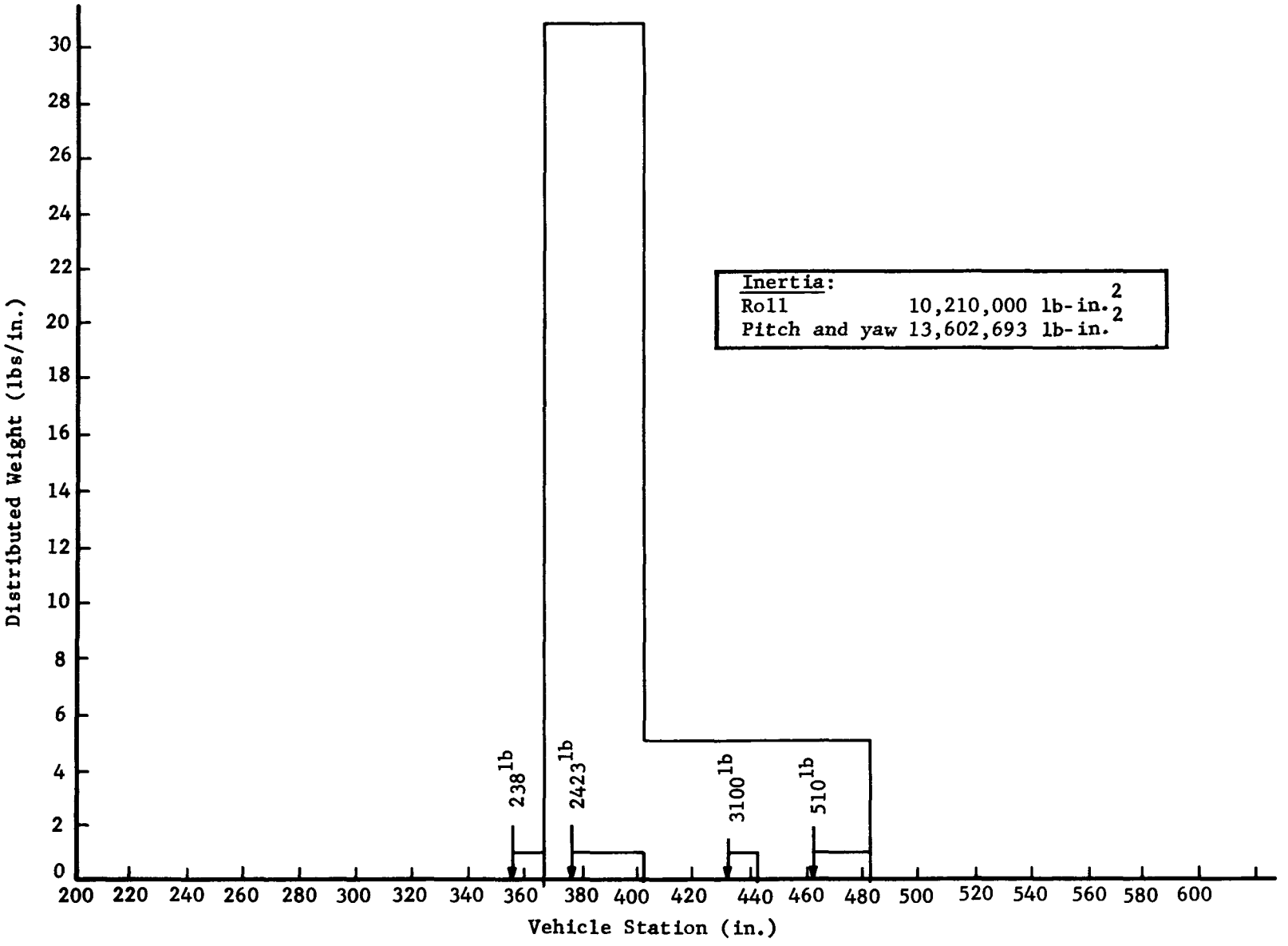

Fig. II-28 Distributed and Concentrated Weight Versus Vehicle Station—Orbital Configuration, before Expansion

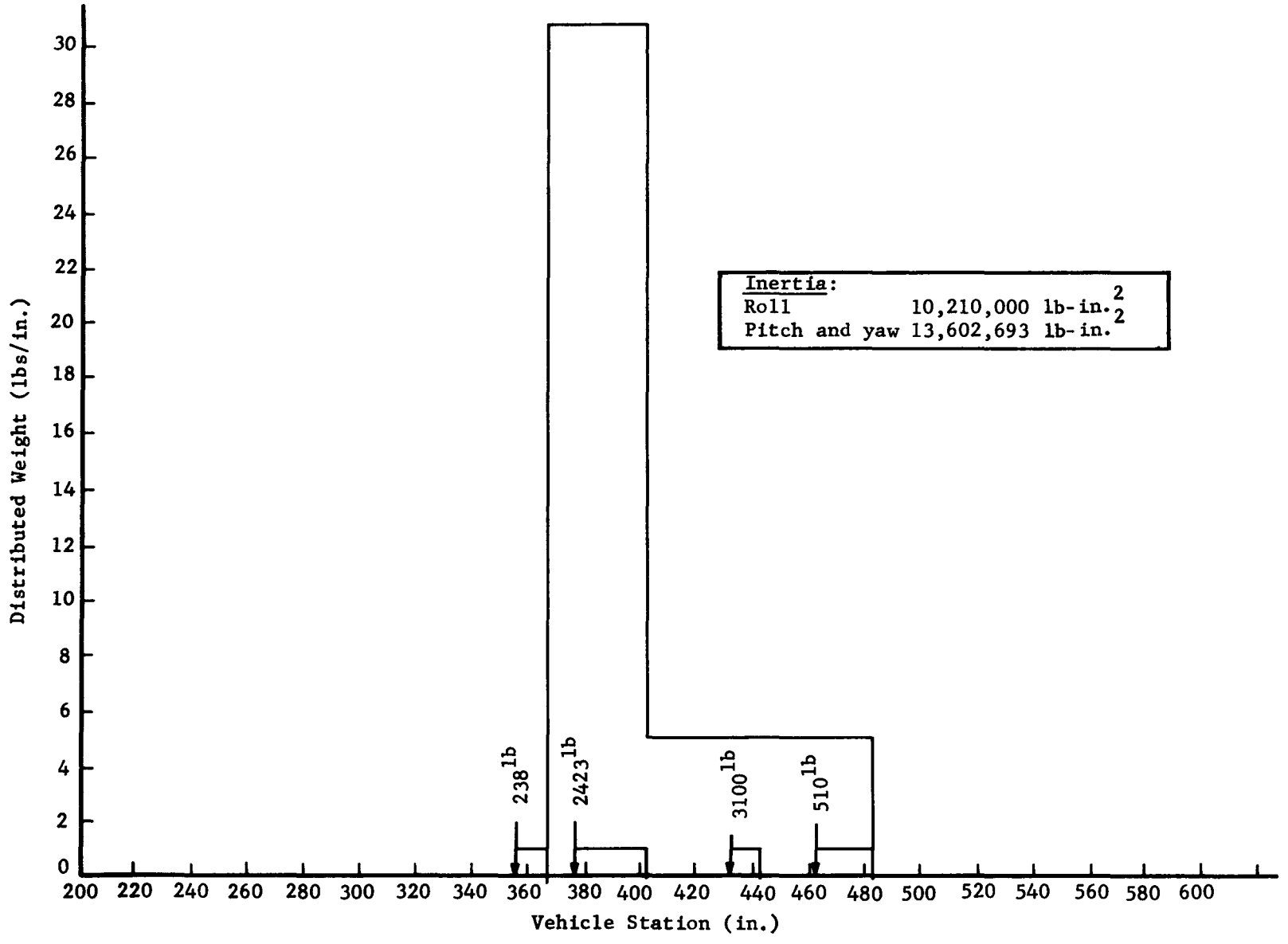

Fig. II-28 Distributed and Concentrated Weight Versus Vehicle Station—Orbital Configuration, before Expansion

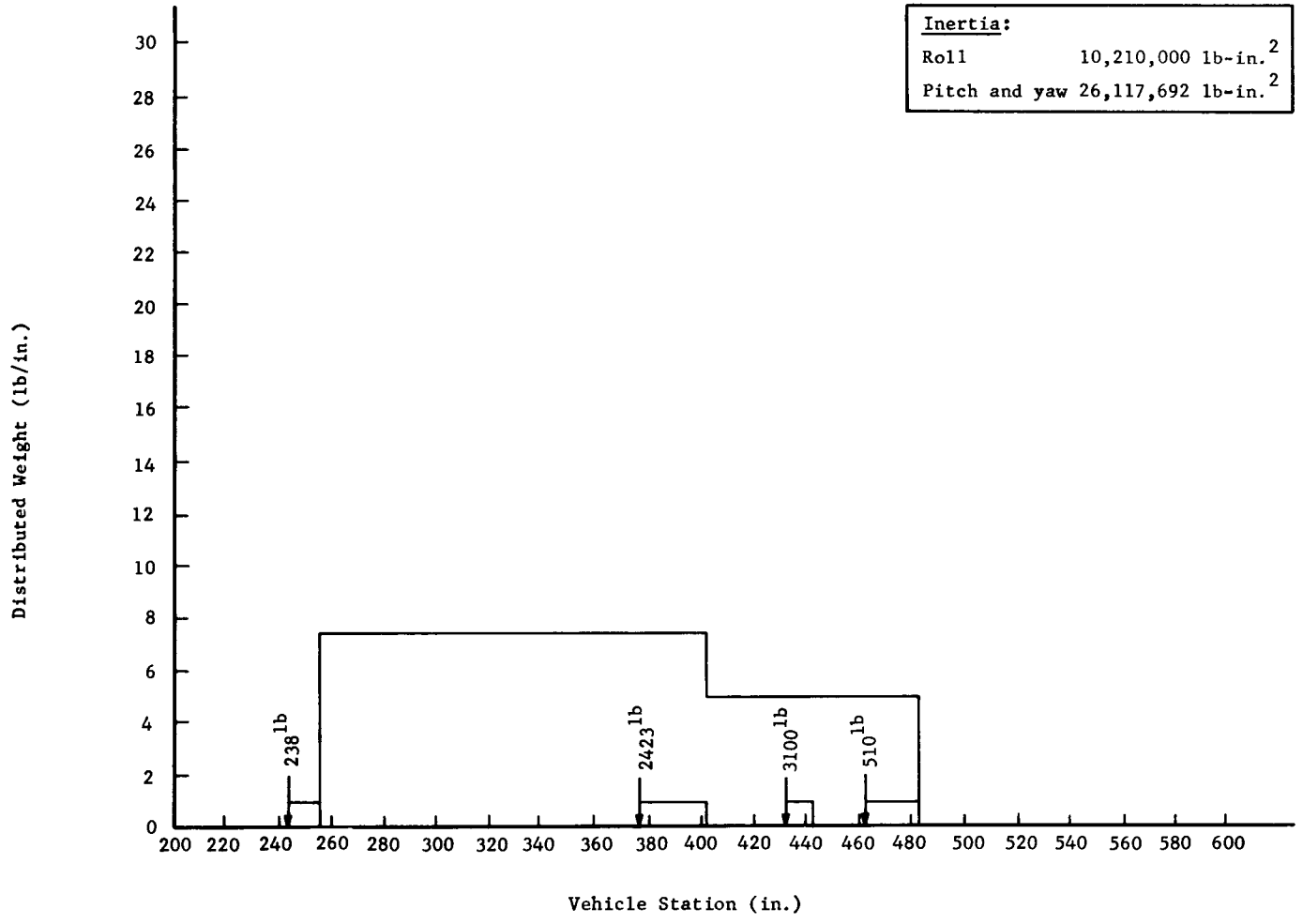

Fig. II-29 Distributed and Concentrated Weight Versus Vehicle Station - Orbital Configuration, Expanded

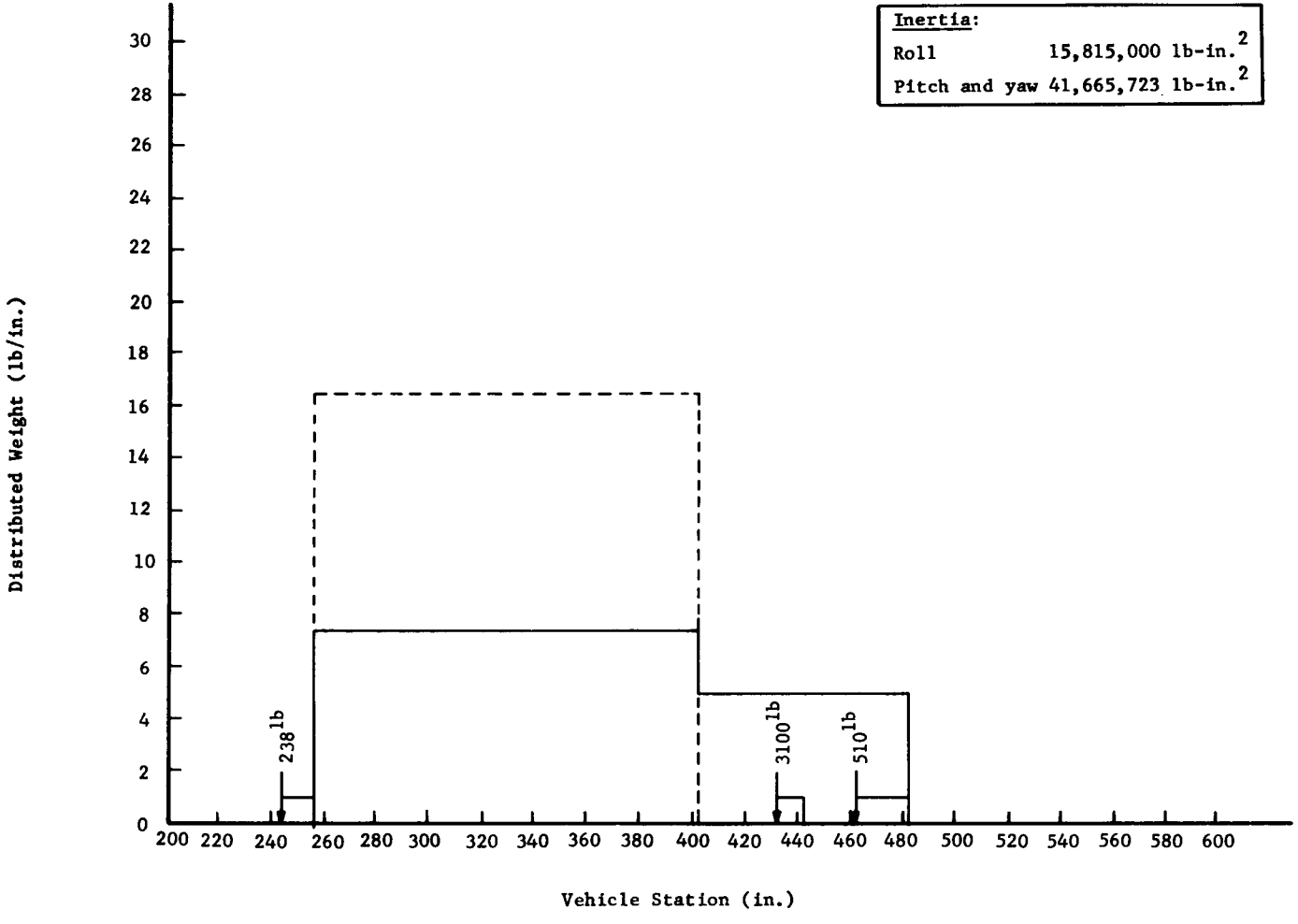

Fig. II-30 Distributed and Concentrated Weight Versus Vehicle Station - Orbital Configuration, Expanded, Solar Collectors Deployed and Equipment Distributed

III. SPACE ENVIRONMENTAL EFFECTS

A. SPACE RADIATION

Data presented in Fig. III-1, III-2, and III-3 show exposures of the expandable space structure to Van Allen protons.

Figure III-4 shows biological doses as a function of shielding provided by vehicle walls.

Figures III-2 and III-3 indicate that during a 24-hr time span, only six of the orbits expose the vehicle to Van Allen protons. By multiplying an ordinate taken from Fig. III-4 by total flux values in Fig. III-2 and III-3, total biological doses can be determined for crew members for one day.

The expandable space structure has a total aluminum thickness in the telescoping walls of 0.060 in. This amounts to a total shielding weight provided by the skins of 0.864 lb/sq ft or 0.423 gr/sq cm. Based upon Fig. III-2, III-3 and III-4, the crew would receive a monthly dose of approximately 4 rem. This is well below design limits shown in Fig. II-6.

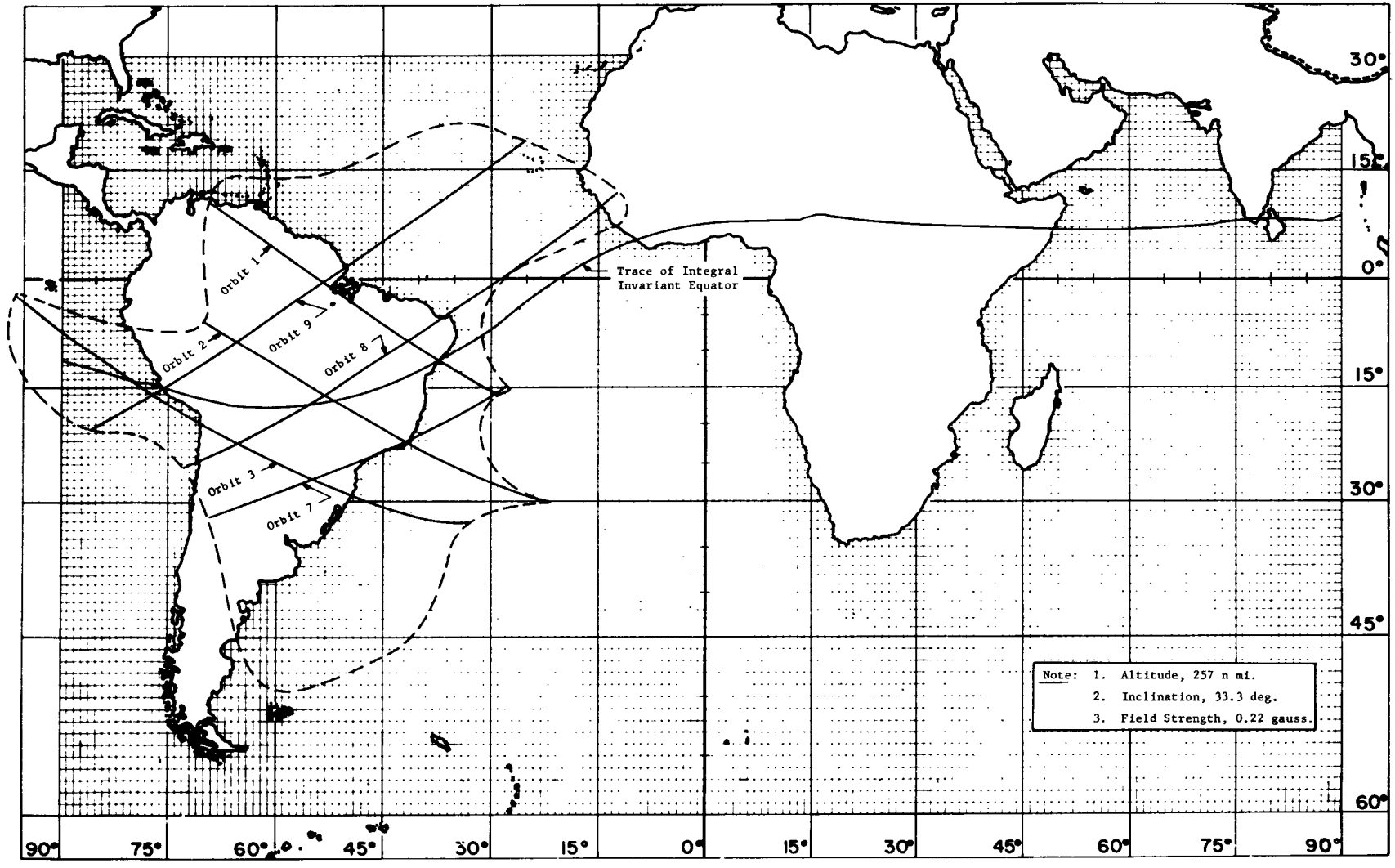

Fig. III-1 Orbiting Vehicle Ground Traces of Orbits Penetrating the Van Allen Belt

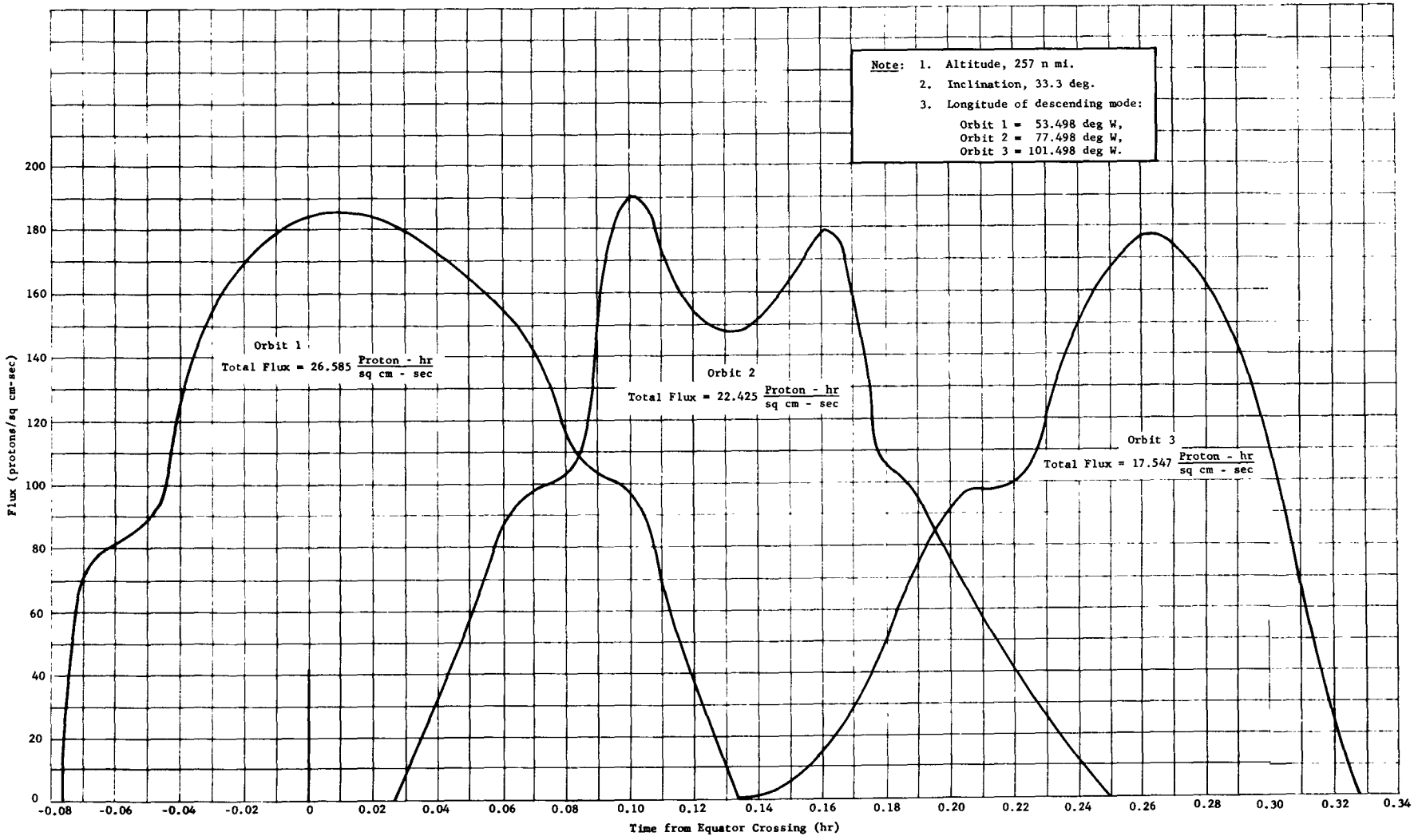

Fig. III-2 Time Histories of Vehicle Exposure to Van Allen Protons, Orbits 1, 2, and 3

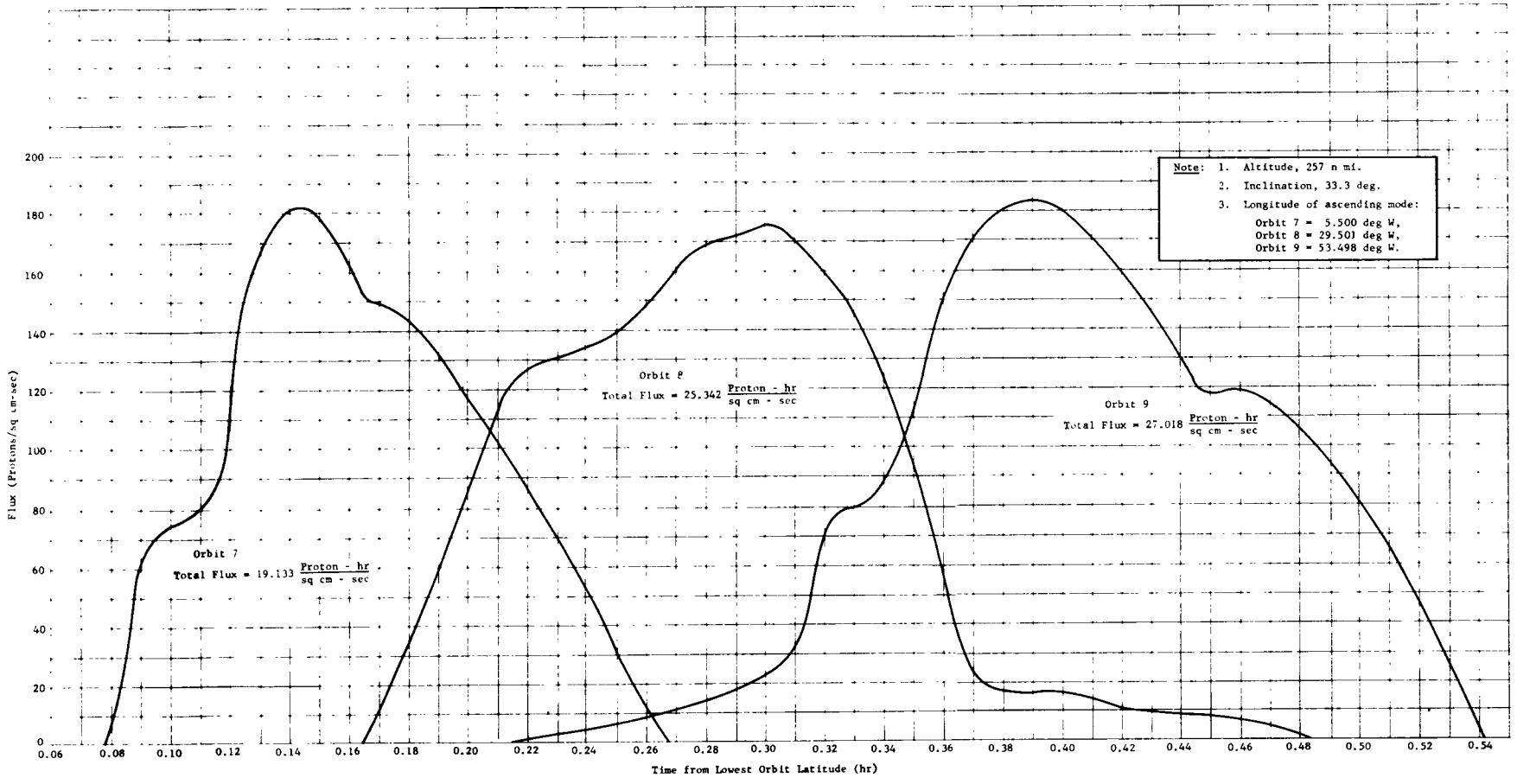

Fig. III-3 Time Histories of Vehicle Exposure to Van Allen Protons, Orbits 7, 8, and 9

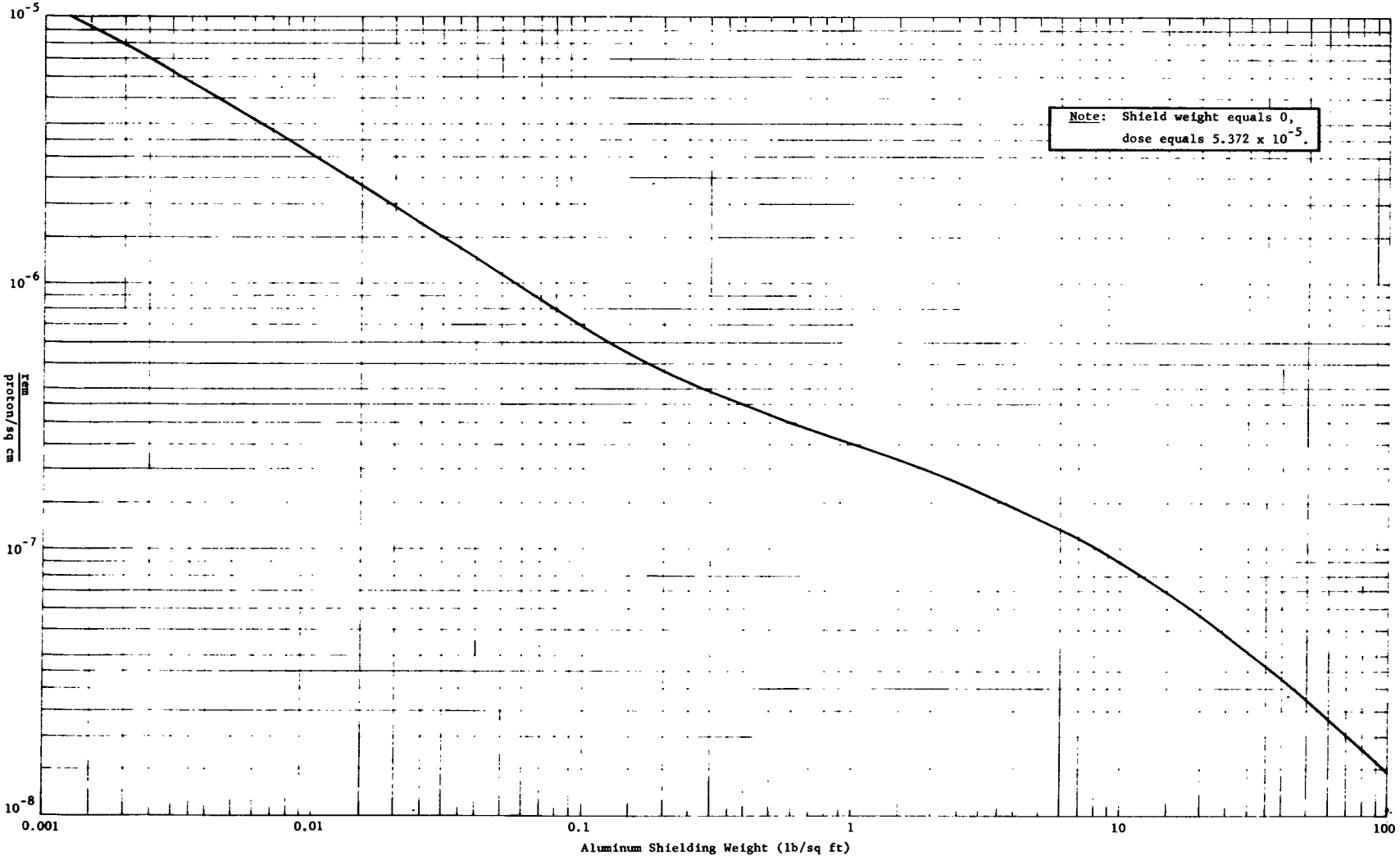

Fig. III-4 Biological Dose for Unit Incident Proton Flux, Energy Range 10 to 700 Mev

B. METEOROID HYPERVELOCITY TESTS

During the period from 8 October to 15 November 1962 the data shown in Fig. III-5 were obtained in the two-stage light-gas gun facility of the Denver Research Institute. Eight shots were fired in the first test package purchased by Martin, and nine in the second.

Objectives of the tests were to determine the penetration characteristics of structural aluminum sheet and plate in single thickness, as a basis for later tests on double-wall constructions, and to develop and evaluate a method for launching several projectiles at each shot.

Projectiles were glass balls of a commercial grade in assorted sizes. These were individually checked for roundness and homogeneity, and weighed before loading onto the polyethylene sabot that carried them through the gun. Each shot consisted of five balls plus the sabot. Ball sizes were chosen in each case to bracket the size expected to produce a marginal puncture in the target.

The shots were all fired under nominally identical gun conditions. Velocities varied from 17,000 fps to 18,400 fps, with one shot at 13,800 fps because of an expanded barrel.

An ideal shot is one in which all five ball impacts are identifiable and located well away from the hole caused by the sabot. In addition, some, but not all, of the balls should penetrate the target. Such a shot provides a bracket on the size of the ball that will just penetrate the target under the same conditions. If desired, a closer bracket can be established by a succeeding shot with several ball sizes between the two that established the bracket.

In addition to the critical ball size, hole diameter data can be obtained from the punctures, and crater data from the other impacts. Figure III-5 indicates a preliminary grouping of hole diameter data obtained in this way. In this simple correlation, the data are shown to be fairly consistent. Also, the qualitative effects of target hardness and projectile velocity agree with intuitive estimates. The sharp cutoff between a ball size that will produce a puncture, and a smaller one that will not is apparent.

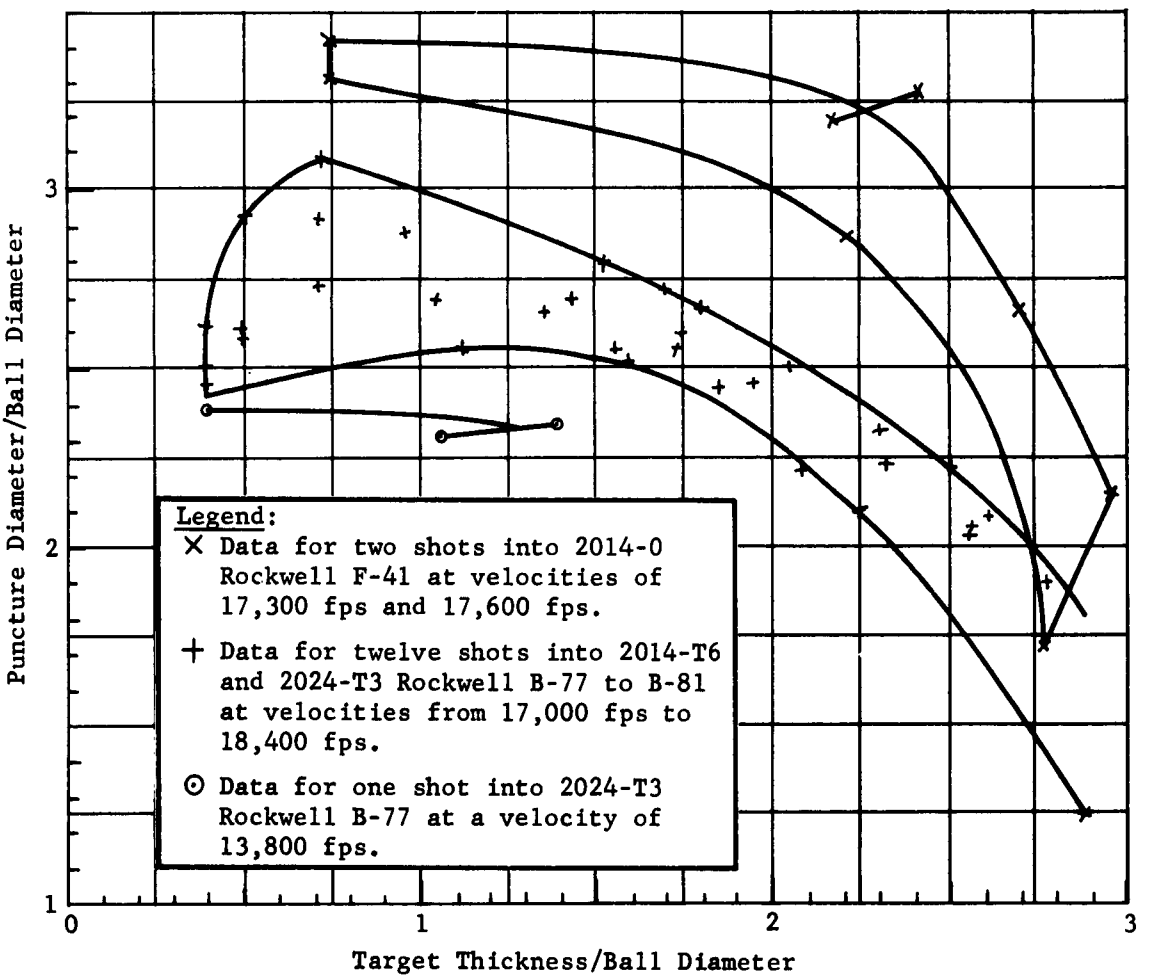

Fig. III-5 Hypervelocity Puncture Diameter Data

A more careful and complete analysis of the data is being made, with plans for a series of shots at a nominal velocity of 25,000 fps.

Figure III-6 shows a representative target after firing, and indicates the certainty with which punctures may be assigned to the balls that produced them.

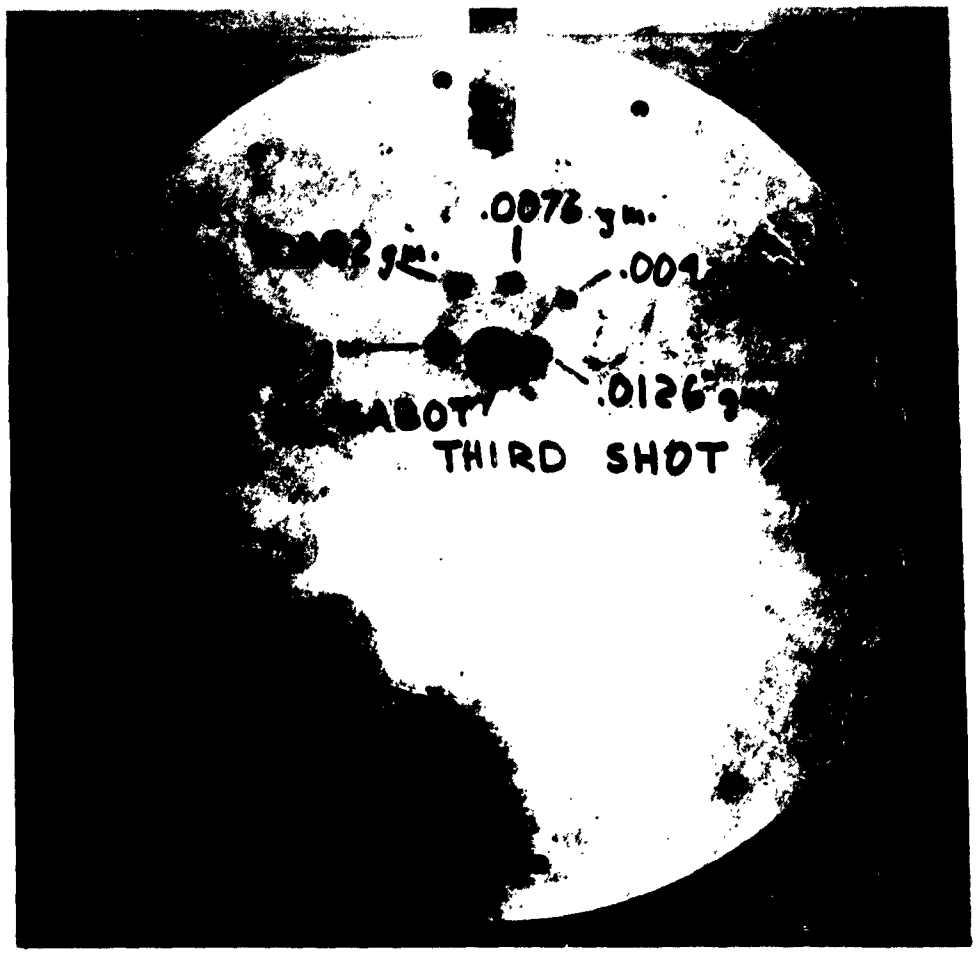

Fig. III-6 Typical Target After Firing

C. THERMAL RADIATION -- ORBITAL HEATING

Heat transfer analyses have been programed and run on the IBM 7090 computer. Objectives were to:

1) Determine temperature history of the structure;

2) Evaluate temperature gradients between the inner and outer walls and across the joints of the vehicle;

3) Determine the internal thermal environment of the vehicle in cases where internal environments are not held constant.

Two analyses were made. The first was preliminary in nature. It assumed several broad parameters.

Vehicle configuration was an aluminum structure with telescoping walls of double-wall construction with cavity insulation, and an external surface having optical properties of sand-blasted aluminum.

1. Analysis No. 1

A constant heat flux of 442 Btu/sq ft/hr was imposed on one side of the cylindrical part of the vehicle; the opposite side is constantly exposed to deep space. Reflected solar and direct radiation from the earth were neglected. No internal heat generation for the vehicle was assumed. Element breakdown of the structure is shown in Fig. III-7.

Using the above assumptions, results indicated that the vehicle would overheat considerably. Typical results are shown in Fig. III-8 and III-9.

IBM runs were made to evaluate the effect of internal radiation within the structure and a "super" insulation between the inner and the outer walls. Three problems were considered as follows:

Problem 1 -- No insulation between walls, and no internal radiant heat exchange (internally insulated);

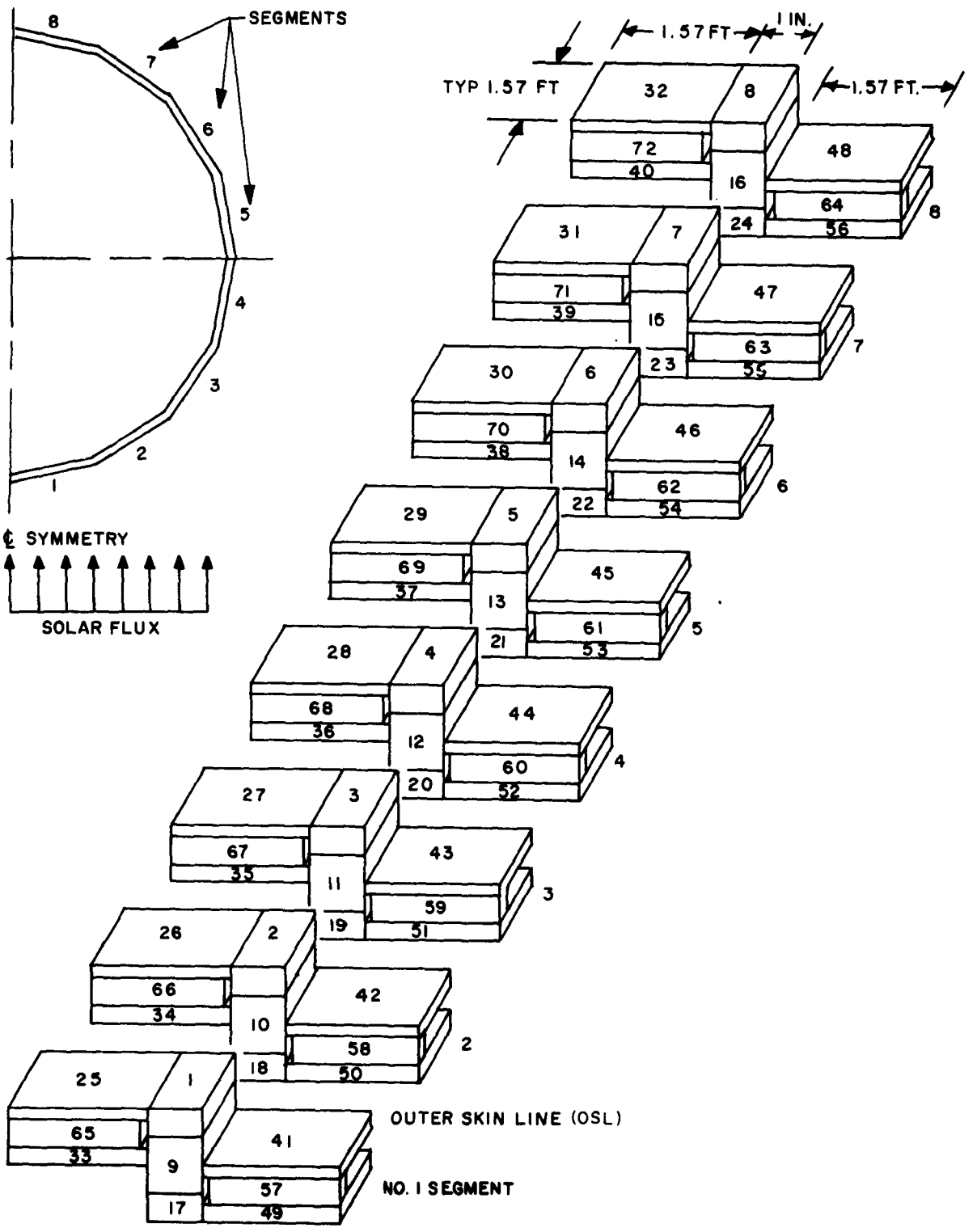

Fig. III-7 Element Breakdown for Structural Heating Analysis No. 1

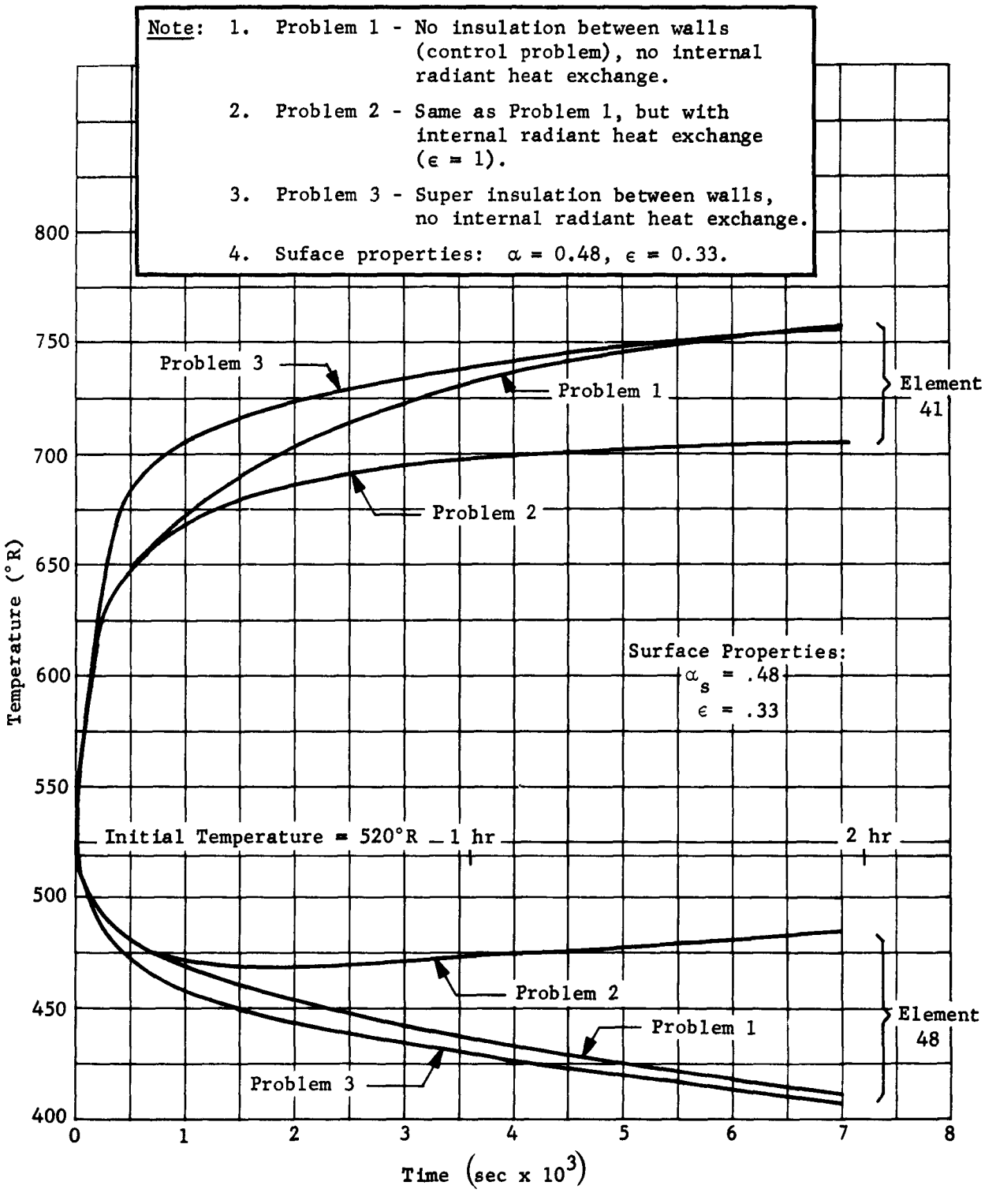

Fig. III-8 Comparison of Hot and Cold Side Temperatures for Outer Wall Only

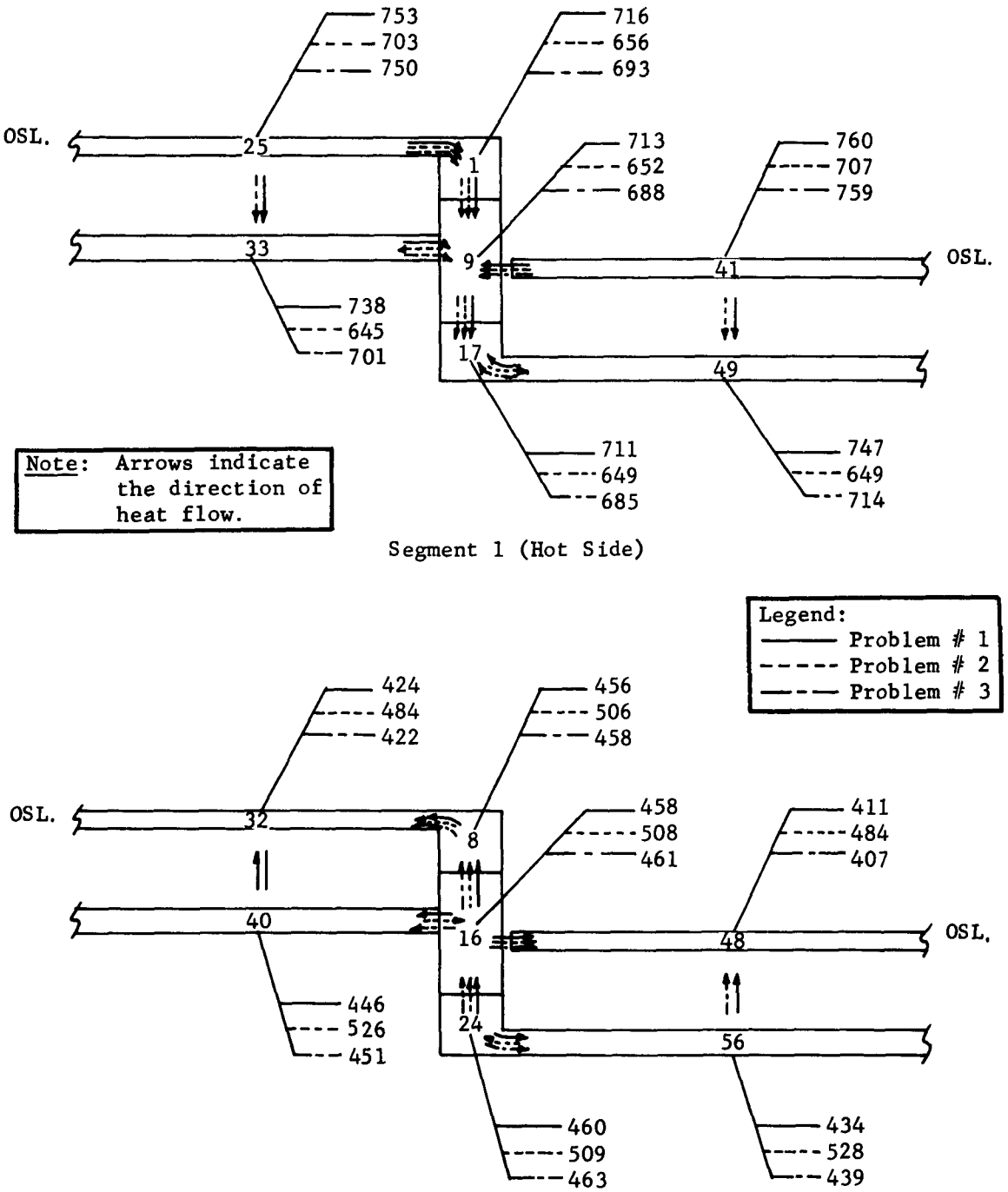

Segment 1 (Hot Side)

Segment 8 (Cold Side)

Fig. III-9 Temperature Distribution Within the Structure after 2 Hr

Problem 2 -- Same as Problem 1 except with internal radiant heat exchange, assuming an ideal emissivity of one for the internal wall;

Problem 3 -- Assumes a "super" insulation (such as the NRC-2 or the Linde SI-4) between the outer and the inner wall, and no internal radiant heat exchange (internally insulated).

These three problems are qualitatively compared in Fig. III-8. Here, the extreme high and low temperature elements for the outer wall are plotted as functions of time starting with an initial overall temperature of 520°R(60°F). The major temperature changes take place within the first 30 min of orbital flight, and by the end of 2 hr the temperatures have all approached close to the equilibrium state. Problem 3 shows the most extreme temperatures (759 to 407°R) found on the outer skin. This may be attributed to the reduced cooling effect of the inner wall on the hot side due to the insulation layer, and the reduced heating effect of the inner wall on the cold side of the space structure. Of the three problems shown, Problem 2 is the least severe temperature problem. This can be explained by a rather extensive radiant heat exchange internally within the space structure, which was obtained by using an ideal black body emissivity of 1. The temperature difference between Problems 1 and 3 and Problem 2 becomes more pronounced with time.

The actual temperature distribution within the structure at the end of 2 hr is shown in Fig. III-9. Information can be obtained for other time intervals from IBM printouts.

Considering the temperature distribution, certain recommendations on solar heating control can be made. To equalize the temperature extremes on the opposing sides, rotation about the longitudinal axis might be considered. However, for this to be effective the rotational speed would have to be 10 min/rev or greater. The tendency here would be to stabilize the temperatures around some mean value, (in this case 590°R or 130°F) on the exterior. If rotation is not desirable other methods could be used:

1) Externally -

Use of a low absorptivity (0.2) coating on the side facing the sun, and a low emissivity (0.03) coating on the dark side of the structure. (This assumes that the spade structure is oriented with respect to the sun, with one side facing sun at all times);

2) Internally -

a) Coat the interior surfaces between the two walls with a low emissivity (0.03) coating,

b) Use super insulation between walls,

c) Replace aluminum inner and outer supports or frames with a low thermal conductivity material (steel, fiberglas, etc),

d) Coat interior of the pressure seal bag with a high emissivity (0.95) coating.

Item 1 would decrease the net heat input on the hot side and decrease the heat loss on the cold side thus reducing the temperature extremes. Items 2a and 2b would both reduce the radiant heat exchange between the inner and outer walls. This case was worked in Problem 3, and as seen in Fig. III-9, the effect was to increase the temperature difference between the inner and outer skin panels. Item 2c would be a promising method because the amount of heat conducted through the supports or frames between the skin panels is about equal to radiative energy passed between panels. Decreasing the thermal conductivity of these supports and frame by one order of magnitude would have the same temperature effect as the introduction of insulation between panels. The last item, 2d, increases the heat exchange across the compartment thus reducing the temperature difference between the hot and cool sides. This case was worked as Problem 2 and the temperature trends are shown in Fig. III-9.

2. Analysis No. 2

The second analysis was based on more realistic parameters. An orbit of 250 n mi altitude and an inclination of 33.3 deg was chosen. Vehicle configuration was aluminum structure, the telescoping walls being of double-wall construction with cavity insulation in one case, and without it in another case. The external surfaces of the outer skin panels were coated with a material having a solar absorptivity value of 0.2, and an infrared emissivity value of 0.8. A circulating atmosphere of 70°F was assumed for the inside of the vehicle.

External heat flux applied was that given in Section II B. The variable heat flux was obtained from a program run on the IBM 7094 computer. Thermal heating results in temperature-time history form are shown for two complete orbits in Fig. III-10.

As can be seen from this figure, extremely cool temperatures exist in the outer wall. This may be attributed to the small absorptivity/emissivity ratio used in this analysis. If these temperatures are undesirable, they may be altered upward by manipulating the α/ϵ ratio for the outer wall. However, a change in temperature of the inner wall can be expected. Increasing α/ϵ would cause a rise in temperatures for both inner and outer walls.

Figure III-11 is a diagram showing the elemental structural breakdown. Included is the orientation of the vehicle with respect to earth. For this analysis, side 5 faces the earth throughout the orbit.

Figures III-12 thru III-19 afford a quick look at temperatures of all sides at various times from the end of the first orbit to the end of the second orbit. Note that although the temperatures at the end of two orbits have not reached a steady-state periodic function, the temperatures are within a few degrees of that condition. For this analysis the program had been run both with and without insulation between the walls. Since the largest difference in temperatures for analyses with insulation as compared with those without insulation amounted to only a few degrees, the only results shown in Fig. III-8 are those without insulation.

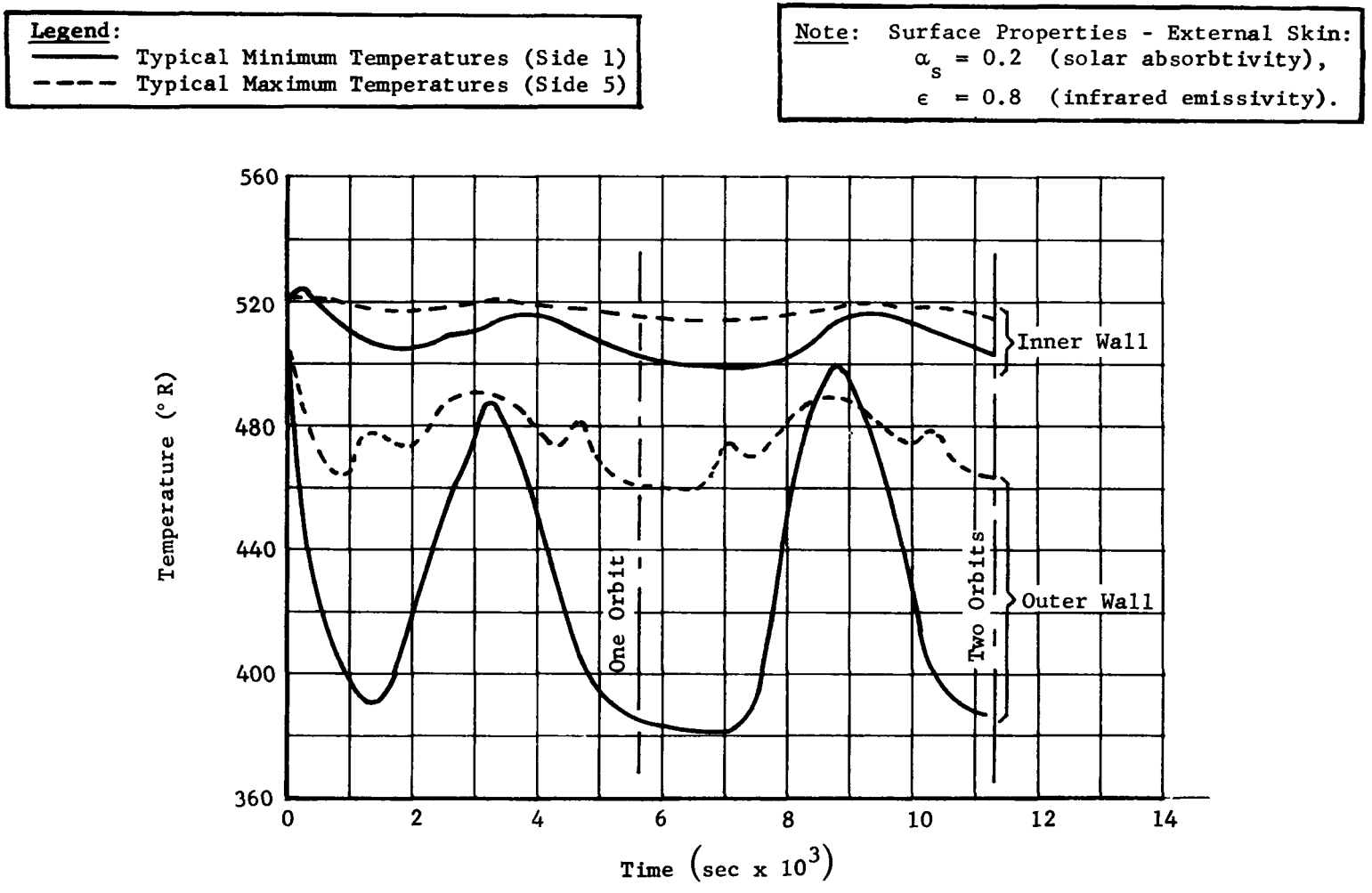

Fig. III-10 Wall Temperature Versus Time

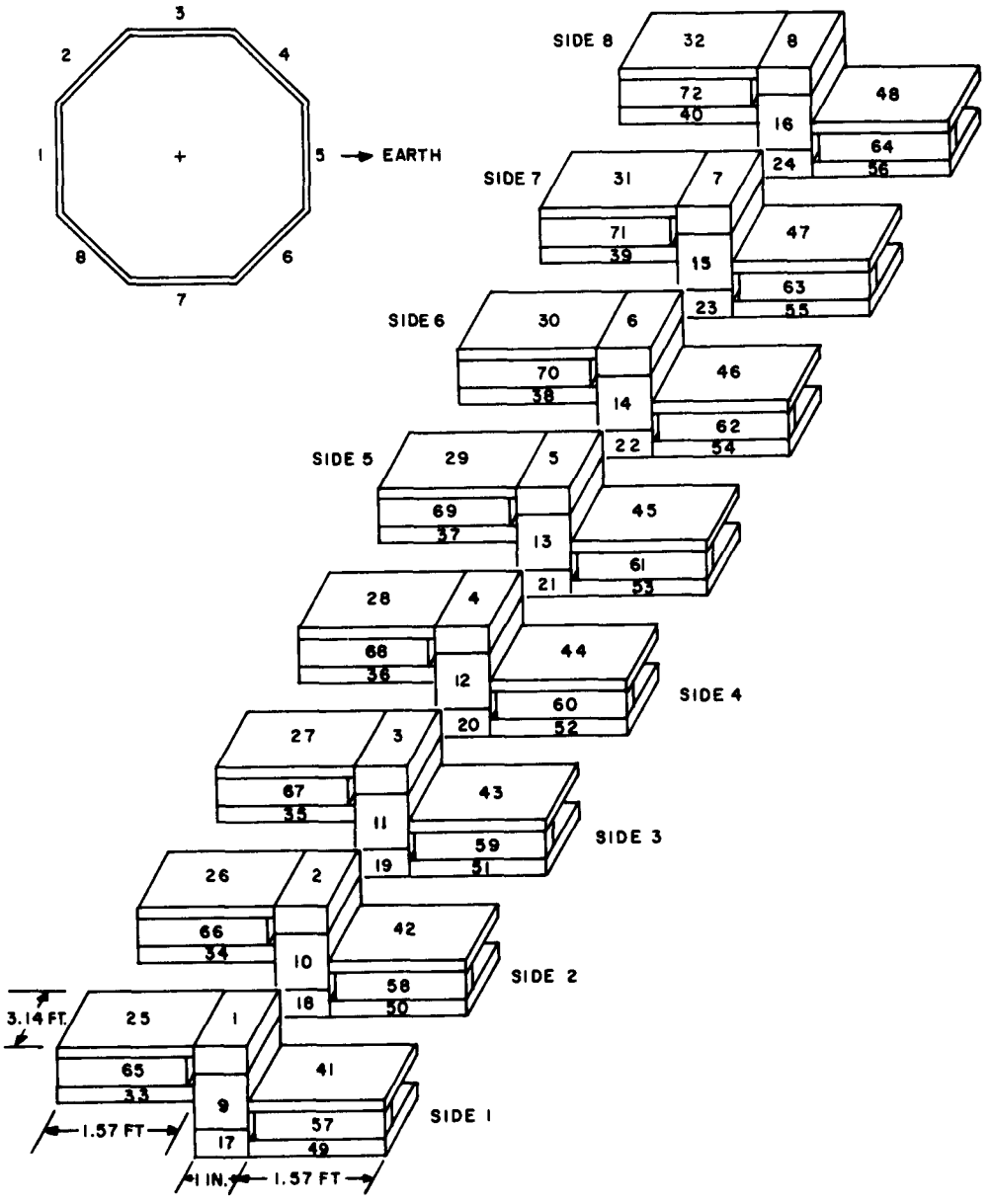

Fig. III-11 Element Breakdown for Structural Heating Analysis No. 2

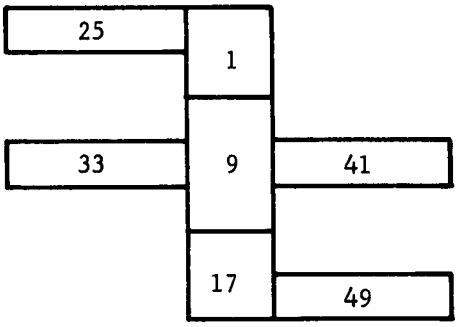

Time (sec)	Temperature (°R)		
5,580	401	485	
	505	491	386
		494	503
6,600	399	482	
	503	488	382
		491	502
7,800	444	479	
	503	483	434
		485	501
9,000	494	495	
	516	496	494
		498	516
10,200	417	493	
	512	498	408
		501	512
11,280	401	483	
	504	490	386
		493	503

Fig. III-12 Temperature Distribution within the Structure of Side 1 at Various Times during the Second Orbit

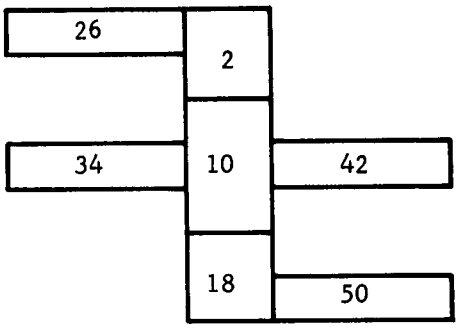

Time (sec)	Temperature (°R)		
5,580	403	484	
	505	490	389
		493	503
6,600	400	478	
	502	484	385
		488	500
7,800	436	479	
	503	483	426
		485	501
9,000	474	491	
	513	493	472
		495	512
10,200	416	489	
	510	495	407
		498	509
11,280	402	482	
	504	488	388
		491	503

Fig. III-13 Temperature Distribution within the Structure of Side 2 at Various Times during the Second Orbit

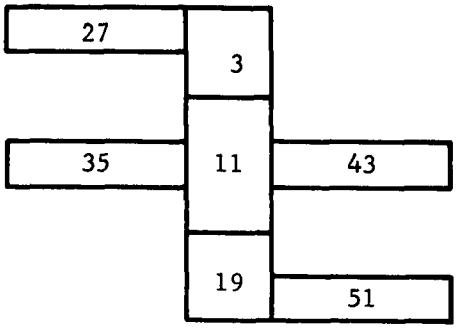

Time (sec)	Temperature (°R)		
5,580	420	485	
	506	489	409
		493	505
6,600	420	483	
	515	488	409
		491	504
7,800	425	482	
	505	487	414
		489	504
9,000	432	484	
	507	488	423
		491	506
10,200	422	506	
	506	489	412
		492	506
11,280	420	504	
	505	488	409
		491	504

Fig. III-14 Temperature Distribution within the Structure of Side 3 at Various Times during the Second Orbit

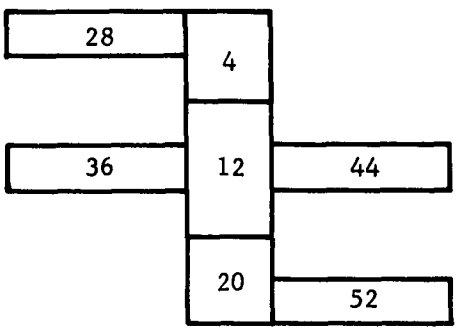

Time (sec)	Temperature (°R)		
5,580	449	497	
	513	501	442
		503	512
6,600	446	495	
	512	499	439
		501	511
7,800	452	494	
	511	497	444
		499	510
9,000	469	497	
	514	500	465
		502	514
10,200	460	498	
	514	501	454
		503	513
11,280	447	496	
	512	500	440
		502	512

Fig. III-15 Temperature Distribution within the Structure of Side 4 at Various Times during the Second Orbit

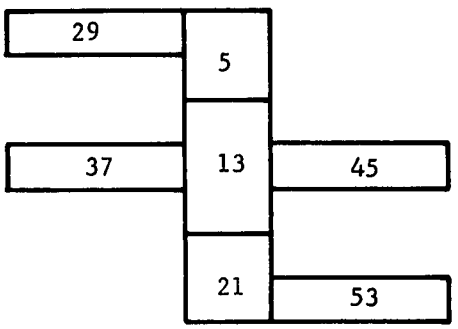

Time (sec)	Temperature (°R)		
5,580	462	504	
	505	507	457
		509	516
6,600	460	501	
	515	504	455
		506	514
7,800	477	503	
	516	505	473
		506	516
9,000	494	506	
	519	508	487
		509	519
10,200	479	506	
	518	508	475
		510	518
11,280	464	504	
	516	507	459
		509	516

Fig. III-16 Temperature Distribution within the Structure of Side 5 at Various Times during the Second Orbit

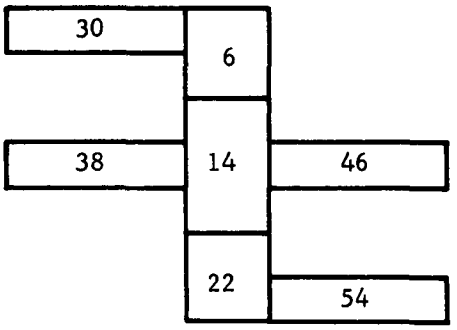

Time (sec)	Temperature (°R)		
5,580	447	497	
	513	501	439
		503	512
6,600	445	494	
	511	498	438
		500	511
7,800	458	495	
	512	498	452
		500	512
9,000	468	498	
	515	501	464
		503	514
10,200	459	498	
	514	501	453
		503	513

Fig. III-17 Temperature Distribution within the Structure of Side 6 at Various Times during the Second Orbit

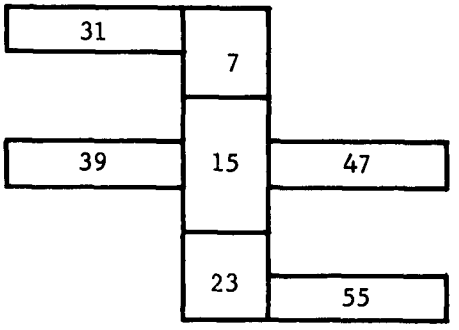

Time (sec)	Temperature (°R)		
5,580	420	484	
	506	489	409
		492	505
6,600	419	483	
	505	488	408
		491	504
7,800	424	482	
	505	487	414
		489	504
9,000	431	484	
	507	488	422
		491	506
10,200	421	484	
	506	489	412
		492	505
11,280	421	483	
	506	488	411
		491	505

Fig. III-18 Temperature Distribution within the Structure of Side 7 at Various Times during the Second Orbit

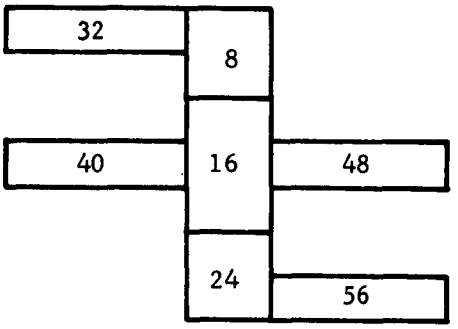

Time (sec)	Temperature (°R)		
5,580	403	484	
	505	490	388
		493	503
6,600	400	478	
	502	484	385
		488	500
7,800	437	479	
	503	483	426
		485	501
9,000	474	491	
	513	493	472
		495	512
10,200	416	489	
	510	495	407
		498	509
11,280	402	482	
	504	488	388
		491	502

Fig. III-19 Temperature Distribution within the Structure of Side 8 at Various Times during the Second Orbit

IV. MATERIALS

A. TEST PROGRAM PHILOSOPHY

The primary purpose of the ESS materials program is to obtain existing data describing materials that will be used in the ESS design, and to generate test data, when necessary, on the long-term compatibility of materials with a space environment.

A wealth of test data on materials is available describing the short-term performance of materials in a simulated space environment. However, in many areas the data are not applicable to the design of a space structure such as ESS, with a life expectancy of one year or more. All materials that are planned for the ESS design need not be tested. Only those materials whose degradation would affect the performance of the structure in space will be evaluated by test. For other materials, maximum use of materials information gathered as a result of testing by other agencies will be used.

Both metallic and nonmetallic candidate materials that will be tested have been chosen. The interim selections were made based on their short-term compatibilities with a space environment, their availability, and ease of fabrication. The candidate materials will be evaluated for physical and mechanical property changes after exposure to the operating environments of temperature, vacuum, and ultraviolet radiation.

B. MATERIALS TEST PROGRAM

The materials test program is divided into material category tests and tests involving composites of materials, as in the case of typical wall sections. Several categories of materials will be tested. Table IV-1 presents the candidates selected and the proposed tests.

Table IV-1 Proposed Materials Test Program

Materials and End Use	Environmental Exposure	Material Candidate	Tests	Proposed Designated Test Procedures
Rubber Impregnated Fabric	Hard Vacuum Ozone	1. Neoprene-Coated Dacron Fabric EX-2095	Breaking Strength Warp and Fill	CCC-T-191b Method 5100
			Peel Strength "T"	MMS-H-411
Internal Pressure Bladder	Heat Aging	2. 121-KP506	Low-Temperature Flexure	CC-T-191b-5874
		3. Polyurethane-Coated Dacron Fabric EX-2099	Tear Strength Warp and Fill	Fed Std 601-4211
			Permeability	ASTM D815
			Abrasion Resistance	CCC-T-191b-5306
		4. Hycar-Coated Dacron Fabric 139-KP509	Weight Change	Fed Std 601-6631 Mod
			Flammability	CCC-T-191b-5904
Insulation	Hard Vacuum	5. TG 15,000 AA Fiber	Thermal Conductivity	ASTM-C420 Mod
			Tensile Strength	ASTM-D62 Mod
			Edgewise Compression	None
Between Wall Thermal Insulation		NRC-2 Aluminum 6. Mylar	Vibration Resistance	Titan II Criteria
Gasket Materials	Hard Vacuum Ultraviolet Radiation	Polyurethane Rubber 7. EX-2099	Ultimate Tensile Strength	Fed Std 601-4111
			Ultimate Elongation %	Fed Std 601-4121
			Modulus at 300 psi	
Ring Frame Seals	Ozone	8. Neoprene Rubber EX-2095	Compression Set	Fed Std 601-3311
	Heat Aging	9. 121-KP506	Hardness Change	Fed Std 601-3021
		Hycar Rubber	Weight Change	Fed Std 601-6631
		10. 139-KP-509	Permeability	AS7M D815
Filled Teflon	Hard Vacuum Ultraviolet Radiation	11. Rulon - A	Ultimate Tensile Stength	ASTM D1457
			Ultimate Elongation %	ASTM D1417
Guide Rails and Rub Strips	Ozone		Weight Change	Fed Std 601-6631
			Coefficient of Friction	Mod LFW-1 Test
Sealants	Hard Vacuum Ozone	12. EC-1675	Lap Shear Strength	ASTM D816
			Permeability	ASTM-D815
Faying Surfaces	Heat Aging	13. Pro-Seal 793	Hardness Change	Fed Std 601-3021
			Weight Change	Fed Std 601-6631
		14. RTV-60		
Coatings	Hard Vacuum Ultraviolet Radiation	15. Methyl Silicone 63W	Adhesion	Fed Std 141-6301
			α/ϵ Measurements	None
Thermal Protective Coatings	Heat Aging Artificial Weathering	16. Inorganic Coating	Weight Change	Weight Determined on Dry Specimen
Nonstructural Adhesives	Hard Vacuum Heat Aging Low Temperature	17. Room Temperature Curing Epoxy	Lap Shear Strength	ASTM-D1002
Crack Propogation Aluminum Tests	Ambient	7075-T6 2024-T3 7079-T51	Long-Term Crack Propogation Ballistic Penetration Tear Test	None

Note:

Items 1, 3, 7, and 8 supplied by U. S. Rubber Company, Providence, Rhode Island.

Items 2, 4, 9, and 10 supplied by B. F. Goodrich Company, Akron, Ohio.

Item 5, Thompsoglas TG-15,000, AA Fiber, supplied by HI Thompson Fiberglas Company, Gardina, California.

Item 6, NRC-2 Aluminized Mylar supplied by Nation Research Corporation, Palo Alto, California.

Item 11, Rulon A ceramic-filled Teflon supplied by Dixon Corporation, Bristol, Rhode Island.

Item 12, EC 1675 supplied by 3M Company, St. Paul, Minnesota.

Item 13, Pro Seal 793, supplied by Coast Pre-Seal and Manufacturing Company, Compton, California.

Item 14, RTV-60, Supplied by General Electric Company, Waterford, New York.

Item 15, 63W Methyl Silicone Paint supplied by Ball Brothers Research Corporation, Boulder, Colorado.

Item 16, Inorganic Coating, formulated by Armour Research Foundation, Chicago, Illinois, Reference Interim Report No. Arf. 3207-14, November 1962.

Item 17, Epon 934 Epoxy Adhesive, Supplied by Shell Chemical Company, Pittsburg, California.

1. Insulation Tests

The thermal protection system planned for ESS requires a lightweight, efficient, insulation material. The material must be readily available, relatively easy to apply, and must withstand launch loads. The material candidates are a bonded fibrous material and a multilayer super insulation.

The purpose of the tests will be to determine the physical and mechanical properties of the materials. The physical property that will be determined is thermal conductivity vs temperature in a vacuum. The mechanical properties that will be determined are buckling strength, tensile strength, and vibration resistance. Installation tests will also be performed.

2. Rubber Impregnated Fabric Tests (Internal Pressure Bladder)

Bladder materials will be tested for solar heating, ozone, and exposure to high oxygen concentrations to determine changes in breaking strength, vulcanized bond strength, and tear strength. The changes in physical properties that will be determined are weight change, abrasion resistance, and permeability. The materials will also be tested for flexibility at operational temperatures. Folding characteristics of the rubberized fabric bladder will be determined to ensure proper operation on deployment of the telescoping sections.

3. Gasket Materials Test (Ring Frame Seals)

The object of the gasket material test will be to determine the property changes of elastomer materials after exposure to operating conditions. The environmental conditions are solar heating, hard vacuum, ultraviolet radiation, and ozone. The physical and mechanical property changes that will be determined are ultimate tensile strength, percent elongation, modulus, compression set, hardness change, weight loss, and permeability.

4. Thermal Protective Coating Tests

The thermal protective system planned for ESS requires a passive thermal protective coating to be applied to the exterior meteoroid bumper panels. The coating tests will determine the changes in physical and mechanical properties on exposure to launch heating, hard vacuum, ultraviolet radiation, temperature extremes of approximately -150 to 400°F, and weathering. The property changes to be determined in the coatings are changes in optical and thermal properties, weight changes, and changes in adhesive strength.

5. Teflon Guide and Rub Strips

The object of these tests is to determine the property changes of ceramic-filled Teflon after exposure to hard vacuum and ultraviolet radiation. The properties that will be investigated are ultimate tensile strength, percent elongation, and weight loss. A structural test will be performed to test the feasibility of the guide rail design.

6. Sealing Tests

The sealing tests will determine the performance of the various sealing systems necessary to completely seal the inner aluminum wall at joints and fasteners. These tests will be performed using a positive pressure of 15 psig. Additional tests will be performed on the sealant materials to determine the changes in properties after exposure to hard vacuum, heat, and ozone. The properties that will be evaluated are weight change, hardness change, and permeability.

In conjunction with the sealing tests, a program has been devised to determine the best methods of sealing the inner aluminum wall and the rubberized fabric cylinder in case of damage during flight. This investigation will test patch-sealing techniques, as well as rapid curing sealants.

7. Self-Sealing Tests

The self-sealing system may be used in two areas: within the plys of the rubber bladder, and along the inner aluminum wall. Various combinations of self-sealing materials and design concepts will be tested. The initial tests will be performed using simple puncture techniques; the final tests will use high speed particles.

8. Radiation Tests

Radiation testing of materials will not be required for reasons given in the following paragraphs.

In a 257 n mi orbit of 33.3 deg inclination Van Allen fringe doses are not expected to exceed approximately 1 rad/year, even during high solar flare activity. Total radiation dose is therefore not expected to exceed approximately 50 rad/year from all natural sources.

Any nonmetallic material will have a considerable lifetime before being affected by these radiations. For example, an elastomer whose threshold of radiation damage is 10^8 ergs/gr carbon (10^6 rad) should have a lifetime of approximately 10^5 years when considering only the natural radiation environment.

Considerations relative to the effect of space radiations on metals used in the expandable vehicle are even less significant.

V. FUNCTIONAL DEVELOPMENT TESTS

A. BLADDER MEMBRANE MODEL

A ¼-scale model test was devised to broadly determine folding characteristics of a self-sealing type double-wall bladder. A viscous sealant material was placed in the cavity of a double-wall sleeve to simulate a bladder of this type. The detail objectives of the test were to determine how severely folding would affect a viscous sealant material, and to determine folding characteristics of the sleeve.

The results of the test indicate that sharp creases caused by folding do not displace the sealant. However, on re-extending the model, separation can occur between the viscous sealant and the outer wall of the sleeve. It was found that the separations tend to heal after a short time under pressure inside the sleeve.

Also, the test indicated that the sleeve can be readily folded by applying a small vacuum inside the sleeve during contraction.

Figures V-1 thru V-5 are sequence photographs of the test. Figure V-6 shows sealant-outer wall separation.

The material used was a double layer of 0.010-in. thick Kel-F film. The cavity between the layers was filled with a thick solution of dyed plexiglas.

Fig. V-1 Model before Contraction, Sleeve Fully Extended

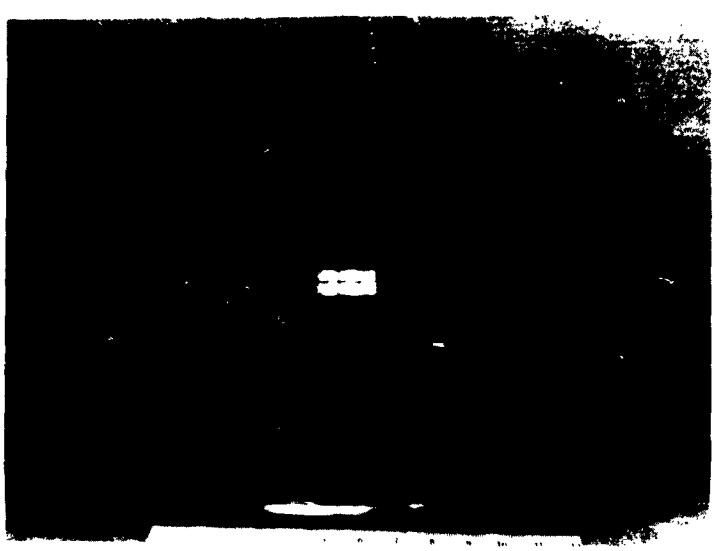

Fig. V-2 Model Partly Contracted, Sleeve Partly Folded

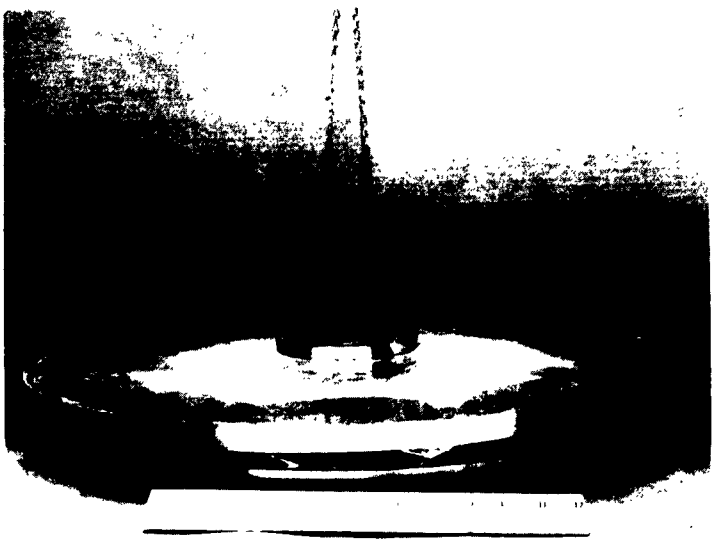

Fig. V-3 Model Fully Contracted

Fig. V-4 Top View of Model Fully Contracted

Fig. V-5 Model Extended after Full Contraction

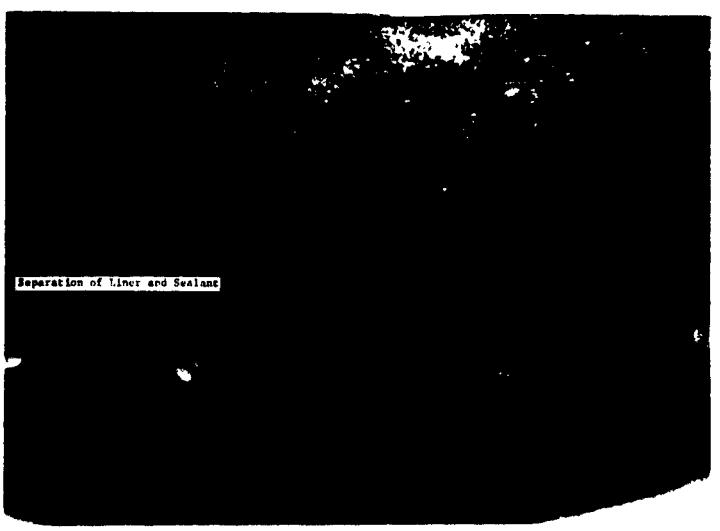

Fig. V-6 Close-up of Liner after Re-extension

B. FULL-SCALE OPERABLE MOCKUP

An operable mockup was designed and built to study the telescoping action of large diameter, thin-walled nested cylinders, and bladder action during contraction and expansion of the cylinders (Fig. V-7, V-8, and V-9). Air pressure of 0.05 psig was used to expand the cylinder.

Initial expansion and contraction tests were conducted to determine the tendency of the cylinders to bind. Pressure continuity between the cylinders was obtained by an arbitrarily chosen liner taped to the inner walls. During these tests, external forces were applied in an attempt to force the cylinders to bind. However, the cylinders realigned themselves in the direction of motion and continued to deploy.

Later, expansion and contraction tests were run to evaluate bladder folding action. In these tests a bladder material closely simulating that proposed for design was installed in the mockup. The bladder material was 0.022-in. thick, two-ply nèoprene coated nylon fabric.

The first test run in this series was made with a bungee cord attached to the bladder at eight places, equally spaced around the circumference (Fig. V-10 and V-11). During installation the cord was stretched to provide a 15-lb pull on the bungee when the bladder was fully expanded. This system required 0.10 psig internal pressure to expand the specimen. On reducing the pressure, the cord immediately began pulling the bladder away from the wall at the points where the cord was attached. The cord had no immediate effect at the re-entrant corner. The specimen failed to retract fully.

A second run performed without the cord also required 0.10 psig to expand the specimen. The retraction characteristics were very poor and the specimen did not fully retract.

A third run, also without the cord, was made with talc spread between the lower segment wall and the bladder. The internal pressure required to expand the specimen for this run dropped to 0.05 psig. The specimen fully retracted when the internal pressure was reduced (Fig. V-12).

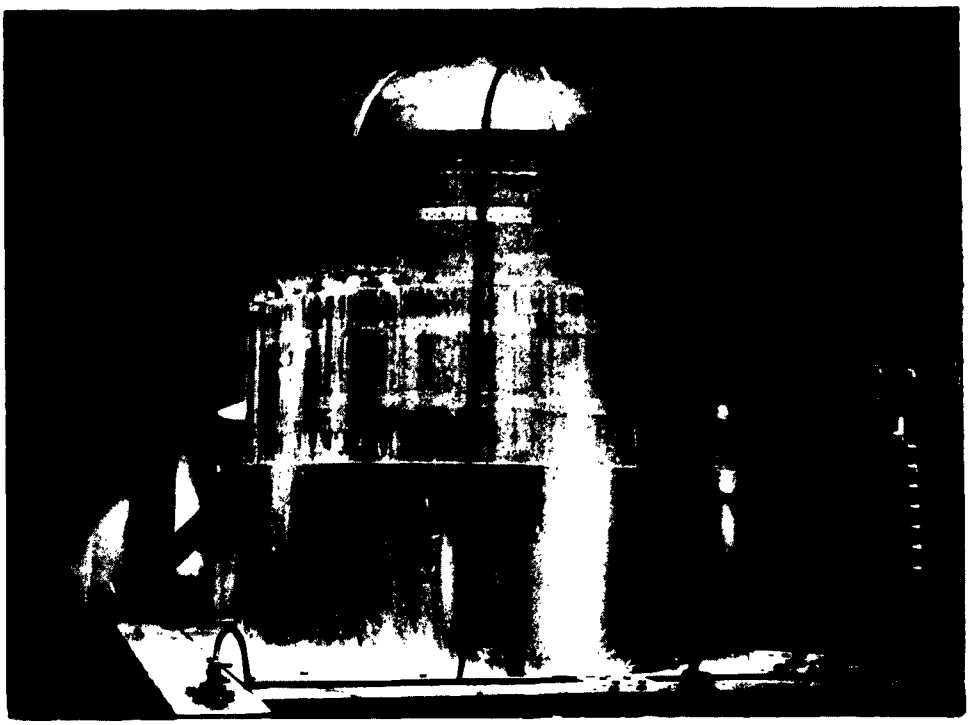

Fig. V-7 Operable Mockup in Expanded Position

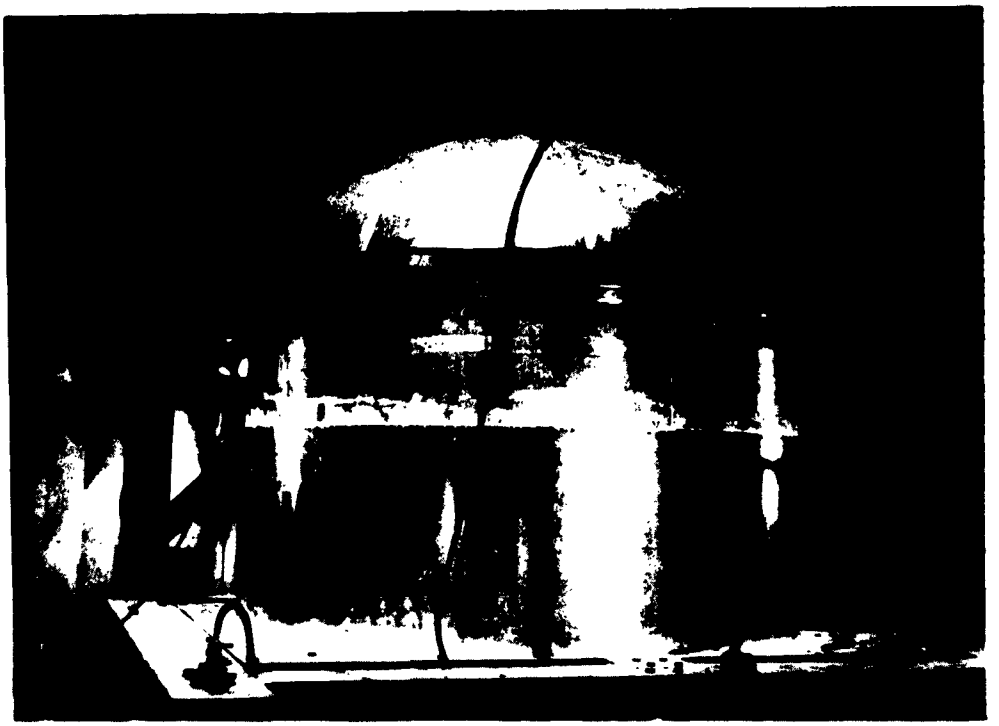

Fig. V-8 Operable Mockup in Contracted Position

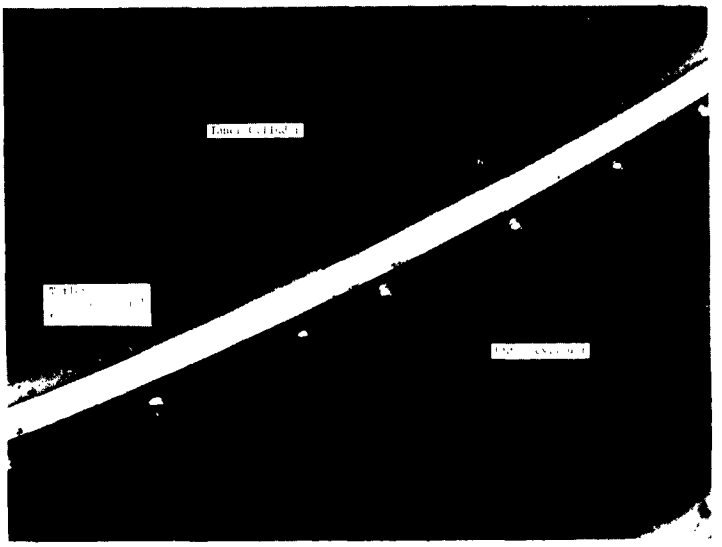

Fig. V-9 Close-up of Sliding Joint (Indentical Joint Exists at Base of Inner Cylinder)

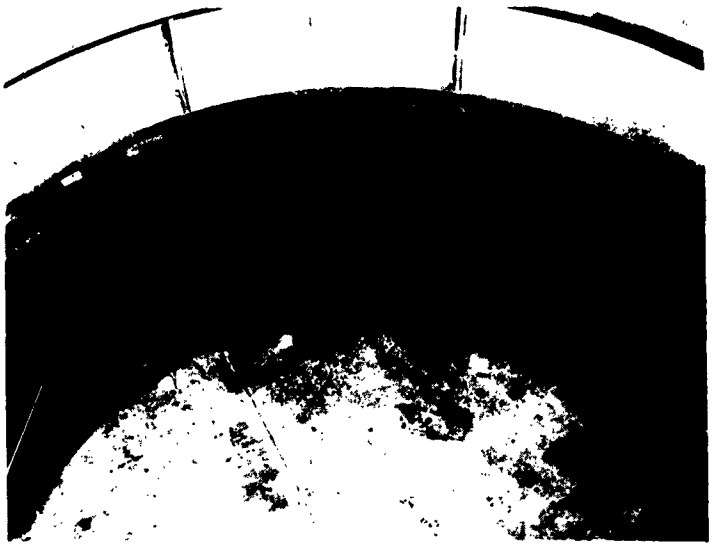

Fig. V-10 Two-Ply Neoprene-Impregnated Nylon Liner, 0.022-in. Thickness, Mockup Expanded with Bungee Cord Attached at Eight Places

Fig. V-11 Two-Ply Neoprene-Impregnated Nylon Liner, 0.022-in. Thickness, Liner Configuration after Mockup Contraction

Fig. V-12 Two-Ply Neoprene-Impregnated Nylon Liner, 0.022-in. Thickness, Bladder Configuration after Mockup Retraction, Talc between Wall and Liner

C. EXTENSION LOCK MODEL

An operable model of an extension lock is being fabricated to ascertain the design. See Section II for design requirements of the extension lock.

VI. MANUFACTURING AND TOOL DESIGN

The Manufacturing Division during Phase I has been studying methods and processes that may be used to fabricate detail parts and assemblies of the vehicle. The results of these studies have produced a relatively firm manufacturing plan that is based on evaluations of manufacturing feasibility and costs. Product quality and reliability have been paramount factors in the evaluation of alternative manufacturing methods and processes.

A. MANUFACTURING TESTS

In the large-diameter machined frames, control of tolerances of related diameters presents problems in material selection, control, and process planning. Preliminary manufacturing tests were conducted concerning these problems.

The first manufacturing feasibility test was performed by fabricating two 8-ft diameter ring frames, the cross sections simulating a potential ring frame design. The first ring was made of 2-in. thick 6061-T6 aluminum plate, sawed into four straight bars, sized, performed, and machined. This ring was fabricated without aid of stress-relieving or heat-treating operations. The second ring was made the same way, except that the material was 6061-T6 aluminum bar stock, and was stress-relieved between the rough and finish machining operations.

The most significant conclusions drawn from these tests are:

1) Dimensional tolerance in the machined frames would be unreliable when using machine stock fabricated by fusion-welding ring segments;

2) Dimensional tolerance control can be improved by stress-relieving the rough machined part before performing the finish machine operations.

Detail descriptions, photographs, and results of these tests are given in the appendix.

B. ASSEMBLY TOOLING - PRELIMINARY MANUFACTURING AND ASSEMBLY PLAN

Conclusions relative to tool design, obtained from results of the tests described previously, are that the methods to hold the rings are time consuming, inadequate, and unpredictable. The possibility of overstressing the rings during fabrication operations was great.

Subsequent tooling studies resulted in a design approach that permits the machine tool to function later as a part of the assembly fixture. This concept is shown in Fig. VI-1.

The concept permits the assembly in one fixture of the five cylindrical sections comprising the vehicle. After assembly of a section, the upper and lower tool rings remain with the section for handling. They are not removed until nesting of the five sections to form the vehicle.

Fig. VI-1 Assembly Fixture - Preliminary Concept

VII. VALUE ENGINEERING

The broad objective of the value engineering program is to insure the provision of a product that fulfills all its functional requirements at minimum cost, considering cost as the basic parameter.

Three major examples of the application of value engineering principles are found in decisions made to date on the forward closure, interlocking frames, and aft closure.

A. FORWARD CLOSURE

Cost avoidance, through the use of existing components, is demonstrated by the adoption of a salvaged dome. This dome, initially a test article in another program, had been inventoried for scrap and was available to any program that could use it. Examination of the dome revealed that it would be suitable for use in this program.

B. INTERLOCKING FRAMES

The interlocking frames present a problem in producibility. Obtaining tolerance control required to assure proper function of the frames presents a major problem, considering the sizes and shapes of the frames. The design calls for machining the frames from stress-relieved 7079 aluminum alloy ring-rolled forgings. Several other designs, modifications, and manufacturing techniques were evaluated on the basis of cost and producibility before the present design was selected.

Based on quantity, cost, and function, the machined-from-ring-rolled-forging design is the best method of producing the frames. However, the effectiveness of using stress-relieved material to achieve the required tolerances is subject to confirmation. A proper combination of stress relief and manufacturing technique is anticipated to yield frames within the required tolerance limits.

The aft closure design is an aluminum honeycomb sandwich structure. Based on cost, weight, function, reliability, and availability, the aluminum honeycomb structure was found to offer certain advantages over the other flat-closure designs considered.

VIII. CONCLUSIONS AND RECOMMENDATIONS

At this stage of Phase I, the conclusions and recommendations can be enumerated as critical problem areas and recommendations for future work.

A. PROBLEM AREAS

Critical problem areas that require solution before completion of Phase I are described in the following paragraphs.

Structural Sealing - The structural design must be compatible with the sealing method chosen to ensure a reliable secondary seal. Compatibility of sealants and sealant application processes with vacuum chamber testing may affect detail design of the vehicle.

Bladder Folding - Methods to control bladder folding during contraction of the vehicle have not been established. Talc placed between bladder and pressure wall to facilitate sealing may not be the final design choice.

Machined Frame Tolerance Control - Tolerance control, both diametrical and out-of-plane warping, is important from the standpoint of sliding action and reliable sealing. Previous tests of welded rings show that warping may be a problem in machined rings of this diameter and thickness due to residual stresses.

Cleanliness Requirements - Vacuum chamber testing will set the requirements for cleanliness of the structure rather than operational considerations.

B. RECOMMENDATIONS FOR FUTURE WORK IN PHASE I

Work items required for completion of Phase I, except as noted, are described in the following paragraphs.

1. Design

Formal engineering drawings of the vehicle will be completed and submitted for approval.

2. Analysis

The status of the following analyses is:

1) Loads, stress, and dynamics analyses will be completed;

2) Weight analysis and weight statements will be completed;

3) Orbital heating analyses will continue into the second quarter to firm-up requirements for thermal control. Definite need for thermal insulation and fiberglas components in the structure will be determined. Thermal coating requirements on external skin panels will be firmly established.

3. Materials Studies

Material studies are covering the following areas:

1) Thermal and mechanical properties of the two candidate insulation materials will be determined under vacuum conditions;

2) Structural sealants and sealant application processes now being called out on design drawings will be verified. Seven test panels for this testing were built during the first quarter;

3) Work will proceed on the 3-month environmental tests. Physical and mechanical properties of the materials will be determined in the "as received" condition, and specimens will be placed in environmental chambers for the initial 3-month exposures;

4) Self-sealing tests will begin using double-wall bladder material and wire puncture techniques;

5) Hand patch sealing tests for the bladder and the internal aluminum skin will proceed;

6) Bladder folding tests will continue as the design affects this area. These tests will include items such as folding varying thickness of bladder material for stowage.

4. Manufacturing

Two frames that will duplicate production parts will be machined to verify proposed designs and tolerance limitations. The frames will be machined from ring-rolled forgings that have specifications identical to those called out on design drawings.

Other manufacturing activities will include design support where required. Activities will include continued support relative to the 8-ft diameter operable mockup, fabrication of panels for materials testing, and the fabrication of an operable mockup of the extension locks discussed in Section IIC.

5. Test Plan

The test plan, establishing requirements for vehicle testing, will be started during February and completed during the quarter. Preparation of test procedures will begin during March.

Early in the quarter potential subcontractors for space simulator testing will be contacted, and cleanliness requirements, system interfaces, and structural interfaces affecting vehicle detail design will be determined. Schedule requirements will also be established on a preliminary basis.

APPENDIX

MANUFACTURING TESTS

A. RING FRAME MACHINING TEST - RING NO. 1

An 8-ft diameter ring was fabricated from 6061-T6 material to determine the metal reaction during processing. Figures A-1 thru A-6 are photographs of ring fabrication. The material used was 2 x 1 x 84-in. long bars sawed out of 1-in. plate stock. The process consisted of the following steps:

1) Four bars planed to rectangle cross section;

2) Bars slotted on the planer to dimensions on Fig. A-7;

3) Deburr;

4) Roll to 48-in. inside radius;

5) Trim ends to 73.750-in. inside length;

6) Bevel ends and weld into a ring;

7) Ring-roll and straighten;

8) Machine one surface, mill cutter;

9) Machine opposite surface and I.D. to dimensions on Fig. A-8;

10) Chem-Mill to remove 0.010 per surface;

11) Machine one surface, single point tool;

12) Force ring into nearly round shape, clamp on outside, machine inside diameter per Fig. A-9. Holding ring stationary, move clamps to inside, machine surface B and outside surfaces per Fig. A-9. Measure flatness and ovality runout;

13) Unclamp ring. Measure flatness and ovality runout;

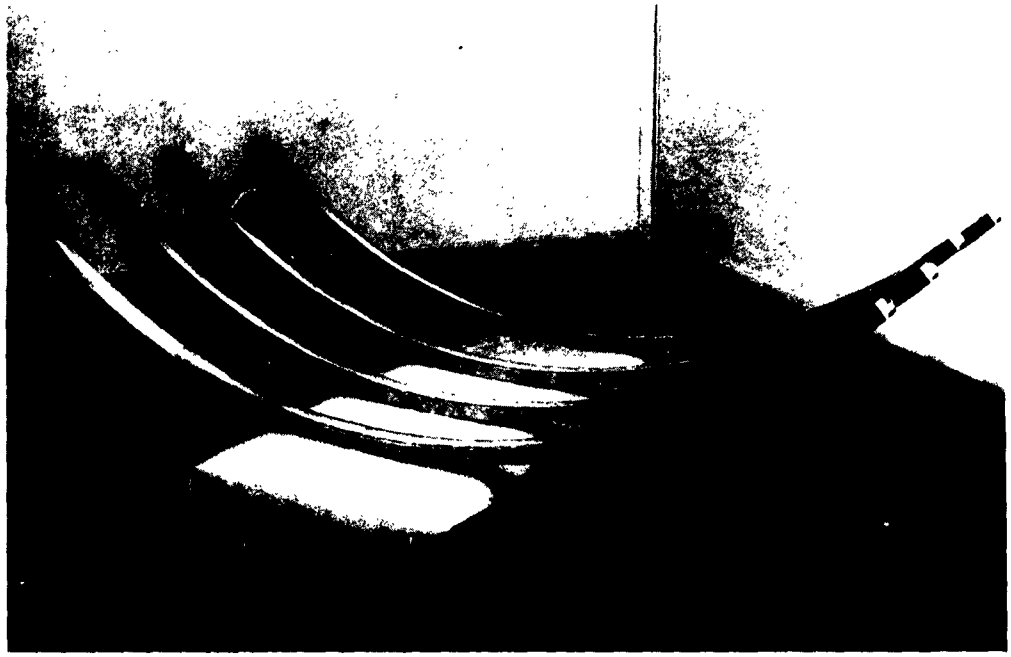

Fig. A-1 Frame Quadrants

Fig. A-2 Cross Sections of Frame Quadrants at Weld Preparations

Fig. A-3 Quadrants Prepared for Assembly by Fusion Welding

Fig. A-4 Quadrants Assembled and Readied for Welding

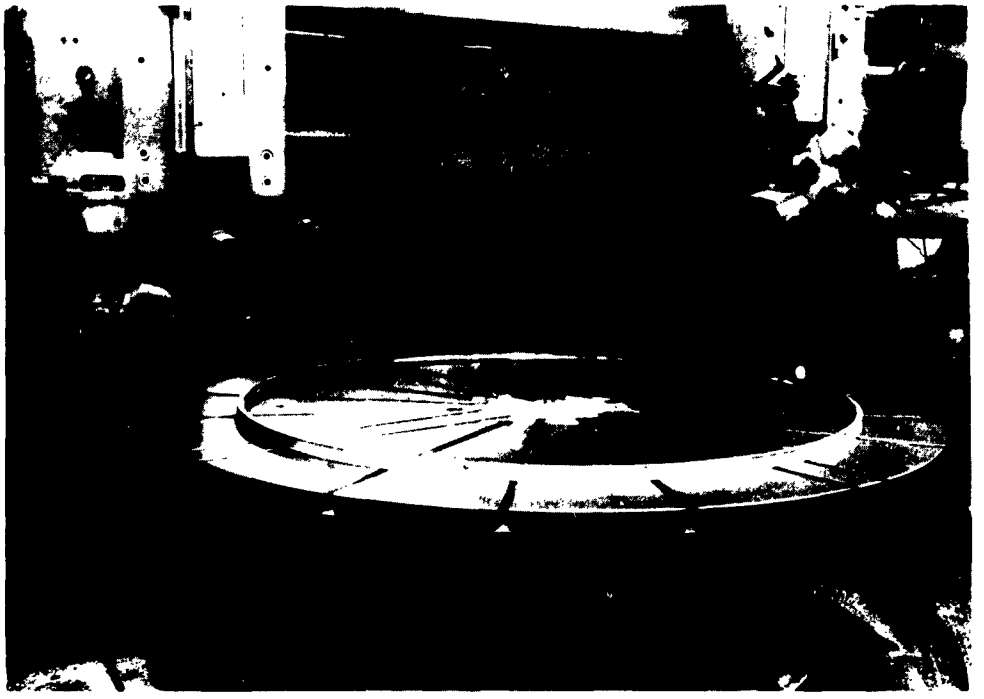

Fig. A-5 Frame Ready for Turning

Fig. A-6 Frame Being Machined

14) Rivet 0.040 x 3-in. skin to inside of ring. Measure outer diameter.

Steps 1, 2, 3, 4, 5, 6, and 7 - Due to the unsymmetrical cross section, the bars twisted during rolling. Hand straightening corrected the twist to allow work to continue. During welding the change in ring shape was readily visible as the weld joints cooled. Ring-rolling was not of value in rounding out the part because of the wide variation of metal strength in the weld zone as compared to the base metal. Again hand straightening was required. (All dimensions on Fig. A-7 thru A-14 are in inches unless otherwise noted.)

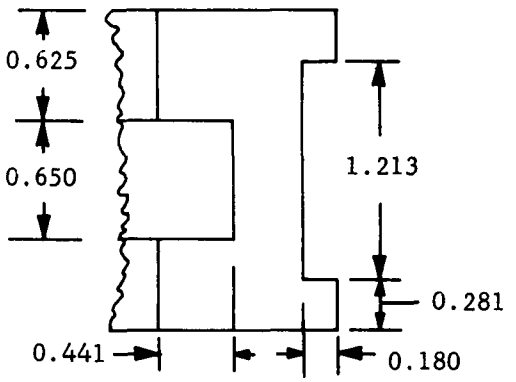

Fig. A-7 Slotted Cross Section

Step 8 - The ring was then positioned on the Betts vertical lathe. Shims were placed under the ring before clamping so that clamp pressure would not distort the part. Surface A (Fig. A-8) was machined to produce a flat surface. The machining was accomplished by a 2-1/2-in. diameter milling cutter on a Bridgeport head. Before machining, Surface A varied in height by 0.146 in. Metal was removed down to 0.005 in. under the lowest indicated point.

After machining surface A, a maximum of 0.003 in. variation was present when the ring was clamped down. On release of the clamps, with the ring still resting on the shims, a height variation of 0.022 in. was indicated.

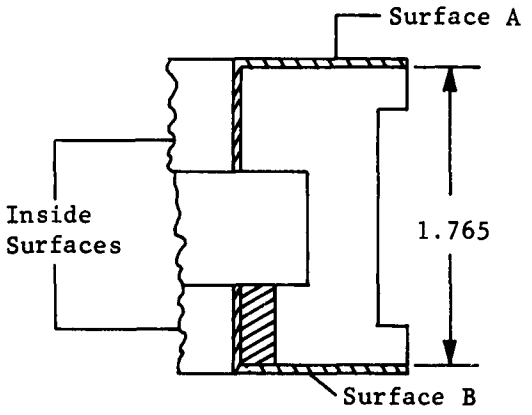

Fig. A-8 Initial Machining

Step 9 - The ring was turned over, placing surface A on the Betts table. With feeler gages, it was determined that the maximum gap between the ring and the table was 0.013 in. at one point. The ring contacted the table at 11 of the 16 approximately equally spaced points around the ring.

Being careful to prevent deforming the natural circular shape of the ring, it was centered on the table and clamped down. The inside surface indicated a total ovality runout of 0.140 in. Surface B and the inside surfaces were then machined per Fig. A-8, again using the milling head.

After machining the inside surfaces, ovality indicated 0.003 in. total runout.

Once again the clamps were to be repositioned to the opposite side of the ring. As the clamps were loosened, the ring moved about 1/8 in. until the fifteenth clamp was released, when it moved 1-in. With all clamps released and the ring resting on the Betts table, the following inside diameters were measured. The variation between the maximum and minimum inside diameter was 2 9/32 in.

Location	Inside Diameter (in.)
7-15	95 13/32
8-16	95 1/2
9-1	95 1/8
10-2	94 5/16
11-3	93 7/16
12-4	93 7/32
13-5	93 7/8
14-6	94 13/16

The weld joints are located at points 1 3/4, 5 3/4, 9 3/4, and 13 3/4.

Step 10 - The ring was chem-milled to remove 0.010 in. from all surfaces. After the operation, the cross-sectional height measured 1.738 to 1.744 in. Again the inside diameter and flatness were measured.

Location	Inside Diameter (in.)
7-15	95 15/32
8-16	95 9/16
9-1	95 3/32
10-2	94 3/16
11-3	93 9/32
12-4	93 7/32
13-5	94 1/16
14-6	94 31/32

The variation between the maximum and minimum inside diameter was 2 11/32 in. Flatness, measured with feeler gage between ring and Betts table was 0.021 in. maximum.

Step 11 - Without any attempt to round out the ring, it was centered on the Betts table, clamped down and turned to remove 0.030 in. from surface A (Fig. A-9) using a 0.030-in radius single point tool bit. The feed and depth of the cut was kept small to minimize strain input to the ring. After machining, and with the clamps released, the ring flatness was within 0.020 in.

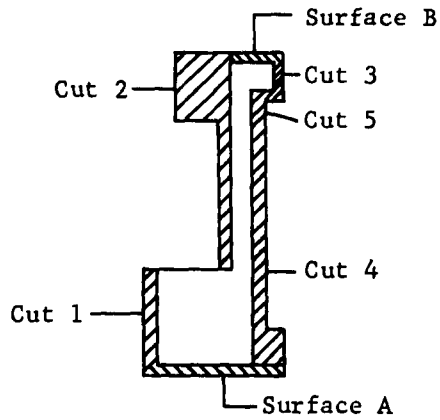

Fig. A-9 Final Machining

Step 12 - Sixteen location blocks were positioned on the Betts table and machined to provide true location and diameter points with relation to the machine and the ring. The ring was then forced over the blocks with surface A down. When the ring was clamped down, ovality runout at the clamps was 0.022 in., while runout midway between the clamps was 0.088 in. Machining was initiated with the premise that a single point, 0.030-in. radius tool bit would be used with light feeds and depth of cuts to clean up all surfaces and, if sufficient metal was present, to remove 0.030 in. below the cleanup point.

Cuts 1 and 2 (Fig. A-9) were made, then the clamps were changed to the inside, care was taken to prevent movement of the ring during the process. To be certain the ring did not move, the ring was indicated at each clamp location while changing the clamps. Surface B and cuts 3, 4, and 5 were then accomplished.

Before releasing of the clamps, the following flatness and ovality runout measurements were made (see Fig. A-10).

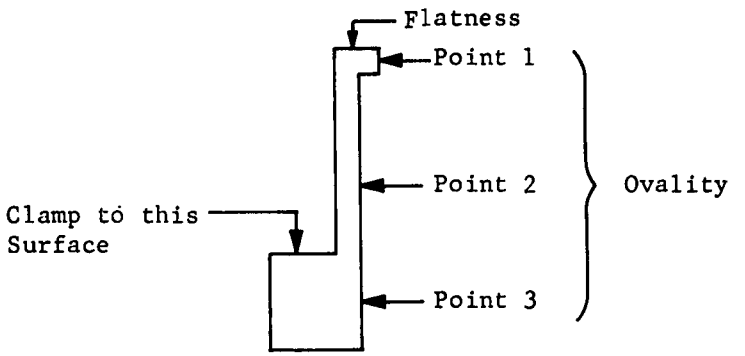

Fig. A-10 Measurement Locations

Quadrant	Flatness (in.)	Ovality (in.)		
		Point 1	Point 2	Point 3
1	0	0	0	0
2	0.001	-0.008	-0.001	0.001
3	0.013	-0.012	0.001	0.003
3-1/2	--	--	-0.005 min	--
4	0.008	-0.009	-0.003	0.002
5	0.004	-0.006	-0.002	0.002
5-1/2	--	--	--	0.005 max
6	0.002	0.003	0.001	-0.001
7	0	0	-0.002	0.001
8	0.002	-0.001	-0.002	0
9	0.001	-0.004	-0.002	0.002
10	0.002	-0.011	-0.003	0.002
10-1/2	--	-0.018 min	--	--
11	0.004	-0.009	-0.003	0.002
12	0.025	-0.008	-0.005 min	0.004
12-1/2	-0.008 min	--	--	--
13	0.004	-0.007	-0.003	0.001
13-1/2	0.028 max	--	--	--
14	-0.001	0	-0.001	0.001
15	-0.002	0.004	-0.002	0.001
16	0.003	0.025	0.005 max	-0.005 min
16-1/2	--	0.028 max	--	--
Variation	0.036	0.046	0.010	0.010

The outer diameter at the small flange of ring was measured as 95-9/16 in. by steel tape. The cross section dimensions are shown in Fig. A-11.

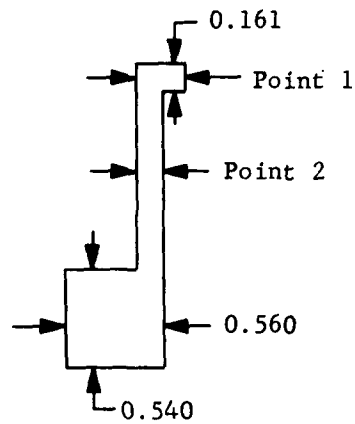

Fig. A-11 Cross Section Dimensions

Measurements indicated dimensions shown in the following tabulation:

Quadrant	Point 1 (in.)	Point 2 (in.)	Quadrant	Point 1 (in.)	Point 2 (in.)
1	0.263	0.139	9	0.267	0.142
2	0.265	0.144	10	0.265	0.143
3	0.273	0.155	11	0.269	0.145
4	0.279	0.155	12	0.276	0.149
5	0.277	0.151	13	0.276	0.142
6	0.265	0.139	14	0.268	0.140
7	0.267	0.140	15	0.270	0.148
8	0.270	0.144	16	0.278	0.134

Step 13 - All clamps were removed and again flatness and ovality was determined. Flatness was measured by use of feeler gages between the ring and the table. Flatness gage dimensions were:

Quadrant	Gage (in.)	Quadrant	Gage (in.)
1	0.025	9	0
2	0.005	10	0.010
3	0.033	11	0.039
4	0.015	12	0.043
5	0.005	13	0.013
6	0.015	14	0.046
7	0.025	15	0.069 max
8	0 min	16	0.039

Ovality small flange diameters were:

Location	Diameter (in.)
7-15	97 13/16
8-16	98 1/6
9-1	96 13/16
10-2	94 7/8
11-3	92 13/16
12-4	92 3/4
13-5	94 19/32
14-6	96 3/4

The variation between the maximum and minimum diameter was 5 5/16 in.

Step 14 - To the inside surface of the ring, a 0.040 x 3-in. skin was riveted using 3/32 in. annealed aluminum rivets located on 3/4 in. centers staggered 1/2 in. vertically. The rivets were squeeze upset.

Ovality small flange dimensions after riveting were:

Location	Diameter (in.)
7-15	97 27/32
8-16	98 1/8
9-1	97 3/32
10-2	95 1/4
11-3	93 1/32
12-4	92 25/32
13-5	94 3/8
14-6	96 21/32

The variation between the maximum and minimum diameter was 5 11/32 in.

Conclusions - Several conclusions appear valid in view of the results obtained. These are:

1) In the squaring up of the initial bars, it was necessary to cut them undersize due to crooked sawing when the bars were cut from the plate stock. Greater clean-up allowance should be present, preferably 3/16 in. per side;

2) Bars sawed from plate stock are not desirable, since each bar has residual rolling stresses which differ from those in the other bars. Bar stock is most desirable;

3) The bars should not be slotted unsymmetrically before rolling. This resulted in twisting during rolling;

4) Stress relieving is highly desirable to relieve the weld joint stresses. If the starting material is 6061-T6, stress relieving can be expected to effect the base metal properties;

5) Ring rolling is of no value if the ring has a metal characteristics variation as wide as welded sections have. In fact, rolling complicates the problem;

6) No proof of the effect of machining the ring with a milling cutter as compared to single, point turning could be ascertained;

7) By careful operation, it is practical to make a large diameter, thin ring, flat within 0.030 in., and on a special basis to 0.015 in. Considering the thinness of the ring, it is questionable as to how long this flatness could be retained through normal handling of the part;

8) Riveting of a thin skin to the ring with annealed rivets produced no distortion.

B. RING FRAME MACHINING TEST - RING NO. 2

The first test ring processed had a 5 11/32 in. variation in measured diameters. This variation was attributed to a number of factors. A second test ring was processed in a revised manner to prove that more nearly circular rings could be fabricated. The second ring has only a 13/32 in. variation between maximum and minimum diameters.

Starting material was 6061-T6 rectangular bar stock, 2 x 1 in. While adequate material was on hand to make an 8-ft diameter ring, the length of the three pieces was such that four sections could not be used. Three sections were welded together to form the ring. The complete process was as follows:

1) Trim three bars to 113 1/2 ± 1/4 in. length;

2) Roll form to 47 7/16-in. inside radius;

3) Layout to trim to 99 23/64 ± 1/64-in. inside length;

4) Trim to length;

5) Bevel bar ends and weld to form 94.875-in. I.D. ring, Remove excess weld bead;

Steps 1, 2, 3, 4, 5, 6, and 7 - No particular problems were encountered. The rolled bar sections were compared to the desired radius before welding and were found to be within 1/16 in. One bar end was twisted slightly in relation to the end butting against it when welded. This was attributed to the surface where the sections were laid, since it was not flat.

After stress relieving and some straightening, a distorted area was found. The area was approximately 0.100 in. out of round within a length of 12 in. Attempts to remove the distortion were not successful, resulting in removal of considerable metal at all other points around the inside surface during subsequent machining.

Step 8 - With the ring resting free on the Betts table, a height variation of 0.145 in. was indicated. Shims were placed between the ring and the table so that when clamps were applied, the ring was not distorted. After facing off the upper surface and removal of all clamps, the machined surface was flat within 0.011 in.

Step 9 - Resting freely on the Betts table, machined surface down, the maximum feeler gage which could be inserted between the table and ring was 0.008 in. at one point only.

Without distorting the ring, it was centered on the Betts table as closely as practical. After clamping down, the inside surface had a total ovality runout of 0.237 in., of which 0.108 in. was present in the single deformed area.

The inside surface was machined to completely clean up, then the initial roughing cut was made. All machining was performed with a single point tool bit.

Steps 10 and 11 - The clamps were relocated to the inside of the ring, thus clearing the top and outside surfaces for machining. The top and outside surfaces were machined. Due to the excessive metal removal required to clean up the inside and outside surface, the upper small flange was machined off, resulting in a cross section shown in Fig. A-14.

6) Stress relieve at 300°F for 4 hr and lay ring flat;

7) Straighten to correct roundness and flatness to ±1/32 in.;

8) Locate on Betts, face side 1 up for cleaning;

9) Turn ring over, center it on Betts table, turn I.D. to clean up, and turn I.D. to 19/32 in. and 7/16 in. per Fig. A-12;

10) Move clamps to inside of ring. (Restrain ring from movement while moving clamps.) Face top surface to 1.875 ± 0.010 in. height;

11) Turn O.D. to clean up, turn O.D. to 3/8 in. and 1/4 in. per Fig. A-12. Measure and record O.D. ovality;

12) Release clamps, measure, and record O.D. ovality;

13) Stress relieve at 300°F for 4 hr and lay ring flat;

14) Straighten ring to correct roundness and flatness to ±1/32 in.;

15) Center ring on Betts table, turn lower flange of I.D. to clean up, turn complete I.D. surface to produce dimensions per Fig. A-13;

16) Move clamps to inside of ring. (Restrain ring from movement while changing clamps.) Turn complete O.D. surface to produce dimensions per Fig. A-13.

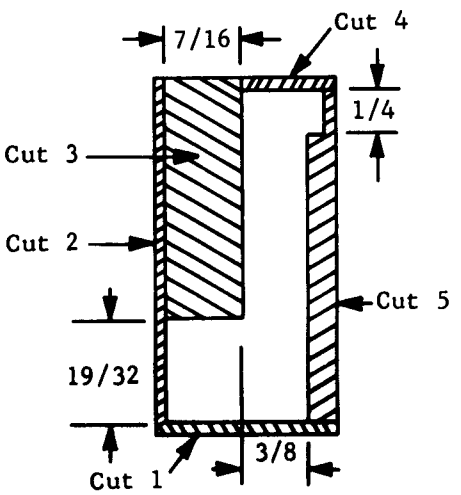

Fig. A-12 Rough Machining

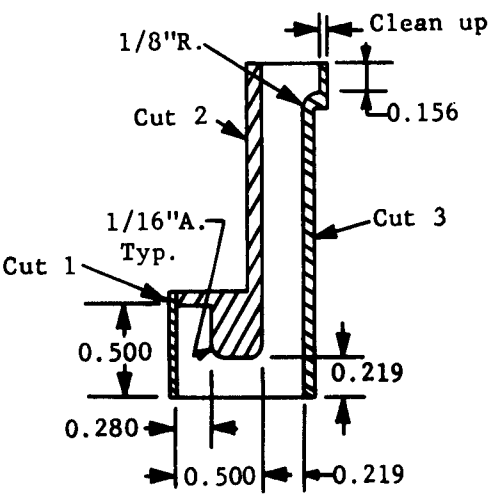

Fig. A-13 Finish Machining

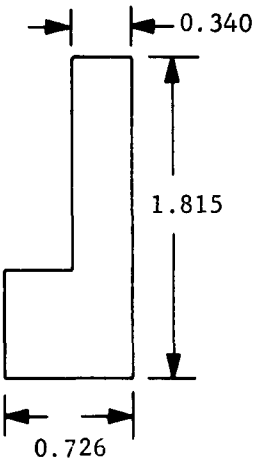

Fig. A-14 Rough Machining Completed

Step 12 - Before and after releasing the clamps, measurements of flatness and O.D. ovality runout were made. When the ring was initially placed on the Betts table, 16 location numbers corresponding to the centers between the tee slots of the table were marked on the ring. These numbers were retained through all operations and all measurements were made at these points. The measurements obtained were as follows:

Location	Clamped (in.)		Unclamped (in.)	
	Ovality	Flatness	Ovality	Flatness
1	0.300	0.201	0.990	0.300
2	0.302	0 201	0.630	0.308
3	0.300	0.201	0.400	0.314
3-1/2	-	-	0.315 min	-
4	0.301	0.203	0.370	0.315
4-1/2	0.292 min	-	-	-
5	0.301	0.201	0.710	0.307
6	0.303	0 204 max	0.890	0.317
7	0 302	0.202	0.925	0.315
8	0.303	0.202	0.850	0.305
9	0 301	0 202	0.680	0.289
9-1/2	0.305 max	-	-	-
10	0.300	0.202	0.615	0.301
11	0.302	0.201	0.570	0.298
12	0.303	0.201	0.485	0.296
13	0 302	0.201	0.620	0.314
13-1/2	-	-	-	0.330 max
14	0.302	0.202	0.780	0.327
15	0 302	0.201	0 940	0.310
16	0 303	0.200 min	1.110	0.292
16-1/2	-	-	1.165 max	0.281 min
Variation	0.013	0.004	0.850	0.049

O.D. measurments by steel tape were:

Location	O.D. (in.)
16-8	97 5/16 max
1-9	96 15/16
2-10	96 17/32
3-11	96 1/4
4-12	96 1/16 min
5-13	96 19/32
6-14	97
7-15	97 7/32

The variation between the maximum and minimum diameter was 1 1/4 in. Welds were located at 5-1/5, 10-1/2, and 16-1/5.

Step 13 - After stress relieving, the diameters were again measured. It was found that the maximum and minimum were still at locations 16-8 and 4-12, respectively, with a variation of 1 5/32 in.

To determine if any large change in metal physical properties occurred during the stress relieving operations, ends from the original rolled bar sections were processed along with the ring. Rockwell hardness measurements were made before and after the operations. An average increase in hardness from F-89 to F-91 was experienced.

Step 14 - Manual straightening was then performed on the ring. When placed on the Betts table, total ovality runout was 0.151 in. and flatness by feeler gage was 0.031 in.

Steel tape measurements of the O.D. was determined as follows:

Location	O.D. (in.)
16-8	96 21/32 min
1-9	96 11/16
2-10	96 11/16
3-11	96 3/4
4-12	96 13/16
5-13	96 13/16
6-14	96 27/32 max
7-15	96 23/32

The variation between the maximum and minimum diameter was 3/16 in.

Step 15 - Sixteen locating blocks were fixed to the Betts table and machined to the approximate I.D. of the ring. The ring was forced over these blocks to round it out, then clamps were applied to the outside of the ring. After clamping but before machining, the I.D. ovality runout was 0.076 in. After machining, the I.D. ovality runout was 0.010 in. Machining the lower flange inside surface to clean up was done first, then using this surface as a dimensioning base, all other inside surfaces were machined to the dimensions on Fig. A-13.

Step 16 - The clamps were moved from the outside to the inside of the ring while care was exercised to prevent the ring from moving. The O.D. was then machined to the clean-up point only, since insufficient material remained to produce the originally intended cross section. The final configuration dimensions are shown in Fig. A-15.

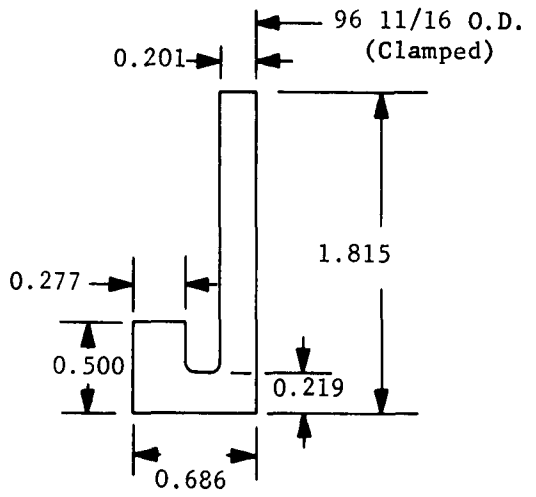

Fig. A-15 Final Configuration

Measurements of O.D. ovality and flatness were made in both the clamped and fully released positions. Since the upper surface was not machined, change in flatness values are given rather than the directly measured values.

Location	Ovality (in.)		Change in Flatness (in.)
	Clamped	Unclamped	
1	0 min	0.500	0
2	0.001	0.295	0.008
3	0.001	0.249	0.013
3-1/2	-	0.221	-
4	0.0005	0.275	0.013
5	0.001	0.382	0.001
6	0.001	0 345	0 011
6-1/2	-	0 240	-
7	0.001	0.283	0.008
8	0.001	0 257	0.007
9	0.001	0.285	0.006
10	0.001	0 365	-0.002
11	0.0007	0 381	0.012
12	0.0005	0.275	0.003
12-1/2	-	0.100	-
13	0.0007	0.047	0.023
13-1/2	-	0.039 min	0.021
14	0.001	0.072	0.031 max
15	0.001	0 197	0.007
16	0.0005	0 452	-0.005 min
16-1/2	0.0015 max	0 538 max	0.011
Variation	0 0015	0.499	0 036

O.D. measurements by steel tape were:

Location	O.D. (in.)
16-8	96 25/32
1-9	96 7/8 max
2-10	96 3/4
3-11	96 23/32
4-12	96 5/8
5-13	96 15/32 min
6-14	96 15/32
7-15	96 9/16

The variation between the maximum and minimum diameter was 13/32 in.

After 3 days storage on a rack with the 7-15 diameter being vertical, a change in ring diameters occurred. The variation was found to be 21/32 in. with the 2-10 and 6-14 diameters being maximum at 96 15/16 in. and minimum at 96 9/32 in., respectively.

To better illustrate the flexibility of the ring, the 6-14 diameter changed from 96 9/32 to 97 1/4 in. with the ring erected vertically so that the 6-14 diameter was parallel to the floor and only the weight of the ring acted as a compressive force.

Conclusions - The following conclusions appear valid as a result of processing this ring and comparing it to the initial ring:

1) When fabricating a thin-wall ring of this type, the following procedure is desirable:

   a) Start with bar stock of the longest practical length to minimize weld joints,

   b) Initial rolling should be done carefully to obtain as nearly a perfect section of a circle as can be produced,

c) Low temperature stress relieving reduces distortion and should be done at least after welding and after rough machining,

d) Manual straightening can be of value, but it is time consuming and requires an experienced, capable operator;

2) While a much better degree of roundness was achieved, the problem of making a ring to a definite diameter is still present. In each case, machining to a clean-up point has bettered roundness, but resulted in leaving insufficient metal to produce the desired configuration. To achieve both roundness and configuration for rings of this design, thoroughness in starting with properly rolled segments and care in manual straightening operations are necessities. Larger stock allowances should be made for diametrical dimensions than for dimensions parallel to the center axis, preferably 1/4 in. per side diametrically, and 3/16 in. per side axially;

3) To frequently fabricate rings of this nature, a minimum facilities requirement would be a large layout table that could accommodate 10-ft diameter rings and have a flat surface for alignment purposes during welding. This same table could provide the reference surface for straightening, and with portable hydraulic systems, straightening could be done right on the table;

4) Forcing the ring into a more round condition and then machining it should be avoided whenever possible. First, it is extremely difficult to make a ring round within 0.030 in., and second, the stress setup by forcing it into shape will not be dissipated during machining. Thus, on release, the ring will again distort;

5) The following tolerances appear feasible for a ring of this design:

	Normally (in.)	Special Basis (in.)
Flatness	0.030 max	0.015 max
Roundness	0.500 max	0.300 max
Diameters (clamped)	±0.015	±0.010

DISTRIBUTION LIST

DEPARTMENT OF THE AIR FORCE	NUMBER OF COPIES
ASD/ASRCTF (T. L. Campbell) Wright-Patterson AFB, Ohio	6
ASD/ASRMDS-21 (F. R. Barnett) Wright-Patterson AFB, Ohio	6
ASD/ASRC (Dr. Lovelace) Wright-Patterson AFB, Ohio	1
ASD/ASRCE (Mr. J. Teres) Wright-Patterson AFB, Ohio	1
ASD/ASRCE (Mrs. H. Ragen) Wright-Patterson AFB, Ohio	2
ASD/ASRCM Wright-Patterson AFB, Ohio	1
Armed Services Technical Information Agency ASTIA (TISIA-2) Arlington Hall Station Arlington 12, Virginia	29
SSD/SSRTH (Lt. Col. J. Clyde) AF Unit Post Office Los Angeles 45, California	1
SSD/SPRE-2 (Maj. W. Iller) AF Unit Post Office Los Angeles 45, California	1
Aerospace Corporation Attn: Mr. Ezra Hatcher Palo Alto, California	1
Foreign Technology Division (TB-E2B) Wright-Patterson AFB, Ohio	1
U.S.A.F., Directorate of Research & Development Attn: Lt. Col. J. B. Shipp, Jr. Room 4-D-313, The Pentagon Washington 25, D.C.	1

Hq AFSC (SCTAA Maj. Griswold) 1
Washington 25, D.C.

AFFTC 1
Edwards AFB, California

DEPARTMENT OF THE ARMY

Commander 1
Army Research Office
Arlington Mall Station
Arlington 12, Virginia

Chief of Research and Development 1
U.S. Army Research and Development Liaison Group
Attn: Dr. D. Stein
APO 757, New York, N.Y.

Office, Chief of Ordnance 1
Attn: OBDTE-Materials
Department of the Army
Washington 25, D.C.

Commanding General 1
U.S. Army Ballistic Missile Agency
Documentation and Technical Information Branch
ORDAB-IKE
Redstone Arsenal, Alabama

Command General 1
U.S. Army Rocket and Guided Missile Agency
ORDXR-RGS
Redstone Arsenal, Alabama

Command General 1
Ordnance Materials Research Office
Watertown Arsenal
RID
Watertown 72, Massachusetts

DEPARTMENT OF DEFENSE

Office of the Director of Defense Research & Engrg. 1
Attn: Mr. J. C. Barrett
Room 3D-1067, The Pentagon
Washington 25, D.C.

Advanced Research Project Agency 1
Attn: Dr. G. Hack
The Pentagon
Washington 25, D.C.

Defense Metals Information Center 1
Battelle Memorial Institute
505 King Avenue
Columbus 1, Ohio

DEPARTMENT OF THE NAVY

Department of the Navy 1
Office of Naval Research
Attn: Code 423
Washington 25, D.C.

Commander 1
U.S. Naval Research Laboratory
Attn: J. B. Strauley
Anacostia Station
Washington 25, D.C.

Department of the Navy 1
Special Projects Office
Attn: SP271
Washington 25, D.C.

GOVERNMENT AGENCIES

National Aeronautics & Space Administration 1
Attn: Mr. G. C. Deutch
Washington, D.C.

National Aeronautics & Space Administration 1
George C. Marshall Space Flight Center
Attn: M-8AM-M/Dr. W. Lucas
Huntsville, Alabama

National Aeronautics & Space Administration 1
Attn: Mr. Robert W. Leonard
Langley Research Center
Langley Field, Virginia

Jet Propulsion Laboratory 1
California Institute of Technology
Attn: Dr. L. Jaffe
4300 Oak Grove Drive
Pasadena, California

DEFENSE CONTRACTORS

Aerones Manufacturing Company 1
Technical Library
1712 Germantown Road
Middletown, Ohio

Aeronatronics 1
Division of Ford Motor Company
Technical Library
Ford Road
Newport Beach, California

AiResearch Manufacturing Company 1
Div. of The Garrett Corporation
9851-9951 Sepulveda Blvd.
Los Angeles 45, California

American Machine & Foundry Company 1
Attn: C. J. Muccolino
Stanford, Connecticut

Arthur D. Little, Inc. 1
Attn: Mr. R. S. Binekley
Acorn Park
Cambridge, Massachusetts

Avco Corporation 1
Nashville Division
Nashville 1, Tennessee

Bell Aerosystems Company 1
Technical Library
P.O. Box 1
Buffalo 5, New York

B. F. Goodrich Corporation 1
Aerospace & Defense Products
Akron, Ohio

The Boeing Company 1
Aerospace Division
Technical Library
Seattle, Washington

Ling Temco-Vought, Inc. 1
Chance Vought Corporation
Attn: J. Millsap
P.O. Box 5907
Dallas 22, Texas

Chrysler Corporation 1
Missile Division
Technical Library
P.O. Box 2628
Detroit 31, Michigan

Curtiss-Wright Corporation 1
Wright Aeronautical Division
Technical Library
Wood-Ridge, New Jersey

Douglas Aircraft Company, Inc. 1
Missiles & Space Systems Division
Technical Library
3000 Ocean Park Blvd.
Santa Monica, California

General Dynamics Corporation 1
Astronautics Division
Technical Library
Mail Zone 580-60X
P.O. Box 1128
San Diego 12, California

General Electric Corporation 1
MSVD
Valley Forge Space Technology Center
P.O. Box 8555
Philadelphia 1, Pennsylvania

Goodyear Aircraft Corporation 1
Attn: P. Baldwin
Akron, Ohio

Grumman Aircraft Corporation 1
Bethpage, L.I., New York

G. T. Sehjeddahl Company 1
Northfield, Minnesota

Hughes Aircraft Division 1
Technical Library
Florence & Teale Streets
Culver City, California

Lockheed-California Company 1
Division of Lockheed Aircraft Corp.
Attn: R. B. Liddell
Burbank, California

Marquardt Aircraft Corporation 1
Technical Library
16555 Saticoy Street
Van Nuys, California

McDonnell Aircraft Corporation 1
Technical Library
P.O. Box 516
St. Louis 3, Missouri

Narmco 1
Division of Telecomputing
8125 Aero Drive
San Diego, California

North American Aviation, Inc. 1
Attn: R. H. Crotaley, Mgr. of Applied Science
International Airport
Los Angeles 45, California

Northrop Corporation 1
Norair Division
Attn: G. Mangurin
1001 E. Broadway
Hawthorne, California

Radio Corporation of America 1
Astro-Electronics Division
Princeton, New Jersey

Republic Aviation Corporation Technical Library Farmingdale, L.I., New York	1
Ryan Aeronautical Company Technical Library 2701 Barbor Drive San Diego 12, California	1
Space-General Corporation Div. of Aerojet General Attn: R. Brodsky El Monto, California	1
U.S. Rubber Company Research Center Wayne, New Jersey	1

Aeronautical Systems Division
Wright-Patterson Air Force Base, Ohio
Rpt Nr ASD-TDR-7-943a(1). EXPANDABLE SPACE STRUCTURE
Interim Technical Documentary Report. Feb 63, 144 p, incl. illus., Tables.

Unclassified Rpt.

The needs and requirements for expandable semirigid space structures are discussed and problem areas described. A representative space mission profile is defined at an altitude of 257 n mi and 33.3 deg inclination. Preliminary design criteria, including structural loads and space environmental conditions, are established. Effects of thermal radiation, meteoroids, and space radiation are discussed. Results of thermal heat balance analyses programed on the IBM 7090 are presented. Structural safety factors are defined. A structural configuration is chosen from the standpoints of strength, operational reliability, manufacturing feasibility, and minimum weight and cost. Preliminary tooling and fabrication studies are described.

1. Space Station, Expandable
2. Materials, Evaluation
3. Materials, Machining
4. Materials, Testing
5. Meteoroid Puncture
6. Heating, Solar
7. Bladders, Pressure

I. ASD Project Nr. 7-943a and 1368
II. Contract AF33(657)-9733
III. Martin Company, Denver, Colorado
IV. Knox, P.M., Corell, A. Lane, E.
V. ASD-CR-63-4
VI. Not in ASTIA collection.

Aeronautical Systems Division
Wright-Patterson Air Force Base, Ohio
Rpt Nr ASD-TDR-7-943a(1). EXPANDABLE SPACE STRUCTURE
Interim Technical Documentary Report. Feb 63, 144 p, incl. illus., Tables.

Unclassified Rpt.

The needs and requirements for expandable semirigid space structures are discussed and problem areas described. A representative space mission profile is defined at an altitude of 257 n mi and 33.3 deg inclination. Preliminary design criteria, including structural loads and space environmental conditions, are established. Effects of thermal radiation, meteoroids, and space radiation are discussed. Results of thermal heat balance analyses programed on the IBM 7090 are presented. Structural safety factors are defined. A structural configuration is chosen from the standpoints of strength, operational reliability, manufacturing feasibility, and minimum weight and cost. Preliminary tooling and fabrication studies are described.

1. Space Station, Expandable
2. Materials, Evaluation
3. Materials, Machining
4. Materials, Testing
5. Meteoroid Puncture
6. Heating, Solar
7. Bladders, Pressure

I. ASD Project Nr. 7-943a and 1368
II. Contract AF33(657)-9733
III. Martin Company, Denver, Colorado
IV. Knox, P.M., Corell, A. Lane, E.
V. ASD-CR-63-4
VI. Not in ASTIA collection.

Aeronautical Systems Division
Wright-Patterson Air Force Base, Ohio
Rpt Nr ASD-TDR-7-943a(1). EXPANDABLE SPACE STRUCTURE
Interim Technical Documentary Report. Feb 63, 144 p, incl. illus., Tables.

Unclassified Rpt.

The needs and requirements for expandable semirigid space structures are discussed and problem areas described. A representative space mission profile is defined at an altitude of 257 n mi and 33.3 deg inclination. Preliminary design criteria, including structural loads and space environmental conditions, are established. Effects of thermal radiation, meteoroids, and space radiation are discussed. Results of thermal heat balance analyses programed on the IBM 7090 are presented. Structural safety factors are defined. A structural configuration is chosen from the standpoints of strength, operational reliability, manufacturing feasibility, and minimum weight and cost. Preliminary tooling and fabrication studies are described.

1. Space Station, Expandable
2. Materials, Evaluation
3. Materials, Machining
4. Materials, Testing
5. Meteoroid Puncture
6. Heating, Solar
7. Bladders, Pressure

I. ASD Project Nr. 7-943a and 1368
II. Contract AF33(657)-9733
III. Martin Company, Denver, Colorado
IV. Knox, P.M., Corell, A. Lane, E.
V. ASD-CR-63-4
VI. Not in ASTIA collection.

Aeronautical Systems Division
Wright-Patterson Air Force Base, Ohio
Rpt Nr ASD-TDR-7-943a(1). EXPANDABLE SPACE STRUCTURE
Interim Technical Documentary Report. Feb 63, 144 p, incl. illus., Tables.

Unclassified Rpt.

The needs and requirements for expandable semirigid space structures are discussed and problem areas described. A representative space mission profile is defined at an altitude of 257 n mi and 33.3 deg inclination. Preliminary design criteria, including structural loads and space environmental conditions, are established. Effects of thermal radiation, meteoroids, and space radiation are discussed. Results of thermal heat balance analyses programed on the IBM 7090 are presented. Structural safety factors are defined. A structural configuration is chosen from the standpoints of strength, operational reliability, manufacturing feasibility, and minimum weight and cost. Preliminary tooling and fabrication studies are described.

1. Space Station, Expandable
2. Materials, Evaluation
3. Materials, Machining
4. Materials, Testing
5. Meteoroid Puncture
6. Heating, Solar
7. Bladders, Pressure

I. ASD Project Nr. 7-943a and 1368
II. Contract AF33(657)-9733
III. Martin Company, Denver, Colorado
IV. Knox, P.M., Corell, A. Lane, E.
V. ASD-CR-63-4
VI. Not in ASTIA collection.

Aeronautical Systems Division
Wright-Patterson Air Force Base, Ohio
Rpt Nr ASD-TDR-7-943a(1). EXPANDABLE SPACE STRUCTURE
Interim Technical Documentary Report. Feb 63, 144 p, incl. illus., Tables.

Unclassified Rpt.

The needs and requirements for expandable semirigid space structures are discussed and problem areas described. A representative space mission profile is defined at an altitude of 257 n mi and 33.3 deg inclination. Preliminary design criteria, including structural loads and space environmental conditions, are established. Effects of thermal radiation, meteoroids, and space radiation are discussed. Results of thermal heat balance analyses programed on the IBM 7090 are presented. Structural safety factors are defined. A structural configuration is chosen from the standpoints of strength, operational reliability, manufacturing feasibility, and minimum weight and cost. Preliminary tooling and fabrication studies are described.

1. Space Station, Expandable
2. Materials, Evaluation
3. Materials, Machining
4. Materials, Testing
5. Meteoroid Puncture
6. Heating, Solar
7. Bladders, Pressure

I. ASD Project Nr. 7-943a and 1368
II. Contract AF33(657)-9733
III. Martin Company, Denver, Colorado
IV. Knox, P.M., Corell, A. Lane, E.
V. ASD-CR-63-4
VI. Not in ASTIA collection.

Aeronautical Systems Division
Wright-Patterson Air Force Base, Ohio
Rpt Nr ASD-TDR-7-943a(1). EXPANDABLE SPACE STRUCTURE
Interim Technical Documentary Report. Feb 63, 144 p, incl. illus., Tables.

Unclassified Rpt.

The needs and requirements for expandable semirigid space structures are discussed and problem areas described. A representative space mission profile is defined at an altitude of 257 n mi and 33.3 deg inclination. Preliminary design criteria, including structural loads and space environmental conditions, are established. Effects of thermal radiation, meteoroids, and space radiation are discussed. Results of thermal heat balance analyses programed on the IBM 7090 are presented. Structural safety factors are defined. A structural configuration is chosen from the standpoints of strength, operational reliability, manufacturing feasibility, and minimum weight and cost. Preliminary tooling and fabrication studies are described.

1. Space Station, Expandable
2. Materials, Evaluation
3. Materials, Machining
4. Materials, Testing
5. Meteoroid Puncture
6. Heating, Solar
7. Bladders, Pressure

I. ASD Project Nr. 7-943a and 1368
II. Contract AF33(657)-9733
III. Martin Company, Denver, Colorado
IV. Knox, P.M., Corell, A. Lane, E.
V. ASD-CR-63-4
VI. Not in ASTIA collection.

Aeronautical Systems Division
Wright-Patterson Air Force Base, Ohio
Rpt Nr ASD-TDR-7-943a(1). EXPANDABLE SPACE STRUCTURE
Interim Technical Documentary Report. Feb 63, 144 p, incl. illus., Tables.

Unclassified Rpt.

The needs and requirements for expandable semirigid space structures are discussed and problem areas described. A representative space mission profile is defined at an altitude of 257 n mi and 33.3 deg inclination. Preliminary design criteria, including structural loads and space environmental conditions, are established. Effects of thermal radiation, meteoroids, and space radiation are discussed. Results of thermal heat balance analyses programed on the IBM 7090 are presented. Structural safety factors are defined. A structural configuration is chosen from the standpoints of strength, operational reliability, manufacturing feasibility, and minimum weight and cost. Preliminary tooling and fabrication studies are described.

1. Space Station, Expandable
2. Materials, Evaluation
3. Materials, Machining
4. Materials, Testing
5. Meteoroid Puncture
6. Heating, Solar
7. Bladders, Pressure

I. ASD Project Nr. 7-943a and 1368
II. Contract AF33(657)-9733
III. Martin Company, Denver, Colorado
IV. Knox, P.M., Corell, A. Lane, E.
V. ASD-CR-63-4
VI. Not in ASTIA collection.

Aeronautical Systems Division
Wright-Patterson Air Force Base, Ohio
Rpt Nr ASD-TDR-7-943a(1). EXPANDABLE SPACE STRUCTURE
Interim Technical Documentary Report. Feb 63, 144 p, incl. illus., Tables.

Unclassified Rpt.

The needs and requirements for expandable semirigid space structures are discussed and problem areas described. A representative space mission profile is defined at an altitude of 257 n mi and 33.3 deg inclination. Preliminary design criteria, including structural loads and space environmental conditions, are established. Effects of thermal radiation, meteoroids, and space radiation are discussed. Results of thermal heat balance analyses programed on the IBM 7090 are presented. Structural safety factors are defined. A structural configuration is chosen from the standpoints of strength, operational reliability, manu acturing feasibility, and minimum weight and cost. Preliminary tooling and fabrication studies are described.

1. Space Station, Expandable
2. Materials, Evaluation
3. Materials, Machining
4. Materials, Testing
5. Meteoroid Puncture
6. Heating, Solar
7. Bladders, Pressure

I. ASD Project Nr. 7-943a and 1368
II. Contract AF33(657)-9733
III. Martin Company, Denver, Colorado
IV. Knox, P.M., Corell, A. Lane, E.
V. ASD-CR-63-4
VI. Not in ASTIA collection.

MARTIN COMPANY

DENVER
DIVISION
Denver 1,
Colorado

25 March 1963

TO: All Holders of Expandable Space Structure Report No. ASD-TDR-7-943(a)1.

SUBJECT: Errata Sheet for Expandable Space Structure Interim Technical Documentary Report

ENCLOSURE: a) Errata Sheet for Report

b) Corrected Mailing List for Report

Attached to this letter is a copy of Enclosure (a) Errata sheet, and (b) Corrected Mailing List. Please attach Enclosure (a) to your copy of the report, and replace the original mailing list with Enclosure (b).

P. M. Knox, Program Manager
Expandable Space Structure

THE AEROSPACE
DIVISION OF
MARTIN
MARIETTA

Enclosure (a)

Errata Sheet

for

Report No. ASD-TDR-7-943(a)1

1) Page I-3, Paragraph 6, 1st line should read ".....Manned Orbital Development System.....".

2) Page II-12, "Van Allen Electronics" should read "Van Allen Electrons."

3) Page II-24, Bottom arrow of V_E should extend to same surface as V_C bottom arrow.

4) Page II-47, Line 7 (in.) should be ($in.^2$).

5) Figure III-4, Note should read "Shield weight equals 0.864....."

6) Page IV-3, Paragraph 1, last sentence. Replace word "fibrous" with "multilayer."

7) Page VI-1, Paragraph 3, second sentence. Word "performed" should be "preformed."

DISTRIBUTION LIST

Contract AF 33(657)-9733
Project No. 7-943a
1 February 1963

DEPARTMENT OF THE AIR FORCE	NUMBER OF COPIES
ASD/ASRCTF (T. L. Campbell) Wright-Patterson AFB, Ohio	6
ASD/ASRMDS-21 (F. E. Barnett Wright-Patterson AFB, Ohio	6
ASD/ASRC (Dr. Levelace) Wright-Patterson AFB, Ohio	1
ASD/ASRCE (Mr. J. Teres) Wright-Patterson AFB, Ohio	1
ASD/ASRCE (Mrs. H. Ragen) Wright-Patterson AFB, Ohio	2
ASD/ASRCM Wright-Patterson AFB, Ohio	1
Armed Services Technical Information Agency ASTIA (TISIA-2) Arlington Hall Station Arlington 12, Virginia	29
SSD/SSRTH (Lt. Col. J. Clyde) AF Unit Post Office Los Angeles 45, California	1
SSD/SPRE-2 (Maj. W. Iller) AF Unit Post Office Los Angeles 45, California	1
Aerospace Corporation Attn: Mr. Ezra Hatcher Palo Alto, California	1
Foreign Technology Division (TB-E2B) Wright-Patterson AFB, Ohio	1
U.S.A.F., Directorate of Research & Development Attn: Lt. Col. J. B. Shipp, Jr. Room 4-D-313, The Pentagon Washington 25, D. C.	1

	NUMBER OF COPIES
Hq AFSC (SCTAA Maj. Griswold) Washington 25, D. C.	1
AFFTC Edwards AFB, California	1
DEPARTMENT OF THE ARMY	
Commander Army Research Office Arlington Hall Station Arlington 12, Virginia	1
Chief of Research and Development U. S. Army Research and Development Liaison Group Attn: Dr. B. Stein APO 757, New York, N. Y.	1
Office, Chief of Ordnance Attn: ORDTB-Materials Department of the Army Washington 25, D. C.	1
Commanding General U.S. Army Ballistic Missile Agency Documentation and Technical Information Branch ORDAB-IKE Redstone Arsenal, Alabama	1
Commanding General U.S. Army Rocket and Guided Missile Agency ORDXR-RGS Redstone Arsenal, Alabama	1
Commanding General Ordnance Materials Research Office Watertown Arsenal RPD Watertown 72, Massachusetts	1
DEPARTMENT OF DEFENSE	
Office of the Director of Defense Research & Engrg. Attn: Mr. J. C. Barrett Room 3D-1067, The Pentagon Washington 25, D. C.	1

	NUMBER OF COPIES
Advanced Research Project Agency Attn: Dr. G. Mack The Pentagon Washington 25, D. C.	1
Defense Metals Information Center Battelle Memorial Institute 505 King Avenue Columbus 1, Ohio	1
DEPARTMENT OF THE NAVY	
Department of the Navy Office of Naval Research Attn: Code 423 Washington 25, D. C.	1
Commander U.S. Naval Research Laboratory Attn: J. E. Srauley Anacostia Station Washington 25, D. C.	1
Department of the Navy Special Projects Office Attn: SP271 Washington 25, D. C.	1
GOVERNMENT AGENCIES	
National Aeronautics & Space Administration Attn: Mr. G. C. Deutch Washington, D. C.	1
National Aeronautics & Space Administration George C. Marshall Space Flight Center Attn: M-S&M-M/Dr. W. Lucas Huntsville, Alabama	1
NASA Attn: Mr. Robert W. Leonard Langley Research Center Langley Field, Virginia	1

	NUMBER OF COPIES
Jet Propulsion Laboratory California Institute of Technology Attn: Dr. L. Jaffe 4800 Oak Grove Drive Pasadena, California	1

DEFENSE CONTRACTORS

Aerenca Manufacturing Company Technical Library 1712 Germantown Road Middletown, Ohio	1
Aeronutronics Division of Ford Motor Company Technical Library Ford Road Newport Beach, California	1
AiResearch Manufacturing Company Div. of The Garrett Corporation 9851-9951 Sepulveda Blvd. Los Angeles 45, California	1
American Machine & Foundry Company Attn: C. J. Muscolino Stamford, Connecticut	1
Arthur D. Little, Inc. Attn: Mr. R. B. Hinckley Acorn Park Cambridge, Massachusetts	1
AVCO Corporation Nashville Division Nashville 1, Tennessee	1
Bell Aerosystems Company Technical Library P. O. Box 1 Buffalo 5, New York	1
B. F. Goodrich Corporation Aerospace & Defense Products Akron, Ohio	1

	NUMBER OF COPIES
The Boeing Company Aerospace Division Technical Library Seattle, Washington	1
Ling Temco-Vought, Inc. Chance Vought Corporation Attn: J. Millsap P. O. Box 5907 Dallas 22, Texas	1
Chrysler Corporation Missile Division Technical Library P. O. Box 2628 Detroit 21, Michigan	1
Curtiss-Wright Corporation Wright Aeronautical Division Technical Library Wood-Ridge, New Jersey	1
Douglas Aircraft Company, Inc. Missiles & Space Systems Division Technical Library 3000 Ocean Park Blvd. Santa Monica, California	1
General Dynamics Corporation Astronautics Division Technical Library Mail Zone 580-60X P. O. Box 1128 San Diego 12, California	1
General Electric Corporation MSVD Valley Forge Space Technology Center P. O. Box 8555 Philadelphia 1, Pennsylvania	1
Goodyear Aircraft Corporation Attn: F. Baldwin Akron, Ohio	1

	NUMBER OF COPIES
Grumman Aircraft Corporation Bethpage, L. I., New York	1
G. T. Schjeldahl Company Northfield, Minnesota	1
Hughes Aircraft Division Technical Library Florence & Teale Streets Culver City, California	1
Lockheed-California Company Division of Lockheed Aircraft Corp. Attn: R. B. Liddell Burbank, California	1
Marquardt Aircraft Corporation Technical Library 16555 Saticoy Street Van Nuys, California	1
McDonnell Aircraft Corporation Technical Library P. O. Box 516 St. Louis 3, Missouri	1
Narmco Division of Telecomputing 8125 Aero Drive San Diego, California	1
North American Aviation, Inc. Attn: H. H. Cretsley, Mgr. of Applied Science International Airport Los Angeles 45, California	1
Northrop Corporation Norair Division ttn: G. Mangurin 1001 E. Broadway Hawthorne, California	1
Radio Corporation of America Astro-Electronics Division Princeton, New Jersey	1

	NUMBER OF COPIES
Republic Aviation Corporation Technical Library Farmingdale, L. I., New York	1
Ryan Aeronautical Company Technical Library 2701 Harbor Drive San Diego 12, California	1
Space-General Corporation Div. of Aerojet General Attn: R. Brodsky El Monte, California	1
U. S. Rubber Company Research Center Wayne, New Jersey	1